

---

# **THERMOPHILIC MICROORGANISMS AS SOURCE OF VALUE-ADDED MOLECULES AND BIOCATALYSTS FOR LIGNOCELLULOSIC BIOMASS CONVERSION**

---

**Martina Aulitto**

Dottorato in Biotecnologie – 30° ciclo

Università di Napoli Federico II







Dottorato in Biotecnologie – 30° ciclo

Università di Napoli Federico II



---

# **THERMOPHILIC MICROORGANISMS AS SOURCE OF VALUE-ADDED MOLECULES AND BIOCATALYSTS FOR LIGNOCELLULOSIC BIOMASS CONVERSION**

---

**Martina Aulitto**

Dottoranda:	Martina Aulitto
Co-tutor:	Dr. Patrizia Contursi
Relatore:	Prof. Simonetta Bartolucci
Coordinatore:	Prof. Giovanni Sannia



*Ati miei genitori*



*"Nothing in life is to be feared, it is only to be understood.  
Now is the time to understand more, so that we may fear less."*

*Marie Curie*



## INDEX

<b>RIASSUNTO</b>	1
<b>ABSTRACT</b>	7
<b>CHAPTER I</b>	8
1. Thermophiles and biotechnology	9
2. Thermophilic enzymes	9
2.1 Glycosidases	9
2.2 GHs involved in lignocellulose hydrolysis	10
2.2.1 Cellulose conversion by cellulase	10
2.2.2 Hemicellulose conversions by hemicellulase	11
2.3 Discovery of new thermophilic GHs	12
2.3.1 <i>Thermus thermophilus</i> HB27 as source of thermozymes	12
2.3.2 Isolation of a new strain of thermophilic cellulolytic <i>Bacillus coagulans</i>	13
2.4 Synergistic action of thermophilic GHs	13
2.5 Immobilization strategy	14
3. Biorefinery and Bioeconomy	16
3.1 Lignocellulosic biomasses	17
3.2 Industrial process	17
3.2.1 Pre-treatment	17
3.2.2 Saccharification	18
3.2.3 Fermentation	18
3.2.3.1 SHF	18
3.2.3.2 SSF and SSCF	18
3.2.3.3 CBP	18
4. Aim of the work	20
5. References	21
<b>CHAPTER II</b>	25
Thermophilic GHs: discovery, characterization and immobilization	26
1. <i>Thermus thermophilus</i> as source of thermozymes for biotechnological applications: homologous expression and biochemical characterization of an $\alpha$ -galactosidase (paper 2-I)	27
2. A thermophilic enzymatic cocktail for galactomannans degradation (manuscript 2-II)	37
3. A standardized protocol for the UV induction of <i>Sulfolobus</i> spindle- shaped virus 1 (paper 2-III)	46
<b>CHAPTER III</b>	54
Industrial application of thermophilic and cellulolytic lactic acid producer, <i>Bacillus</i> <i>coagulans</i>	55
1. <i>Bacillus coagulans</i> MA-13: a promising thermophilic and cellulolytic strain for the production of lactic acid from lignocellulosic hydrolysate (paper 3-I)	56
2. Seed culture pre-adaptation improves lactic acid production of <i>Bacillus</i> <i>coagulans</i> MA-13 in Simultaneous Saccharification and Fermentation (manuscript 3-II)	71
<b>CONCLUDING REMARKS</b>	85
<b>APPENDIX I</b> –Communications	87
<b>APPENDIX II</b> – List of publications	88
<b>APPENDIX III</b> –Experiences in foreign laboratories	89
<b>APPENDIX IV</b> – Other papers	91





# RIASSUNTO

---

## **Le bioraffinerie e i bioprodotto**

Le “bioraffinerie” identificano gli impianti industriali, che utilizzano matrici di origine biologica, per ottenere i classici prodotti petroliferi (combustibili, carburanti, lubrificanti, materiali plastici), con l’obiettivo di smaltire le eccedenze agricole e di ridurre al minimo l’inquinamento. Le bioconversioni sono realizzate utilizzando materie prime rinnovabili e non incidono, dunque, sul bilancio complessivo dei gas serra. A seconda della biomassa utilizzata, si possono identificare tre generazioni di bioraffinerie: la prima nella quale i prodotti provengono dalla filiera agricola convenzionale; la seconda utilizza scarti di origine agricola o forestale; la terza mira a valorizzare terreni marginali, come quelli non agricoli o marini. La produzione di bioprodotto o biocarburanti è generalmente conseguita attraverso il processo di fermentazione degli zuccheri ricavati dalla biomassa. Un esempio di grande impatto sulla società è stata la produzione di bioetanolo, che ancora oggi è largamente prodotto in Brasile, da biomasse di prima generazione (amido, mais). In questo caso, il livello di produzione non riesce a soddisfare la crescente domanda della società, riscontrando un elevato impatto etico. Inoltre, l’utilizzo di biomasse, destinate all’alimentazione, non fornisce un decremento delle emissioni dei gas serra, ma amplia il conflitto definito “*food versus fuel*”. Una valida alternativa è rappresentata dalle biomasse lignocellulosiche, uno scarto e nel contempo una fonte inesauribile di energia, in quanto sono prodotte in notevoli quantità (100 tonnellate per anno), tali da soddisfare il fabbisogno energetico mondiale. Questa biomassa è costituita da una struttura vegetale molto complessa, che non ne permette un suo diretto utilizzo nelle bioraffinerie. Le biomasse vegetali, infatti, sono caratterizzate da lignina, che serve a cementare le fibre vegetali, da emicellulosa, che costituisce le pareti delle cellule vegetali ed è connessa, attraverso legami ad idrogeno, alla cellulosa. Quest’ultima è una lunga catena di glucosio, che conferisce resistenza ed elasticità alle fibre vegetali. Al fine di utilizzare questa biomassa in scala industriale, il processo convenzionale ne prevede: il pretrattamento (fisico, chimico-fisico, biologico), l’idrolisi enzimatica e infine, la fermentazione. Durante il pretrattamento, il cui risultato è la destrutturazione a livello molecolare della biomassa, la lignina viene allontanata e l’emicellulosa e la cellulosa diventano accessibili agli enzimi. Quest’ultimi agiscono sui polisaccaridi liberando zuccheri semplici, utilizzati successivamente dai microrganismi in metabolismo fermentativo, per la produzione di nuovi bioprodotto (es. etanolo, lattato, succinato).

## **Scoperta di nuove GH termofile**

I costi di produzione degli enzimi impiegati nella saccarificazione della cellulosa e dell’emicellulosa sono i maggiori fattori che incidono negativamente sul processo di bioconversione della biomassa lignocellulosica. Gli enzimi che degradano la cellulosa, sono definiti “cellulasi”, appartengono alla famiglia delle glicosil idrolasi (GH) e catalizzano l’idrolisi dei legami  $\beta$ -1,4-D-glicosidici. Le cellulasi sono enzimi diffusi dal mondo animale a quello vegetale, fino ai funghi, batteri e protozoi, differendo per struttura e meccanismo di reazione. In base alla reazione catalizzata, si distinguono tre classi: endocellulasi, esocellulasi e cellobiasi.

L'emicellulosa, invece, essendo un eteropolisaccaride con una struttura ramificata e non fibrosa, è costituita da una catena principale i cui monomeri sono zuccheri esosi (glucosio, mannosio e galattosio) e pentosi (arabinosio e xilosio), policondensati mediante legami  $\beta$ -1,4. L'emicellulosa, così come le emicellulasi, sono classificate in base alle tipologie di zuccheri. In natura, tra le più diffuse nelle pareti cellulari vegetali, troviamo gli xilani, i mannani, gli arabani e i galattani, rispettivamente idrolizzati da xilanasi (EC:3.2.1.8.), mannanasi (EC:3.2.1.78), arabinasi (EC:3.2.1.99.) e galattosidasi (EC:3.2.1.22.).

- ***Thermus thermophilus*: una fonte di termozimi con applicazioni biotecnologiche**

I microrganismi termofili sono stati estensivamente studiati negli ultimi anni come una ricca fonte di enzimi ad elevato impatto biotecnologico. In particolare, il genere *Thermus* è considerato non solo una fonte di enzimi, ma anche una “cell factory” per la capacità di over-esprimere proteine ricombinanti. In questo progetto di dottorato è stata effettuata l'espressione omologa e la caratterizzazione di un' $\alpha$ -galattosidasi da *Thermus thermophilus* HB27, appartenente alla famiglia delle GH36. L' $\alpha$ -galattosidasi ( $\alpha$ -D-galattopirinoside galattoidrolasi; EC: 3.2.1.22) è una glicosidasi ubiquitaria, prodotta in piante, animali e microrganismi, in grado di idrolizzare  $\alpha$ -D-galattosidi sia semplici, che complessi. In generale, le  $\alpha$ -galattosidasi hanno un vasto potenziale applicativo nelle biotecnologie, dalla degradazione del raffinosio della canna da zucchero, al trattamento della malattia di Fabry.

Analisi bioinformatiche preliminari sono state effettuate sul gene *TTP0072*, localizzato sul megaplasmide pTT27, presente nelle cellule di *Thermus thermophilus* HB27. Attraverso allineamenti multipli, utilizzando la predizione di sequenza amminoacidica, è stato possibile mettere in evidenza la sequenza consenso e particolari residui catalitici, noti già per altre  $\alpha$ -galattosidasi. Il gene è stato clonato in due vettori pET30 per l'espressione in *E. coli* e pMKE2 per l'espressione omologa nel ceppo *T. thermophilus*::nar. In entrambi i casi, la strategia di clonaggio ha previsto l'aggiunta alla proteina ricombinante di un tag di istidine, per facilitarne la purificazione con una cromatografia di affinità. Alla fine del processo di purificazione, la differenza cruciale è stata la quantità di enzima ottenuto dalle due fonti, in quanto nell'ospite mesofilo, la resa della proteina prodotta è stata 0.5 mg/L; diversamente nell'ospite termofilo il livello di espressione raggiunto è stato di dieci volte maggiore (5.0 mg/L). Date le differenze di resa, è stata condotta la caratterizzazione dell' $\alpha$ -galattosidasi prodotta nell'ospite omologo *T. thermophilus*, *TtGalA*. In seguito alla purificazione, per verificare l'identità e lo stato di purezza della proteina, è stata effettuata un'analisi attraverso spettrometria di massa, che ha confermato la massa molecolare del monomero di 55.8 kDa. Ulteriori analisi sono state effettuate per determinare la struttura quaternaria, in particolare è stata eseguita una cromatografia ad esclusione molecolare, accoppiata alla tecnica di light scattering-QELS, da cui si è evidenziato che la proteina è esamerica ed ha un peso molecolare di circa 320 kDa. Per valutare l'attività enzimatica di *TtGalA* è stato effettuato un saggio qualitativo mediante zimografia e successivamente, l'enzima è stato caratterizzato per stabilire la specificità di substrato e le costanti cinetiche. In particolare, per effettuare saggi di attività catalitica a diverse temperature e pH è stato utilizzato il substrato sintetico il pNPG- $\alpha$ -D-galattopiranoside. L'enzima ricombinante ha mostrato avere un'attività ottimale a 90°C e pH 6, mantenendo oltre il 40% di attività relativa in un intervallo di pH tra 5.0 e 8.0 e più del 90% dopo 30 ore a 70°C. In questo contesto, *TtGalA* si è dimostrata

essere una delle più termoattive e termostabili  $\alpha$ -galattosidasi studiate, con un elevato potenziale nel processo di idrolisi della biomassa lignocellulosica.

- **Studio dell'azione sinergica di un' $\alpha$ -galattosidasi e  $\beta$ -mannanasi termofila**

Un punto cruciale nelle bioraffinerie è la saccarificazione delle cellulose ed emicellulose, con il conseguente incremento del contenuto degli zuccheri fermentabili. In particolare, per effettuare la completa idrolisi della frazione emicellulosica, è richiesta l'azione di molteplici enzimi.

Un esempio sono i mannani, una classe di emicellulose, classificati in quattro sottofamiglie a seconda della loro composizione: mannani lineari, glucomannani, galattomannani e galattoglucomannani. Per la loro completa idrolisi è richiesta la cooperazione di diversi enzimi:  $\alpha$ -galattosidasi (EC 3.2.1.21),  $\beta$ -mannanasi (EC 3.2.1.78),  $\beta$ -mannosidasi (EC 3.2.1.25) e  $\beta$ -glucosidasi (EC 3.2.1.21). Diversamente dalla cellulosa, dove la cooperazione tra enzimi avviene sulla catena lineare, per le emicellulose esistono tre differenti classi di sinergia tra enzimi, che idrolizzano la catena lineare e/o le ramificazioni (omosinergia, eterosinergia e antisinergia). Il progetto di dottorato si è focalizzato sullo studio dell'eterosinergia tra due enzimi termofili, l' $\alpha$ -galattosidasi *TtGalA* (descritta in precedenza) e *DturCelB* una  $\beta$ -mannanasi da *Dictyoglomus turgidum*, precedentemente caratterizzata nel nostro gruppo di ricerca. Al fine di stabilire se fosse presente sinergia tra i due enzimi, sono stati utilizzati come substrati, tre galattomannani con differenti rapporti in galattosio-mannosio: i semi di carrube (1:4), il carrubo (1:3.5) e la gomma di guar (1:2). Analisi preliminari sono state eseguite testando i due enzimi singolarmente sui substrati polimerici, da cui si è evinto che *TtGalA* mostra un'attività idrolitica simile ad altre  $\alpha$ -galattosidasi note in letteratura, mentre *DturCelB*, invece, esibisce un'elevata attività su carrubo e semi di carrube, rispetto all'attività su gomma di guar. Quest'ultimo, a causa dell'elevata concentrazione di galattosi nelle catene laterali, influenza negativamente l'attività enzimatica. Per stabilire l'eterosinergia nell'idrolisi dei galattomannani, i due enzimi termofili sono stati incubati a 80°C per 30 minuti. I risultati ottenuti, hanno evidenziato che i due enzimi lavorano cooperativamente su tutti i substrati testati ed in particolare, il maggior grado di sinergia (1.8) è stato ottenuto su semi di carrube, utilizzando nella miscela di saggio il 75% di *TtGalA* e il 25% di *DturCelB*. Inoltre, è stato dimostrato attraverso i saggi sequenziali, che *TtGalA* agisce come primo enzima, rimuovendo l'ingombro sterico dei galattosi e favorendo l'idrolisi di *DturCelB* sulla catena lineare. Dai risultati ottenuti, si può ipotizzare che i due enzimi termofili, *TtGalA* e *DturCelB*, possono essere dei candidati per lo sviluppo di cocktail enzimatici da utilizzare durante il pretrattamento o nella fase di raffreddamento del processo, favorendo la riduzione del costo di saccarificazione.

- **Protocollo di induzione UV per la produzione di particelle virali del virus *Sulfolobus* spindle-shaped virus 1**

Le condizioni di temperatura e pH tipiche dei processi industriali, influenzano negativamente la stabilità della struttura proteica degli enzimi e quindi la loro attività catalitica. Una delle strategie utilizzate per superare questa criticità è l'immobilizzazione enzimatica su supporti inerti insolubili. Per questo motivo in questo progetto di dottorato, un altro aspetto preso in esame è stato la messa a punto di un protocollo per l'induzione di particelle virali archeali (VPs) del virus SSV1, come supporto per l'immobilizzazione degli enzimi termofili.

Il fusellovirus SSV1 è uno dei primi virus archaeali ad essere stato isolato ed è considerato un modello per lo studio dell'interazione virus-ospite. Oltre ad infettare il suo ospite naturale, *Sulfolobus shibatae* (B12), SSV1 è in grado di proliferare anche in cellule di *Sulfolobus solfataricus*. La caratteristica peculiare di questo fusellovirus è l'inducibilità della sua trascrizione e replicazione, in seguito ad esposizione a radiazione UV, con la conseguente produzione di particelle virali rilasciate nel mezzo di coltura senza lisare le cellule ospiti. Nel corso di questo dottorato è stato messo a punto un protocollo d'irradiazione, che inducesse opportunamente il virus, ma che al contempo salvaguardasse il più possibile la vitalità delle cellule ospiti. Una prima analisi è stata condotta sull'effetto dell'irradiazione sulla replicazione virale, in particolare, saggi mediante PCR semi-quantitativa e digestione enzimatica hanno evidenziato che la quantità di DNA virale incrementa maggiormente in cellule trattate con  $45 \text{ J}\cdot\text{m}^{-2}$  ( $0.5 \text{ J}\cdot\text{m}^{-2}\cdot\text{s}^{-1}$ ), rispetto a colture trattate con altre dosi. Inoltre, è stato osservato un elevato numero di particelle virale rilasciate nel mezzo di coltura dopo circa 24 ore dal trattamento (circa  $5 \cdot 10^9$  PFU/ml). La vitalità delle cellule ospiti è stata dimostrata diminuire all'aumentare della dose totale e dell'energia d'irradiazione, utilizzata per trattare le cellule. Questo ha permesso di confermare, come buon compromesso, una dose totale di  $45 \text{ J}\cdot\text{m}^{-2}$  fornita utilizzando un'energia d'irradiazione di  $0.5 \text{ J}\cdot\text{m}^{-2}$  al secondo; infatti, questa dose determina una sopravvivenza cellulare del 37%. Una volta stabilita l'adeguata dose ed energia per l'irradiazione, è stata effettuata un'analisi nel tempo, per valutare dopo quante ore dal trattamento fosse sbloccata la replicazione di SSV1. A tal scopo, esperimenti di PCR semi-quantitativa sono stati allestiti, per stimare le variazioni della quantità di DNA virale nel tempo, dimostrando che poche ore dopo il trattamento (2-4 ore) si verifica uno sblocco della replicazione virale, con un accumulo di DNA dopo circa 8 ore dal trattamento. Inoltre, il successivo decremento (10-24 ore) potrebbe essere spiegato dall'estruzione delle particelle virali, da parte delle cellule infettate (SSV1-InF1), nel mezzo di coltura. Questi esperimenti dimostrano la possibilità di poter indurre la produzione di VPs, al fine di purificarle dal mezzo di coltura e utilizzarle per l'immobilizzazione degli enzimi termofili.

### **Isolamento di nuovi ceppi di microrganismi termofili e cellulolitici**

Una delle principali strategie adottate per la ricerca di nuovi enzimi, da impiegare nel processo di saccarificazione, è l'isolamento di microrganismi in grado di crescere e idrolizzare i polisaccaridi presenti nelle biomasse lignocellulosiche. Una preziosa fonte di microrganismi e biocatalizzatori sono gli ambienti nei quali i microrganismi si sono evoluti sotto pressione selettiva. In studio è stata effettuata la selezione per la ricerca di nuovi ceppi cellulolitici e termofili, per consentire l'identificazione e la caratterizzazione di nuovi enzimi con caratteristiche idonee al processo di idrolisi industriale, quali: alte temperature, pH acidi ed elevata efficienza catalitica.

- ***Bacillus coagulans* MA-13: un ceppo termofilo e cellulolitico per la produzione di acido lattico**

In natura, la degradazione della biomassa lignocellulosica richiede complessi processi, che includono la presenza di microrganismi decompositori. Per cui una delle riserve più ricche di nuove specie cellulolitiche sono proprio i residui agricoli e forestali; in particolare in questa tesi di dottorato sono stati utilizzati come fonte per l'isolamento di microrganismi termofili e cellulolitici, gli scarti di lavorazione dei fagioli. Dopo diversi passaggi di screening, selezione ad elevate temperature (60°C) e utilizzando come unica fonte di carbonio la carta da filtro o la carbossi-metil-cellulosa (CMC), è stato

isolato il microrganismo *Bacillus coagulans* MA-13. Questo batterio è stato selezionato per la sua abilità nell'utilizzare substrati complessi ad una temperatura ottimale di crescita di 55°C. Partendo dal presupposto che diverse specie di *Bacillus* sono in grado di secernere enzimi idrolitici e che *B. coagulans* è in grado di metabolizzare substrati complessi, il surnatante ottenuto dalla crescita è stato testato per individuare la presenza di attività cellulastica, mediante saggi enzimatici su piastra.

*B. coagulans* è anche noto per essere un organismo modello usato per la produzione di acido lattico da biomassa lignocellulosica. Per questo motivo, il nuovo ceppo isolato MA-13 è stato testato per la sua abilità fermentativa utilizzando zuccheri sintetici, esosi e pentosi, presenti nella frazione cellulosica ed emicellulosica. Inoltre, *B. coagulans* MA-13, è stato cresciuto anche utilizzando come fonte di carbonio la melassa, che costituisce un esempio di materia prima grezza ottenuta per concentrazione delle acque madri, ottenute dalla fase di estrazione del saccarosio. Questa è largamente impiegata su scala industriale come fonte di carbonio, in numerosi processi microbiologici e nell'alimentazione animale.

Un'altra caratteristica indispensabile nei microrganismi adibiti alla produzione di biocarburanti e bioprodotto è la tolleranza verso gli inibitori rilasciati durante il pretrattamento della biomassa. Per questo motivo, *B. coagulans* MA-13 è stato cresciuto in presenza della frazione liquida ottenuta dopo il pretrattamento acido della paglia di grano. Questa frazione, definita idrolizzato, contiene furfurali, idrossimetilfurfurali e acido acetico, composti altamente tossici per la vitalità cellulare. Questi esperimenti hanno dimostrato che: i) il ceppo è resistente ad elevate concentrazioni di idrolisato, ii) la produttività specifica di acido lattico aumenta e iii) le rese di acido lattico restano invariate, all'aumentare della concentrazione dell'idrolisato nel mezzo di coltura. L'unico parametro influenzato negativamente dalla presenza degli inibitori è la lunghezza del processo fermentativo, che aumenta significativamente da 18 ore a 48 ore, quando è presente il 95% di idrolisato nel terreno di crescita. Questi risultati, supportano l'ipotesi che il ceppo MA-13 possa essere impiegato nel processo di produzione di acido lattico, utilizzando come fonte di carbonio uno scarto industriale (la melassa) e riducendo al minimo l'apporto di acqua all'interno del processo, poiché sostituita nella totalità dall'idrolisato, ottenuto dopo il processo di pretrattamento.

- ***Bacillus coagulans* MA-13: produzione di acido lattico da scarti agricoli e forestali**

Le bioplastiche sono bioprodotto non derivanti dalla raffinazione del petrolio, con la caratteristica di essere biodegradabili o biocompostabili. L'acido lattico è un precursore delle bioplastiche ed esiste in due forme enantiomeriche (L- e D-), ma soltanto dall'isomero otticamente attivo (L-) è possibile ottenere il polimero cristallino dell'acido polilattico. Dato che il processo biologico utilizzato per ottenere l'isoforma L- è la fermentazione lattica, in questo progetto il ceppo MA-13 è stato testato per la produzione di acido lattico in configurazione SSF (simultanea idrolisi e fermentazione) utilizzando come biomassa la paglia di grano pretrattata con idrolisi acida, ad elevate temperature e pressione. La biomassa è stata ottenuta dal "SP Biorefinery Demo Plant di Örnsköldsvik" (Svezia) e il processo è stato ottimizzato, presso la Chalmers University, sotto la direzione del Prof. Carl Johan Franzén. In questo caso MA-13 è stato propagato in anaerobiosi, ad un pH di 5.5 e una temperatura di 55°C, condizioni ottimali sia per la catalisi enzimatica, che per la crescita e fermentazione del batterio. La particolarità di questo processo è l'aggiunta di una fase di adattamento, in cui le cellule in seguito utilizzate per la fermentazione, sono state propagate in condizioni

controllate in assenza o in presenza di idrolisato (0%-30%-40%-50%), per indagare sulla possibilità di favorire una pressione selettiva verso gli inibitori e migliorare le rese dell'intero processo.

Le cellule sono state cresciute fino alla fase stazionaria precoce (circa 18-20 ore) e raccolte per effettuare l'SSF, utilizzando in un apposito bioreattore per favorire l'agitazione del terreno di coltura contenete la biomassa pretrattata solida. Dai prelievi effettuati, ogni tre ore, sono state condotte analisi mediante HPLC, al fine di quantificare la produzione di acido lattico e monitorare, attraverso la conta cellulare (CFU: unità formanti colonie), la vitalità delle cellule. Dai risultati ottenuti, la resa di acido lattico è la stessa in tutte le condizioni testate, ma nel caso in cui le cellule sono state cresciute in presenza del 30% di idrolizzato, il processo dura 12 ore (invece di 30 ore), con un incremento della produttività massima (2.1 g/L/h), rispetto alle cellule non sottoposte al processo di adattamento. Dai dati ottenuti, il ceppo MA-13, durante la propagazione in presenza di idrolizzato, risulta essere adattato fisiologicamente agli inibitori, poiché è influenzata positivamente sia la velocità del processo di fermentazione, che la produttività di acido lattico. In conclusione, *B. coagulans* MA-13 è un candidato promettente, per la produzione di acido lattico da biomasse lignocellulosiche.

I risultati ottenuti, durante questo progetto di dottorato, dimostrano la potenzialità di enzimi e microrganismi termofili, da utilizzare come nuovi biocalizzatori nell'idrolisi di biomasse lignocellulosiche e nella produzione di materiali ad elevato valore aggiunto.







# ABSTRACT

---

Feedstocks of lignocellulosic biomass represent a widely available and cheap organic material for the production of value added-products. In this context, thermophilic microorganisms are promising candidates both for the production of thermostable variants of carbohydrate-degrading enzymes, as well as for their own ability to thrive under harsh bioprocessing conditions.

The first part of this PhD-thesis was focused on the characterization of new hemicellulolytic enzymes (*TtGalA* and *DturCelB*) from thermophilic source. *TtGalA*, a thermoactive and thermostable  $\alpha$ -galactosidase from *Thermus thermophilus* HB27 was expressed in the native host, displaying an optimal hydrolytic activity at 90° C and pH 6.0 and long-term retained activity (30 hours) at 70°C. *DturCelB* is a  $\beta$ -mannanase from *Dictyoglomus turgidum* characterized in our research group exhibiting optimal catalytic activity at 70°C and pH 5.4. The heterosynergistic functional association between *TtGalA* and *DturCelB* was assayed on galactomannan polysaccharides in simultaneous and sequential assays. Our data showed that the two recombinant enzymes were able to work in synergy on all substrates tested, with *TtGalA* acting as first to remove galactose residues and therefore, exposing cleavage sites to *DturCelB* hydrolysis, thus increasing the degradation efficiency of complex substrates.

Enzymatic immobilization techniques are suitable for enzyme recovery and recirculation. Several such techniques and support materials have been previously proposed, nevertheless the employment of viral particles has not been widely exploited so far. Because of our longstanding experience with archaeal thermophilic viral particles from *Fuselloviridae*, we aim at using them as self-assembling support to immobilize thermophilic carbohydrate-active enzymes. For this purpose, an UV induction protocol was successfully set up for the overproduction of thermophilic SSV1 virus particles.

The second section of this thesis was addressed to the discovery and characterization of a new thermophilic strain (MA-13) of *Bacillus coagulans*. This microorganism was isolated from canned beans manufacturing residues for its ability to grow at 55°C, using carboxymethyl-cellulose and filter paper, as carbon sources. Noteworthy, MA-13 was tested for its ability to secrete soluble endo-1,4- $\beta$ - glucanase enzymes into the culture supernatant. Moreover, it turned to be an efficient lactic acid producer on hydrolysate derived from the pre-treatment of wheat straw by acid-catalyzed hydrolysis and steam explosion. MA-13 was also used to set up the production of lactic acid from renewable lignocellulosic biomasses in SSF configuration.



# Chapter I



# INTRODUCTION

---

## 1. Thermophiles and biotechnology

Microorganisms can be roughly classified, according to the range of temperature at which they can grow, in: i) psychrophiles (below 20°C), ii) mesophiles (from 20° up to 45°C), iii) thermophiles (from 50° up to 70°C) and iv) extremophiles (above 70°C). From biological point of view, the study of these microbes, has an important implication in regard to evolution, for the diversity in their microbial metabolisms and prokaryotic ecosystems [1]. On the other hand, the impact of biotechnology on our lives is inescapable and in addition the comparison between the natural habitats of thermophiles and the typical industrial cultivations reveals both the advantages and the limits of these microorganisms [2]. Today the use of microorganisms has become so prevalent in biotechnology applications, thus rendering their discovery and the genetically modification rights underpin our economy.

In this thesis, the attention was pointed on thermo- and extremophilic microorganisms, for their industrial applications.

## 2. Thermophilic enzymes

Life at high growth temperatures requires cell components stable and biologically active at these extreme temperatures [3]. Although several thermophilic proteins exhibit high thermostability and high temperature optimum, it is still not well understood as to how the proteins from these hyperthermophiles are protected against damage at temperatures, which are detrimental for mesophilic proteins. Although many studies attempted to identify “universal” factors imparting thermostability, protein thermostability is indeed a complex property controlled by several features which may be working additively. Among these sequence-level factors (specific amino acid like Arg and Glu being significantly represented in thermophiles) and structure-level factors (energy of unfolding, number of Van der Waals contacts per residue, number of residues involved in secondary structure) are the most common [4].

Recently another area of interest, that is receiving considerable attention, is the efficient conversion of feedstock into fermentable sugars, through mechanical, chemical and biocatalytic treatments of the raw materials. Thermophilic and thermostable enzymes offer robust catalyst alternative to the mesophilic counterpart, since they can withstand the harsh physical and chemical conditions typical of industrial processes [5, 6].

### 2.1 Glycosidases

In nature, two main classes of biocatalysts are involved in the carbohydrates modifications: Glycosyltransferases (GTs) and Glycoside Hydrolases (GHs). In biological systems, they are responsible for the synthesis and the hydrolysis of the sugars, respectively. These enzymes are classified in families in a database named CAZy (<http://www.cazy.org>) on the basis of their aminoacidic sequence [7]. GTs catalyze the formation of the glycosidic bonds, transferring the sugar moieties from the activated donator to specific acceptor molecules. These families are organized on the basis of their substrate specificity and either in dependence of retaining or inverting mechanism, according to the stereochemistry of the substrates and reaction products. GHs (also named Glycosidases) are a widespread group of enzymes that hydrolyze the glycosidic bond between a carbohydrate and another moiety and are categorized

into over 100 families. These families of enzymes are distinguished in exo- or endo-glycosidase depending on position of the substrate, respectively [8]. Generally, the hydrolysis involves only two amino acids, a proton donator and a nucleophile base, producing a retention or inversion of anomeric configuration of the glycosidic substrate. Therefore, GH are also classified according to the inverting or retaining mechanisms.

Commonly, thermophilic GHs are used for the hydrolysis of lignocellulosic biomasses. In biorefinery, this process named “saccharification” is employed to produce sugars that can be converted through fermentation into value added product. Since these bioprocesses require high temperature, extreme pH and pressure, thermostable and thermoactive enzymes are particularly suitable for this purpose [5]. Furthermore, the thermostable enzymes features may improve the global yield of the process providing additional advantages, as: (1) better enzyme penetration, (2) cell wall disorganization of the raw materials, (3) increase of the substrate solubility and (4) reduction of contamination [5].

Currently, several  $\alpha$ -amylase from *Bacillus acidicola* [9], glucoamylases from *Picrophilus* [10], and  $\alpha$ -pullulanase from *Thermococcus kodakarensis* [11] are used in starch-hydrolysis to replace their mesophilic counterparts.

## **2.2 GHs involved in lignocellulose hydrolysis**

Lignocellulose is the product of the carbon fixation during the photosynthesis of the land plants [12]. During the life of the plants, its role is to provide the structural integrity to withstand the herbivores and pathogens attacks. In detrital food webs, saprophytes and detritivores are involved in the natural decomposition of lignocellulosic-biomass [13]. Since this kind of biomass is generated in large quantities every-day, it could be advantages to exploit it in biorefinery applications. However, lignocellulose is a complex matrix constituted of hemicellulose, which is coated the cellulose by microfibrils. Moreover, polysaccharide components are encapsulated by lignin, rendering lignocellulose recalcitrant to enzymatic digestion [13]. In industrial processes, a chemical and physical pretreatment is employed to disarray the lignin. The resulting polysaccharides are hydrolyzed by the enzymatic mixture based on (hemi)cellulases and auxiliary enzymes needed to obtain an effective saccharification [14]. GHs are the primary enzymes that cleave glycosidic linkages present in cellulose and hemicellulose (Fig. 1)[15].

### **2.2.1 Cellulose conversion by cellulases**

Cellulose is a homo-polysaccharide composed of  $\beta$ -D-glucopyranose units linked together by (1-4)-glycosidic bonds. The cellulose molecules are linear and its length depends on the type of plants of origin. Glucose anhydride, which is formed via the removal of water from each glucose, is polymerized into long cellulose chains that contain 5,000-10,000 glucose units. The basic repeating unit of the cellulose polymer consists of two glucose anhydride units, called a cellobiose units [12]. Cellulose fraction is hydrolyzed by the synergistic action of multiple GHs, acting on internal bonds (e.g., endocellulase: EC 3.2.1.4), extremities (e.g., exocellulase EC 3.2.1.91), and intermediate degradation products (e.g.,  $\beta$ -glucosidase: EC 3.2.1.21). To achieve the complete degradation of the polysaccharide, the cellulolytic bacteria have developed during the evolution, several strategies to produce: i) individual enzymes with accessory proteins (i.e carbohydrate-binding modules (CBM)), ii) complex of proteins with multiple GH domains [16] and iii) cellulosomes, a multi-enzyme machines produced by many cellulolytic microorganisms (Fig. 1A) [16].

### 2.2.2 Hemicellulose conversions by hemicellulase

The second most abundant biopolymer on earth is hemicellulose. Unlike cellulose, hemicellulose is a branched polysaccharide consisting in shorter chains of 500–3,000 sugar units [17]. Hemicelluloses include pentoses (xylose and arabinose), hexoses (glucose, galactose, mannose) and also sugars in their acidified form (glucuronic acid and galacturonic acid) can be present. Among these, mannans comprise linear or branched polymers derived from sugars such as D-mannose, D-galactose and D-glucose [18]. Moreover, they represent the major source of secondary cell wall found in conifers (softwood) and leguminosae. In particular, mannans are classified based on their sugar composition in: i.e. mannans, glucomannans, galactomannans and galactoglucomannans. To achieve the complete degradation of galactoglucomannans, the most complex mannans subfamily, different hydrolytic enzymes such as  $\beta$ -glucosidase (EC 3.2.1.21), endo-mannanase (EC 3.2.1.78), mannosidase (EC 3.2.1.25) and  $\alpha$ -galactosidase (EC 3.2.1.22) are needed (Fig. 1B) [19].

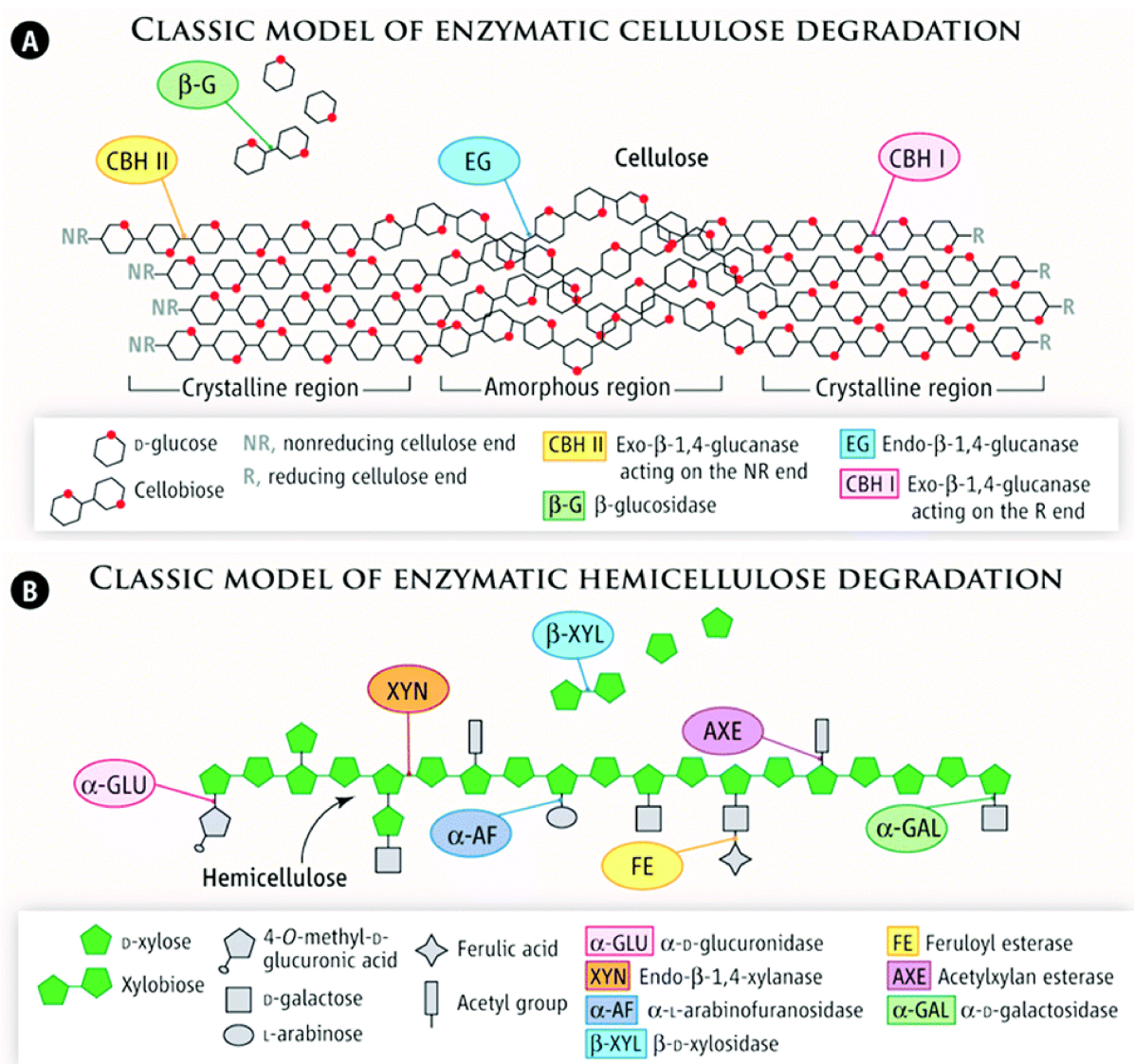


**Figure 1.** Graphical representation of cellulose and hemicellulose degradation [15].

### 2.3 Discovery of new thermophilic GHs

Industrial biotechnology research has been addressed into the discovery of ecofriendly lignocellulose hydrolytic enzymes able to withstand pH, temperature and inhibitory compounds typical of the industrial conditions [20]. The isolation and identification of lignocellulose degrading-microorganisms from natural habitats, together with genomic and metagenomic studies allow the exploitation of a rich reservoir of enzymes with novel activities and/or functional and structural features. High stability and efficient activity over a wide range of temperatures, making them interesting for industrial processes. The main issue for the utilization of thermophilic enzymes, is their market production in large scale. For long time, *Escherichia coli* has been employed to produce thermophilic recombinant enzymes, but in some cases their expression level can be low to achieve amount necessary for industrial scale [20]. For this reason, different genetic systems for both archaeal and bacterial thermophilic microorganisms have been developed. However, the amount of the recombinant proteins is in general lower than that obtained through conventional mesophilic expression systems [21].

#### 2.3.1 *Thermus thermophilus* HB27 as source of thermozymes

*Thermus thermophilus* HB27, a microorganism with high biotechnological potential, has already made an impact on the research community [22]. In particular, its genome sequencing has made possible the discovery of numerous genes crucial for the cell mechanisms and processes such as, replication, transcription and translation. *T. thermophilus* is an aerobic Gram-negative thermophilic bacterium, that grows in a temperature range from 50° and 82°C. Its genome consists of a chromosome (1,894,877 base pair) and of a megaplasmid (pTT27, 232,605 base pair) (Fig. 2) [22].

The cells morphologically appear as thin bacilli and the envelope consists of four layers. The membrane is composed, as all Gram-negative bacteria, primarily of phospholipids and lipopolysaccharides and the structural integrity is guaranteed by a peptidoglycan layer covalently linked to an amorphous material. Another characteristic is the highly competence for natural transformation. The most commonly employed isolates are the strains *T. thermophilus* HB27 and HB8 [23], because the high rates by which they can be transformed by natural competence. Therefore, these strains are widely used as host for the efficient introduction of heterologous DNA and genetic modification, allowing the construction of libraries for large inserts and they are considered a good candidates for the functional screening of genomic and metagenomic library at elevated temperatures [24]. Interestingly, HB8 strain, unlike HB27, can grow in anaerobic conditions performing a partial or complete denitrification or is able to use as final acceptors heavy metals [25]. This additional ability of *T. thermophilus* HB8 was confirmed by the presence of a nitrate reductase gene cluster, absent in HB27 and in other aerobic strains. The cluster encodes for respiratory nitrate reductase operon, strongly induced by the combined effect of nitrate and low oxygen concentration [25].



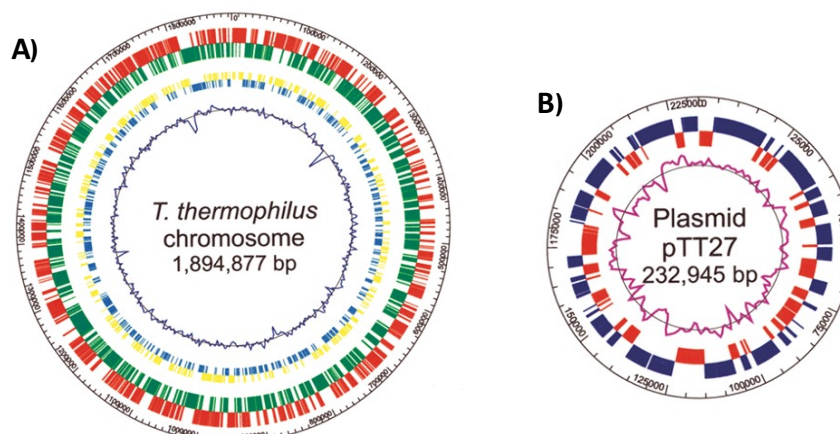


**Figure 2.** Analysis of the chromosome and plasmid pTT27 of *T. thermophilus* HB27 [22].

In order to create a specific expression system for *Thermus* spp., a plasmid pMKE1, containing replicative origins for *E. coli* and *Thermus* spp., a selection gene encoding a thermostable resistance to kanamycin, and a 720 bp DNA region containing the promoter (*Pnar*), was developed [26]. The expression of the proteins was specifically induced by the combined action of nitrate and anoxia in facultative anaerobic derivatives of *T. thermophilus* HB27::nar modified by transferring the gene cluster for nitrate respiration from HB8, through conjugation into the HB27 strain. Subsequently, to increase the protein expression levels, pMKE1 was genetically modified producing a new vector named pMKE2 [27]. This latter one was used in this thesis to express a homologous  $\alpha$ -galactosidase (named *TtGalA*) in the native host (paper 2-I).

### 2.3.2 Isolation of a new strain of thermophilic cellulolytic *Bacillus coagulans*

The discovery of new microorganisms from microbial communities is a promising strategy to identify carbohydrate active-enzymes with new features, in order to widen the application prospective of thermozymes [28]. The suited organisms for the degradation of lignocellulose are the production fungi. Since, their ability to secrete extracellular enzymes, numerous fungi have been isolated and identified, such as *Aspergillus*, *Rhizopus*, and *Trichoderma* species [29-31]. However, the bacteria thriving to the harsh conditions, are also a good candidate for the isolation of novel cellulose hydrolysing enzymes [32]. The intrinsic feature of bacteria is the fast growth rate that improves the competitiveness in the industrial process. Cellulase-producing bacteria have been isolated from various sources such as decaying agricultural wastes [33], soil [28], and extreme environments like hot-springs [34]. In general, the catabolism of cellulolytic strains can be classified in two strategies for the utilization of cellulose [35]. Aerobic bacteria are known to produce free-cellulase into the media to hydrolyse the polymeric substrate. Anaerobic bacteria display a tendency to adhere to cellulose, producing a proteic organelle, the cellulosome [36]. Even if exists a basal classification, various microbial species show a combination of these features [37]. In particular, in this PhD-thesis it was isolated a facultative anaerobic cellulolytic *Bacillus coagulans* strain, from bean manufacturing processing (paper 3-I).

## 2.4 Synergistic action of thermophilic GHs

Since the lignocellulosic wastes are composed of polymeric complexes, their enzymatic degradation is accomplished by numerous carbohydrate-active enzymes, whose collective action increases the hydrolysis yield of cell walls [13]. Typically, these

mixtures act together as a cocktail with complementary, synergistic activities and modes of action. This synergism can be based on the combination of: i) purified proteins ii) individual domains ii) recombinant organisms expressing ligninase, hemicellulase or cellulase encoding genes. For instance, the naturally occurring cellosome synergism is based on the action of non-hydrolytic proteins (i.e. expansin or swollenin) as well as of carbohydrate-binding modules (CBMs). Instead, commercially available cocktails for cellulose digestion are composed of cellobiohydrolases, endoglucanases, and  $\beta$ -glucosidase [38]; while for the hydrolysis of pretreated lignocellulose the synergism among cellulase, xylanase, esterase, and mannanase is exploited. In this PhD-thesis it was studied the synergism between the  $\alpha$ -galactosidase from *Thermus thermophilus* and a  $\beta$ -mannanase from *Dictyoglomus turgidum* on the galactomannan substrates (manuscript 2-II).

## 2.5 Immobilization strategy

The enhancement of enzymes efficiency is one of the current demands of the world's biotechnological industries. One procedure used to increase the enzyme conversion and the stability is the immobilization, i.e. the confinement of enzyme to a solid phase [39]. In the green economy context, the number of enzymes required for the lignocellulosic wastes is very high. Therefore the immobilization strategies is crucial, since this makes possible the enzymes recovery and their recycling [40]. Since, enzyme catalysis takes place in a small region of the protein, i.e. the "active site", the challenge of the immobilization technique is to avoid drastic changes in enzymatic activities, optimum pH, affinity to the substrate, stability. Several methods are used for immobilization, the three of the most common being: i) carrier binding; ii) crosslinking and iii) entrapment.

*Carrier binding* is based on the formation of interactions between enzyme and a support. This method can be further categorized as physical adsorption, ionic binding, covalent binding, metal binding and disulfide binding (Fig. 3A). Among these, the oldest technique is the physical adsorption, where the enzyme is adsorbed to external surface of the support, but it is often too weak to keep the enzyme upon temperature fluctuations, changes in pH, substrate concentration and ionic strength. Therefore, the covalent binding, represents a better alternative. In this case a covalent bond between the amino acid side chains available on the enzyme surface and to the chemical groups on the carrier, is formed. Others non-covalent bindings (i.e. ionic, metal, affinity and disulfide binding) lead to reversible immobilization (Fig. 3A) [41, 42].

*Crosslinking*, also called copolymerization, is an alternative technique developed to overcome the enzymes stabilization during the process. In this method, the enzymes are directly covalently linked to each other, through poly-functional reagents as glutaraldehyde and di-isocyanates (Fig. 3B).

The last type of immobilization is the *entrapment* in which the enzymes embedded in a capsule or fibers made up by semipermeable membrane (i.e. natural, synthetic polymers or gel like structure etc.) (Fig. 3C).

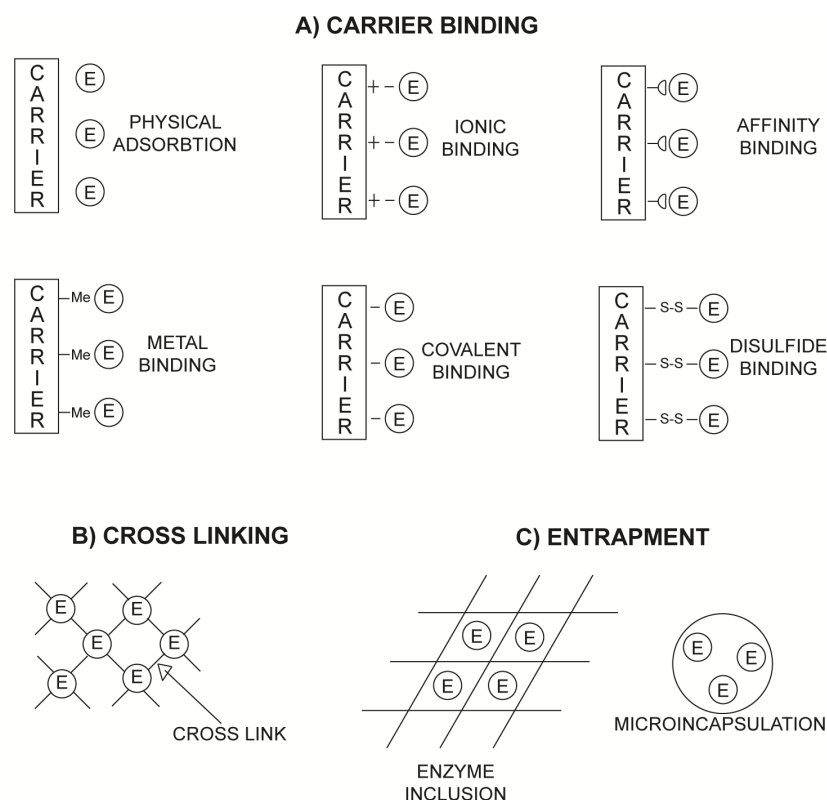


**Figure 3.** Various methods for enzyme immobilization.  
A) Carrier binding; B) Cross linking and C) Entrapment.

On the other hand, the carriers or supports for immobilization are grouped into three major categories: i) natural polymers (i.e. alginate, chitin, collagen, gelatin, cellulose); ii) synthetic polymers (i.e. diethylaminoethyl cellulose, polyvinyl chloride and UV activated polyethylene glycol) and iii) inorganic materials (i.e. zeolites, ceramic, silica, glass) [43].

Enzyme nano-carriers (ENCs) represents a new trend in immobilization techniques and is based on the use of nanoparticles as enzymes support. Virus particles (VPs), are highly ordered nanostructures composed of viral genetic material (either DNA or RNA) embedded inside the capsid which is composed by several copies of virus capsid proteins (CPs) [44]. The main advantages of the employment of VPs resides in their i) nanometric size range, ii) propensity to self-assembly, iii) stability and robustness iv) bioavailability and v) easy production in large amount. Interestingly, CPs can be modified by either genetic or chemical modification to achieve an efficient enzyme immobilization. So far, studies on the use of VPs as nano-scaffolds have been devoted to enzyme selection, enzyme confinement, phage therapy and raw material processing. For instance, a tandem gene construct obtained by fusion of the T7 capsid gene with two ORFs encoding for an  $\alpha$ -amylase from *Bacillus licheniformis* and a xylanase A from *Bacillus halodurans*, was obtained [45].

The high-scale production of VPs can be easily achieved through culturing bacterial and/or archaeal cells infected with bacteriophages and viruses, respectively. Since, *Archaea* thrive in extreme environments, it is expected that archaeal VPs exhibit even more resistance to chemical-physical conditions than the bacterial counterparts. In this PhD thesis, an induction protocol for overproducing thermophilic virus particles (VPs) from the archaeon *Sulfolobus solfataricus* (InF1-SSV1) has been set up (paper 2-III)

with the final aim to exploit them as natural occurring nanoparticles for enzymes immobilization.

### **3. Biorefinery and Bioeconomy**

In biorefinery biomass can be processed to produce value added product, such as biofuels (mainly ethanol, butanol and biodiesel) and bio-based chemicals (lactic acid, itaconic acid, 1,3-propanediol, etc.) [46].

The processes to convert biomass feedstock into bio-products may be classified: “first generation” uses crops; “second generation” uses lignocellulosic residues from agro-industrial residues; and “third generation” is based on the use of algae as biomass [47]. All biorefinery generations are playing an important role in the future development of a bio-based economy. Bioeconomy is an important component of the EU economy and it aims at establishing a connection between functional bioeconomy and synthetic biology for the replacement of fossil fuels [46]. In this context, the outstanding relevance of the bioeconomy is increasing influencing both academia and industry. Specifically, the objective of “Circular economy” is to create an industrial system, in which business creates competitive advantages [48]. Currently, the global renewable biochemicals market is growing in size and importance, and the production of eco-friendly alternatives to petrochemical products, such as plastic polymers are increasing. Fossil-derived plastics (petroplastics) have posed serious problems, due to their extremely long persistence in the environment. Unlike petroplastics, the biodegradable polylactic acid (PLA) is obtained from microbial fermentation and chemical polymerization of the D- and L-lactic acids. Bioplastics made from PLA show similar physical properties as those produced from petroleum-derived polyethylene terephthalate (PET) polymers. Interestingly, PLA-derived bioplastics are used extensively in biomedical applications, such as sutures, dialysis devices, drug capsules, and evaluated as a matrix for tissue engineering. In this PhD-thesis the new thermophilic and cellulolytic *Bacillus coagulans* strain MA-13 was demonstrated a great ability to ferment lignocellulose-derived sugars to lactic acid (paper 3-I and manuscript 3-II).

#### **3.1 Lignocellulosic biomasses**

The feedstocks are the most promising low-cost source alternative to the functioning of modern industrial societies [49]. In addition, forestry, agricultural and agro-industrial biomasses are generated every day in large amount. They are the non-edible portions of the plant, and therefore, they do not interfere with food supplies. All feedstocks produced from available atmospheric CO<sub>2</sub>, water and sunlight through biological photosynthesis are the suitable candidates to fix the production rate of CO<sub>2</sub> to its consumption rate. In particular, through the process of photosynthesis, chlorophyll captures the sun's energy by converting carbon dioxide from the air and water from the ground into carbohydrates, i.e., complex compounds composed of carbon, hydrogen, and oxygen. When carbohydrates are burned, they turn back into carbon dioxide and water, releasing the sun's energy captured [50]. In this way, biomass functions as a sort of natural battery for storing solar energy. Recently, the renewable biomasses have gained increasing research interests, as sustainable source of organic carbon in earth, for the production of fuels and fine chemicals with net zero carbon emission [49].

In general, the lignocellulose biomass composition highly depends on its deriving source (i.e. hardwood, softwood, or grasses). A typical lignocellulosic biomass is composed of cellulose (35-50%), hemicellulose (26-35%) and lignin (14-21%), as well as other minor components (Fig. 4) [49].

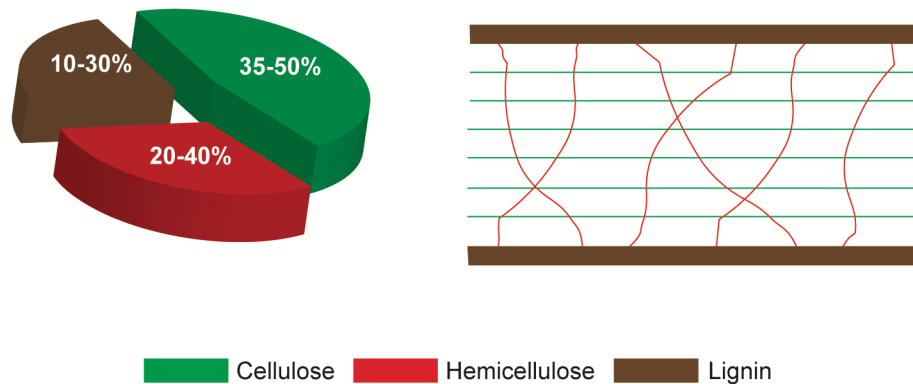


**Figure 4.** Schematic representation of lignocellulosic biomasses.

### 3.2 Bioconversion of lignocellulose

The biological process commonly used for the bioconversion of lignocellulose biomass into value added-products involves: i) pretreatment; ii) saccharification; iii) fermentation of hexose and/or pentose sugars; iv) product purification.

#### 3.2.1 Pre-treatment

The processes that are currently adopted to disrupt the fibrous matrix and to remove lignin is named pretreatment. Several techniques have been explored for removing lignin, such as dilute acid hydrolysis, ammonia fiber expansion (AFEX) and steam explosion being the most studied [14]. The dilute sulfuric acid pretreatment is performed between 140°- 200°C and renders the cellulose more accessible to saccharifying enzymes. This is done to liberate lignin, hemicellulose, and other compounds and makes the cellulosic polymers available for enzymatic degradation [51]. The efficiency of this first process depends on a number of factors, such as hemicellulose composition, biomass density, the presence of non-sugar components (lignin, acid neutralizing ash, and acetyl and other carboxylic acid groups); plant cell structure (including the types of cells or ratios of primary and secondary cell walls) [52].

Pretreatment approach based on alkaline explosive decompression and organic solvent extractions have been successfully applied [53]. This alkaline process, known as ammonia fiber expansion (AFEX), decrystallises the cellulose, hydrolyses hemicellulose, removes and depolymerizes lignin, thereby significantly increasing the rate of enzymatic hydrolysis.

Steam Explosion is one of the most common pretreatment methods and together with the enzymatic saccharification is a promising approach to enhance the amount of fermentable sugars. This pretreatment requires minimum, or in some cases, no chemical addition. Usually, temperatures between 160° and 240°C and pressure between 0.7 and 4.8 MPa are employed [51].

Besides generating suitable substrates for conversion to bio-products, several toxic compounds are produced during the pretreatment [54], that are classified in three classes: furaldehydes (e.g., furfural and 5-hydroxymethylfurfural), weak acids

(e.g., acetic acid, formic acid, and levulinic acid) and phenolics (e.g., vanillin, syringaldehyde, and coniferyl aldehyde) [55]. These components inhibit the growth of the fermenting organisms, reducing the rate of fermentation product and in some cases, the overall yield. To avoid additional process costs of detoxification an alternative approach is to exploit the natural and/or induced tolerance of fermenting microorganisms (bacteria and yeasts) in order to develop a feasible and economic bio-process [56]. In this context, the isolated strain *Bacillus coagulans* MA-13 was characterized not only for the production of lactic acid, as eco-friendly chemicals and for its tolerance towards inhibitors (paper 3-I).

### 3.2.2 Saccharification

Once the cell-wall microfibrils have been compromised by pre-treatments, the carbohydrates are released, becoming accessible to the enzymatic saccharification (hydrolysis) [12]. Multiple factors affecting the process efficiency such as pH, time, temperature as well as the enzyme activity [57]. Traditionally, enzymes are added after cooling down the pre-treated material, thus performing their catalytic activity at lower temperature (50°C) [58]. During the enzymatic saccharification, the acid-catalyzed dehydration of the sugar intermediates into furfural-type components appears negligible, compared to the acid hydrolysis. Although, the enzymatic saccharification is a promising alternative for hydrolysis of lignocellulosic substrates, the high cost of enzyme preparation hinders its applicability on industrial scale [12].

### 3.2.3 Fermentation

There are mainly four approaches to convert complex biomass into bio-products: i) SHF; ii) SSF; iii) SSCF and iv) CBP (Fig. 5).

#### 3.2.3.1 SHF

SHF is a two-step process, in which hydrolysis and fermentation are performed separately (Fig. 5) and conducted under their optimal conditions. The main bottleneck is the accumulation of glucose in the saccharification step, that inhibits the further cellulase activity.

#### 3.2.3.2 SSF and SSCF

In order to overcome the inhibitory effect of sugars on cellulase activity, in the SSF and SSCF, saccharification and fermentation are carried out simultaneously (Fig. 5). SSF includes only hexose fermentation [59], while the SSCF is based on the co-fermentation of pentose and hexose sugars [60]. Both processes are advantageous, since the sugar consumption is rapid, the risk of contamination by other organism is reduced, and the low level of substrate does not influence the fermenting organism and the enzymes [60]. The main issue is the incompatibility between the optimal temperature for hydrolysis (50°C) and fermentation (28°-37°C). On the other hand, the exploitation of the moderate fermenting-thermophiles could be advantageous to increase the efficiency of enzymes activity or the final production yield [61]. Therefore, the recently isolated thermophilic strain of *Bacillus coagulans* MA-13 was tested for production of L-lactic acid in simultaneous saccharification and fermentation (SSF) of wheat straw biomass (manuscript 3-II).

#### 3.2.3.3 CBP

CBP applies in one step enzyme production, saccharification and fermentation [62]. One organism, in one vessel, carries out the whole process (Fig. 5). The choice of this

microbial counterpart is very crucial to obtain a great amount of released sugars and a good fermentation performance [62]. Therefore, several microorganisms have been metabolically modified and are classified in CBP I and CBPII [35]. The former microorganisms are able to degrade polymeric substrates and have been engineered to produce fermentation products. Conversely, when the microorganisms are engineered to add and/or improve the ability to degrade the biomass, belong to CBP II. Therefore, to accomplish this goal the synthetic biology can provide new tools to rewire the desired features for the production of economically viable bio-products and -fuels [35].

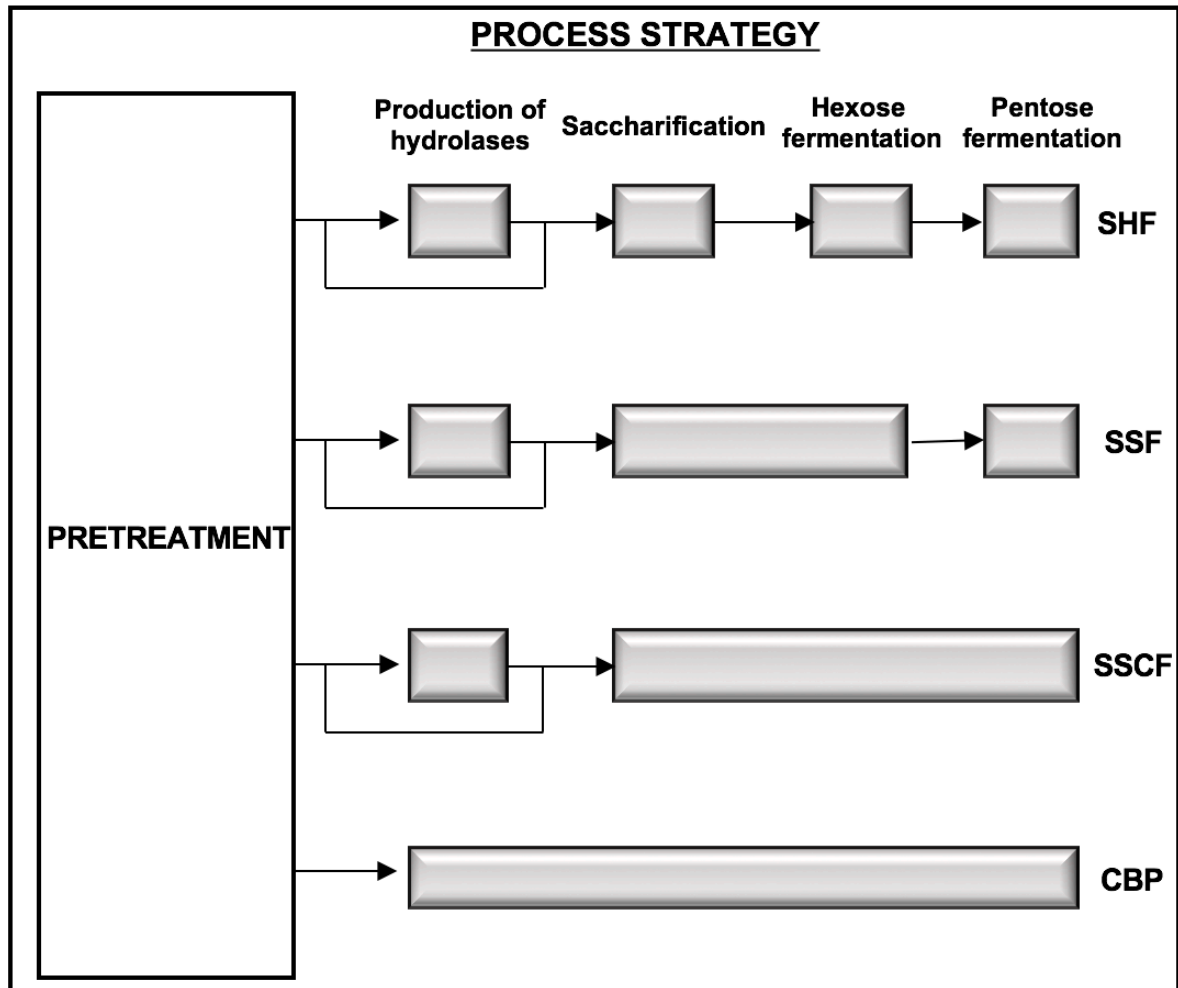


**Figure 5.** The flowchart of the process strategies to produce value-added products from lignocellulosic feedstocks. SHF: separate hydrolysis and fermentation. SSF: simultaneous saccharification and fermentation. SSCF: simultaneous saccharification and co-fermentation. CBP: consolidated bioprocess. Illustration adapted from [63]

#### 4. Aim of the work

The overall aim of this project has been focused on the development of thermophilic biorefinery, based on the use of renewable, cheap and readily available biomasses for the production of a wide variety of value-added products. Thermophilic biorefineries are based on the use of microbial cells and their enzymes, being these latter ones operationally stable at high temperature. This PhD thesis highlights the potential applications of thermophiles and their carbohydrate-active enzymes for the conversion of raw materials into value-added products.

Chapter II describes the characterization of thermophilic hemicellulolytic enzymes as well as the setting up of an induction protocol for the production of archaeal VPs, to be used as carrier for the enzymes immobilization.

Two papers and one submitted manuscript are included in this chapter:

1. *Thermus thermophilus* as source of thermozymes for biotechnological applications: homologous expression and biochemical characterization of an  $\alpha$ -galactosidase (paper 2-I);
2. A thermophilic enzymatic cocktail for galactomannans degradation (manuscript 2-II);
3. A standardized protocol for the UV induction of *Sulfolobus* spindle-shaped virus 1 (paper 2-III).

Chapter III deals with the exploitation of a new strain of *Bacillus coagulans* for lactic acid production in simultaneous saccharification and fermentation process of lignocellulosic biomass.

One paper and one manuscript in preparation are included in this chapter:

1. *Bacillus coagulans* MA-13: a promising thermophilic and cellulolytic strain for the production of lactic acid in lignocellulosic hydrolysate (paper 3-I);
2. Seed culture pre-adaptation improves lactic acid production of *Bacillus coagulans* MA-13 in Simultaneous Saccharification and Fermentation (manuscript 3-II).



## 5. References

1. Oren A: **Molecular ecology of extremely halophilic Archaea and Bacteria.** *FEMS Microbiology Ecology* 2002, **39**:1-7.
2. Strazzulli A, Iacono R, Giglio R, Moracci M, Cobucci-Ponzano B: **Metagenomics of Hyperthermophilic Environments: Biodiversity and Biotechnology.** In *Microbial Ecology of Extreme Environments*. Springer; 2017: 103-135.
3. Elleuche S, Schäfers C, Blank S, Schröder C, Antranikian G: **Exploration of extremophiles for high temperature biotechnological processes.** *Curr Opin Microbiol* 2015, **25**:113-119.
4. Chang C-J, Lee C-C, Chan Y-T, Trudeau DL, Wu M-H, Tsai C-H, Yu S-M, Ho T-HD, Wang AH-J, Hsiao C-D: **Exploring the Mechanism Responsible for Cellulase Thermostability by Structure-Guided Recombination.** *PloS one* 2016, **11**:e0147485.
5. Hoeger IC, Nair SS, Ragauskas AJ, Deng Y, Rojas OJ, Zhu J: **Mechanical deconstruction of lignocellulose cell walls and their enzymatic saccharification.** *Cellulose* 2013, **20**:807-818.
6. A Linares-Pasten J, Andersson M, N Karlsson E: **Thermostable glycoside hydrolases in biorefinery technologies.** *Current Biotechnology* 2014, **3**:26-44.
7. Aulitto M, Fusco S, Fiorentino G, Limauro D, Pedone E, Bartolucci S, Contursi P: **Thermus thermophilus as source of thermozymes for biotechnological applications: homologous expression and biochemical characterization of an  $\alpha$ -galactosidase.** *Microbial Cell Factories* 2017, **16**:28.
8. Cantarel BL, Coutinho PM, Rancurel C, Bernard T, Lombard V, Henrissat B: **The Carbohydrate-Active EnZymes database (CAZy): an expert resource for glycogenomics.** *Nucleic acids research* 2008, **37**:D233-D238.
9. Davies G, Henrissat B: **Structures and mechanisms of glycosyl hydrolases.** *Structure* 1995, **3**:853-859.
10. Sharma A, Satyanarayana T: **Cloning and expression of acidstable, high maltose-forming,  $\text{Ca}^{2+}$ -independent  $[\alpha]$ -amylase from an acidophile *Bacillus acidicola* and its applicability in starch hydrolysis.** *Extremophiles* 2012, **16**:515.
11. Serour E, Antranikian G: **Novel thermoactive glucoamylases from the thermoacidophilic Archaea *Thermoplasma acidophilum*, *Picrophilus torridus* and *Picrophilus oshimae*.** *Antonie Van Leeuwenhoek* 2002, **81**:73-83.
12. Han T, Zeng F, Li Z, Liu L, Wei M, Guan Q, Liang X, Peng Z, Liu M, Qin J: **Biochemical characterization of a recombinant pullulanase from *Thermococcus kodakarensis* KOD1.** *Letters in applied microbiology* 2013, **57**:336-343.
13. Cragg SM, Beckham GT, Bruce NC, Bugg TD, Distel DL, Dupree P, Etxabe AG, Goodell BS, Jellison J, McGeehan JE: **Lignocellulose degradation mechanisms across the Tree of Life.** *Current Opinion in Chemical Biology* 2015, **29**:108-119.
14. Gao D, Chundawat SP, Krishnan C, Balan V, Dale BE: **Mixture optimization of six core glycosyl hydrolases for maximizing saccharification of ammonia fiber expansion (AFEX) pretreated corn stover.** *Bioresource technology* 2010, **101**:2770-2781.
15. Brunecky R, Alahuhta M, Xu Q, Donohoe BS, Crowley MF, Kataeva IA, Yang S-J, Resch MG, Adams MW, Lunin VV: **Revealing nature's cellulase diversity: the digestion mechanism of *Caldicellulosiruptor bescii* CelA.** *Science* 2013, **342**:1513-1516.

16. Pérez J, Munoz-Dorado J, de la Rubia T, Martinez J: **Biodegradation and biological treatments of cellulose, hemicellulose and lignin: an overview.** *International Microbiology* 2002, **5**:53-63.
17. Saha BC: **Hemicellulose bioconversion.** *J Ind Microbiol Biotechnol* 2003, **30**:279-291.
18. Malherbe AR, Rose SH, Viljoen-Bloom M, van Zyl WH: **Expression and evaluation of enzymes required for the hydrolysis of galactomannan.** *J Ind Microbiol Biotechnol* 2014, **41**:1201-1209.
19. Zhang Y-HP, Himmel ME, Mielenz JR: **Outlook for cellulase improvement: screening and selection strategies.** *Biotechnology advances* 2006, **24**:452-481.
20. Rosano GL, Ceccarelli EA: **Recombinant protein expression in Escherichia coli: advances and challenges.** *Front Microbiol* 2014, **5**:172.
21. Henne A, Brüggemann H, Raasch C, Wiezer A, Hartsch T, Liesegang H, Johann A, Lienard T, Gohl O, Martinez-Arias R, et al: **The genome sequence of the extreme thermophile Thermus thermophilus.** *Nat Biotechnol* 2004, **22**:547-553.
22. Brüggemann H, Chen C: **Comparative genomics of Thermus thermophilus: plasticity of the megaplasmid and its contribution to a thermophilic lifestyle.** *Journal of biotechnology* 2006, **124**:654-661.
23. Leis B, Angelov A, Mientus M, Li H, Pham VT, Lauinger B, Bongen P, Pietruszka J, Gonçalves LG, Santos H: **Identification of novel esterase-active enzymes from hot environments by use of the host bacterium Thermus thermophilus.** *Frontiers in microbiology* 2015, **6**.
24. Ramírez-Arcos S, Fernández-Herrero LA, Berenguer J: **A thermophilic nitrate reductase is responsible for the strain specific anaerobic growth of Thermus thermophilus HB8.** *Biochimica et Biophysica Acta (BBA)-Gene Structure and Expression* 1998, **1396**:215-227.
25. Hidalgo A, Betancor L, Moreno R, Zafrá O, Cava F, Fernández-Lafuente R, Guisán JM, Berenguer J: **Thermus thermophilus as a cell factory for the production of a thermophilic Mn-dependent catalase which fails to be synthesized in an active form in Escherichia coli.** *Appl Environ Microbiol* 2004, **70**:3839-3844.
26. Moreno R, Haro A, Castellanos A, Berenguer J: **High-level overproduction of His-tagged Tth DNA polymerase in Thermus thermophilus.** *Appl Environ Microbiol* 2005, **71**:591-593.
27. Irfan M, Safdar A, Syed Q, Nadeem M: **Isolation and screening of cellulolytic bacteria from soil and optimization of cellulase production and activity.** *Turkish Journal of Biochemistry* 2012, **37**:287-293.
28. Krogh KB, Mørkeberg A, Jørgensen H, Frisvad JC, Olsson L: **Screening genus Penicillium for producers of cellulolytic and xylanolytic enzymes.** *Applied biochemistry and biotechnology* 2004, **114**:389-401.
29. Gao J, Weng H, Zhu D, Yuan M, Guan F, Xi Y: **Production and characterization of cellulolytic enzymes from the thermoacidophilic fungal Aspergillus terreus M11 under solid-state cultivation of corn stover.** *Bioresource Technology* 2008, **99**:7623-7629.
30. Rosgaard L, Pedersen S, Langston J, Akerhielm D, Cherry JR, Meyer AS: **Evaluation of minimal Trichoderma reesei cellulase mixtures on differently pretreated Barley straw substrates.** *Biotechnol Prog* 2007, **23**:1270-1276.
31. Niehaus F, Bertoldo C, Kähler M, Antranikian G: **Extremophiles as a source of novel enzymes for industrial application.** *Applied microbiology and biotechnology* 1999, **51**:711-729.

32. Amore A, Pepe O, Ventorino V, Birolo L, Giangrande C, Faraco V: **Industrial waste based compost as a source of novel cellulolytic strains and enzymes.** *FEMS Microbiology letters* 2013, **339**:93-101.
33. Chhabra SR, Kelly RM: **Biochemical characterization of *Thermotoga maritima* endoglucanase Cel74 with and without a carbohydrate binding module (CBM).** *FEBS letters* 2002, **531**:375-380.
34. Lynd LR, Weimer PJ, Van Zyl WH, Pretorius IS: **Microbial cellulose utilization: fundamentals and biotechnology.** *Microbiology and molecular biology reviews* 2002, **66**:506-577.
35. Schwarz W: **The cellulosome and cellulose degradation by anaerobic bacteria.** *Applied microbiology and biotechnology* 2001, **56**:634-649.
36. Haitjema CH, Solomon KV, Henske JK, Theodorou MK, O'Malley MA: **Anaerobic gut fungi: advances in isolation, culture, and cellulolytic enzyme discovery for biofuel production.** *Biotechnology and bioengineering* 2014, **111**:1471-1482.
37. Kostylev M, Wilson D: **Synergistic interactions in cellulose hydrolysis.** *Biofuels* 2012, **3**:61-70.
38. Sheldon RA: **Enzyme immobilization: the quest for optimum performance.** *Advanced Synthesis & Catalysis* 2007, **349**:1289-1307.
39. Bornscheuer UT: **Immobilizing enzymes: how to create more suitable biocatalysts.** *Angewandte Chemie International Edition* 2003, **42**:3336-3337.
40. Fu J, Reinhold J, Woodbury NW: **Peptide-modified surfaces for enzyme immobilization.** *PLoS One* 2011, **6**:e18692.
41. Sardar M, Roy I, Gupta MN: **Simultaneous purification and immobilization of *Aspergillus niger* xylanase on the reversibly soluble polymer Eudragit TM L-100.** *Enzyme and Microbial Technology* 2000, **27**:672-679.
42. Datta S, Christena LR, Rajaram YRS: **Enzyme immobilization: an overview on techniques and support materials.** *3 Biotech* 2013, **3**:1-9.
43. Scarlat N, Dallemand J-F, Monforti-Ferrario F, Nita V: **The role of biomass and bioenergy in a future bioeconomy: policies and facts.** *Environmental Development* 2015, **15**:3-34.
44. Moncada J, Tamayo JA, Cardona CA: **Integrating first, second, and third generation biorefineries: incorporating microalgae into the sugarcane biorefinery.** *Chemical Engineering Science* 2014, **118**:126-140.
45. Genovese A, Acquaye AA, Figueroa A, Koh SL: **Sustainable supply chain management and the transition towards a circular economy: Evidence and some applications.** *Omega* 2017, **66**:344-357.
46. Anwar Z, Gulfranz M, Irshad M: **Agro-industrial lignocellulosic biomass a key to unlock the future bio-energy: a brief review.** *Journal of radiation research and applied sciences* 2014, **7**:163-173.
47. Somerville C, Youngs H, Taylor C, Davis SC, Long SP: **Feedstocks for lignocellulosic biofuels.** *science* 2010, **329**:790-792.
48. Hu F, Ragauskas A: **Pretreatment and lignocellulosic chemistry.** *Bioenergy Research* 2012, **5**:1043-1066.
49. Alvira P, Tomás-Pejó E, Ballesteros M, Negro M: **Pretreatment technologies for an efficient bioethanol production process based on enzymatic hydrolysis: a review.** *Bioresource technology* 2010, **101**:4851-4861.
50. Rocha GdM, Gonçalves AR, Oliveira B, Olivares E, Rossell C: **Steam explosion pretreatment reproduction and alkaline delignification reactions**

- performed on a pilot scale with sugarcane bagasse for bioethanol production. *Industrial Crops and Products* 2012, **35**:274-279.
51. Jönsson LJ, Martín C: **Pretreatment of lignocellulose: Formation of inhibitory by-products and strategies for minimizing their effects.** *Bioresour Technol* 2016, **199**:103-112.
  52. Parawira W, Tekere M: **Biotechnological strategies to overcome inhibitors in lignocellulose hydrolysates for ethanol production: review.** *Critical reviews in biotechnology* 2011, **31**:20-31.
  53. Jönsson LJ, Alriksson B, Nilvebrant N-O: **Bioconversion of lignocellulose: inhibitors and detoxification.** *Biotechnology for Biofuels* 2013, **6**:1.
  54. Keshk SM: **Cellulase Application in Enzymatic Hydrolysis of Biomass.** 2016.
  55. Öhgren K, Bura R, Lesnicki G, Saddler J, Zacchi G: **A comparison between simultaneous saccharification and fermentation and separate hydrolysis and fermentation using steam-pretreated corn stover.** *Process Biochemistry* 2007, **42**:834-839.
  56. Olofsson K, Bertilsson M, Lidén G: **A short review on SSF—an interesting process option for ethanol production from lignocellulosic feedstocks.** *Biotechnology for biofuels* 2008, **1**:7.
  57. Morales-Rodriguez R, Gernaey KV, Meyer AS, Sin G: **A mathematical model for simultaneous saccharification and co-fermentation (SSCF) of C6 and C5 sugars.** *Chinese Journal of Chemical Engineering* 2011, **19**:185-191.
  58. Chang T, Yao S: **Thermophilic, lignocellulolytic bacteria for ethanol production: current state and perspectives.** *Applied microbiology and biotechnology* 2011, **92**:13 .
  59. Yamada R, Hasunuma T, Kondo A: **Endowing non-cellulolytic microorganisms with cellulolytic activity aiming for consolidated bioprocessing.** *Biotechnology advances* 2013, **31**:754-763.





# CHAPTER II





## Chapter II:

### Thermophilic GHs: discovery, characterization and immobilization

The load of enzyme cost to the economics of second generation biorefinery is the main bottleneck of the entire process. Considering that the second most abundant biopolymer on the earth is the hemicellulose, one of the most urgent request is to achieve its complete hydrolysis and conversion. For this purpose the concerted action of different hydrolytic enzymes: beta-glucosidases (EC 3.2.1.21), endo-mannanases (EC 3.2.1.78), mannosidases (EC 3.2.1.25) and  $\alpha$ -galactosidases (EC 3.2.1.22) is required.

This chapter deals with results concerning: i) the characterization of new hemicellulolytic enzymes and ii) the production of archeal VPs for the immobilization and recirculation of enzymes. In the section 2-I the paper “***Thermus thermophilus* as source of thermozymes for biotechnological applications: homologous expression and biochemical characterization of an  $\alpha$ -galactosidase**” is focused on *TtGalA* the most thermoactive and thermostable  $\alpha$ -galactosidases discovered so far, thus pointing to the exploitation of *Thermus thermophilus* as a potential cell factory for the production of thermostable enzymes.

The manuscript 2-II “**A thermophilic enzymatic cocktail for galactomannans degradation**”, is based on the study of the synergy between *TtGalA* and *DturCelB*, i.e. a  $\beta$ -mannanase from *Dictyogloumus turgidum*. In this study it was demonstrated the heterosynergistic activity on galactomannan substrates of these two recombinant thermophilic enzymes, using simultaneous and sequential assays. The results highlighted points to the use of thermophilic enzymatic cocktails to pre-hydrolyze the biomass right after the pretreatment, prior to the conventional saccharification step.

Additionally, to further reduce the cost of the entire process, more tolerant and stable enzymes are needed to maintain optimal catalytic activity under inhibitory conditions, such as high temperature, low pH, presence of inhibitors. In this regard, a possible strategy is the immobilization of enzymes onto nano-carriers. Since our group has an extensive experience in the study of thermophilic viruses, we attempt at exploiting them as carriers for enzyme immobilization. For this purpose, a large scale production of VPs is required. The paper 2-III “**A standardized protocol for the UV induction of *Sulfolobus* spindle-shaped virus 1**” describes the development of a new UV irradiation method to overproduce SSV1 VPs representing a robust support suitable to withstand the extreme temperature, acidity/alkalinity, pressure and salinity typical of industrial processes.

## RESEARCH

## Open Access



# *Thermus thermophilus* as source of thermozymes for biotechnological applications: homologous expression and biochemical characterization of an $\alpha$ -galactosidase

Martina Aulitto<sup>1</sup>, Salvatore Fusco<sup>2</sup>, Gabriella Fiorentino<sup>1</sup>, Danila Limauro<sup>1</sup>, Emilia Pedone<sup>1</sup>, Simonetta Bartolucci<sup>1</sup> and Patrizia Contursi<sup>1\*</sup>

## Abstract

**Background:** The genus *Thermus*, which has been considered for a long time as a fruitful source of biotechnological relevant enzymes, has emerged more recently as suitable host to overproduce thermozymes. Among these,  $\alpha$ -galactosidases are widely used in several industrial bioprocesses that require high working temperatures and for which thermostable variants offer considerable advantages over their thermolabile counterparts.

**Results:** *Thermus thermophilus* HB27 strain was used for the homologous expression of the TTP0072 gene encoding for an  $\alpha$ -galactosidase (TtGalA). Interestingly, a soluble and active histidine-tagged enzyme was produced in larger amounts (5 mg/L) in this thermophilic host than in *Escherichia coli* (0.5 mg/L). The purified recombinant enzyme showed an optimal activity at 90 °C and retained more than 40% of activity over a broad range of pH (from 5 to 8).

**Conclusions:** TtGalA is among the most thermoactive and thermostable  $\alpha$ -galactosidases discovered so far, thus pointing to *T. thermophilus* as cell factory for the recombinant production of biocatalysts active at temperature values over 90 °C.

**Keywords:**  $\alpha$ -Galactosidase, *Thermus thermophilus*, Thermozymes, Recombinant expression, Thermostability

## Background

After cellulose, the second most abundant biopolymer on earth is hemicellulose, an heterogeneous polymer of pentoses (xylose and arabinose) and hexoses (glucose, galactose, mannose) [1]. Among these, mannans comprise linear or branched polymers derived from sugars such as D-mannose, D-galactose and D-glucose. Moreover, they represent the major source of secondary cell wall found in conifers (softwood) and leguminosae [2]. Based on their sugar composition, mannans are classified in four

subfamilies: i.e. mannans, glucomannans, galactomannans and galactoglucomannans. The concerted action of different hydrolytic enzymes such as  $\beta$ -glucosidases (EC 3.2.1.21), endo-mannanases (EC 3.2.1.78), mannosidases (EC 3.2.1.25) and  $\alpha$ -galactosidases (EC 3.2.1.22) is needed to achieve the degradation of galactoglucomannans, the most complex mannans subfamily [3].

$\alpha$ -Galactosidases ( $\alpha$ -D-galactoside galactohydrolase EC 3.2.1.22) are exoglycosidases that catalyse the cleavage of the terminal non-reducing  $\alpha$ -1,6-linked galactose residues present in different galactose-containing oligo- and polysaccharides.  $\alpha$ -Galactosidases are widely distributed in microorganisms, plants, animals and mammals, including humans [4]. The localization of  $\alpha$ -galactosidases can be cytoplasmic (e.g. *Escherichia*

\*Correspondence: contursi@unina.it

<sup>1</sup> Dipartimento di Biologia, Università degli Studi di Napoli Federico II, Complesso Universitario Monte S. Angelo, Via Cinthia, 80126 Naples, Italy  
Full list of author information is available at the end of the article



© The Author(s) 2017. This article is distributed under the terms of the Creative Commons Attribution 4.0 International License (<http://creativecommons.org/licenses/by/4.0/>), which permits unrestricted use, distribution, and reproduction in any medium, provided you give appropriate credit to the original author(s) and the source, provide a link to the Creative Commons license, and indicate if changes were made. The Creative Commons Public Domain Dedication waiver (<http://creativecommons.org/publicdomain/zero/1.0/>) applies to the data made available in this article, unless otherwise stated.

*coli*), lysosomal (e.g. *Homo sapiens*) or extracellular (e.g. yeast) [5, 6].

$\alpha$ -Galactosidases have a great potential in both biotechnological and medical applications. For instance, these enzymes are used for the treatment of Fabry's disease [7], in xenotransplantation [8] and in blood group transformation for safety transfusion [9]. Furthermore,  $\alpha$ -galactosidases offer a promising solution for the degradation of raffinose in beet sugar industry [10], pulp and paper manufacturing [11] as well as in soy food [12] and animal feed processing [13].

The interest towards enzymes hydrolysing hemicellulose, such as  $\alpha$ -galactosidases, has particularly increased in recent years. Indeed, they are extensively used in synergic combination with cellulases [14] for the production of bioethanol from lignocellulose [15]. In this regard, it is noteworthy that the pretreatment of raw lignocellulosic material requires elevated temperatures; therefore, thermostable and thermoactive enzymes are suitable for this purpose [16], since they can withstand high temperature, extreme pH and pressure, as well as the presence of some inhibitors, including toxic metals. Furthermore, as catalysts, thermostable enzymes might provide additional advantages, since higher temperatures often promote: (1) better enzyme penetration, (2) cell wall disorganisation of the raw materials, (3) increase of the substrate solubility and (4) reduction of contamination. Over all, these features may improve the global yield of the process [17].

In recent years, the thermophilic microorganism *T. thermophilus* has emerged as a rich source of polymer-degrading enzymes (e.g.  $\alpha$ -amylases, xylanases, esterases, lipases, proteases and pullulanases). Indeed, this thermophilic bacterium is able to grow on different organic sources such as various proteinaceous and carbohydrate substrates [18].

Although *E. coli* has been successfully employed to produce thermophilic recombinant proteins/enzymes [19–24], in some cases their expression level can be too low to perform functional and structural characterization as well as to exploit their biotechnological potential [25–27]. For this reason, efficient and reliable “hot” expression systems are needed.

Some genetic systems for both archaeal and bacterial thermophilic microorganisms have been designed [28–32]. However, the amount of the recombinant proteins is in general lower than that achieved through conventional mesophilic expression systems [33].

A thermophilic expression system for *T. thermophilus* HB27 was previously developed and proved to be suitable to achieve high expression levels of heterologous proteins [34, 35]. Therefore, we have used this system to produce a novel  $\alpha$ -galactosidase (named *TtGalA*) from *T. thermophilus* HB27. In particular, the coding gene was

over-expressed in the native host and the recombinant enzyme was purified and characterized. *TtGalA* exhibits an optimal hydrolytic activity at high temperature (90 °C and pH 6.0), a good catalytic efficiency ( $k_{\text{cat}} = 709.7/\text{s}$ ) and a significant thermostability (30 h at 70 °C), which are all interesting features for industrial applications.

## Results and discussion

The genus *Thermus* comprises thermophilic and hyper-thermophilic bacteria [18], which represent genetic reservoirs of several thermozymes potentially useful for industrial bioprocesses at high temperature [36, 37]. This aspect, along with other intrinsic features such as the natural competence of many strains, high growth rates and biomass yields, make these thermophiles suitable models for the production of thermozymes [27, 38].

In this work we have used *T. thermophilus* HB27::*nar* as host for the homologous expression of a novel  $\alpha$ -galactosidase (*TtGalA*), one of the most thermoactive  $\alpha$ -galactosidases identified so far.

## Sequence analysis

An in-depth survey of the carbohydrate-active enzymes database CAZy (<http://www.cazy.org/>) was carried out to identify putative  $\alpha$ -galactosidases in the genome of *T. thermophilus* HB27. The only protein sequence retrieved is encoded by TTP0072 (Accession No. AAS82402) and shows high sequence identity with previously characterized  $\alpha$ -galactosidases from *Thermus* sp. strain T2 (75%; Accession No. BAA76597), *Thermus brockianus* (73%; Accession No. AF135398), *Thermotoga neapolitana* (36%; Accession No. AF011400), *Thermotoga maritima* (35%; Accession No. AJ001776), *Sulfolobus solfataricus* (39%; Accession No. Q97U94) and *H. sapiens* (23%; Accession No. CAA29232.1). In general, sequence identities among the analysed proteins fall into regions that are “signature” of the catalytic activity and/or of the structural properties of  $\alpha$ -galactosidases. A multiple alignment (Fig. 1a) revealed the presence of a consensus motif (FEVFQID<sub>193</sub>GW) in the TTP0072 translated sequence characteristic of  $\alpha$ -galactosidases. This is generally localised within the central region of bacterial enzymes (CAZy family GH36) or at the amino-terminal region of eukaryotic variants (CAZy family GH27). The presence of such a sequence points out to a common reaction mechanism and/or a similar substrate binding site [39]. Two aspartic residues i.e. D193–194 underlined in the above consensus sequence are followed by a cysteine or a glycine in the GH27 or GH36 members, respectively. Moreover, GH27 and GH36 families share another common feature, which is the presence of two additional aspartic acids involved in the acid–base catalytic mechanism (D301 and D355 in the protein from *T. thermophilus* HB27,



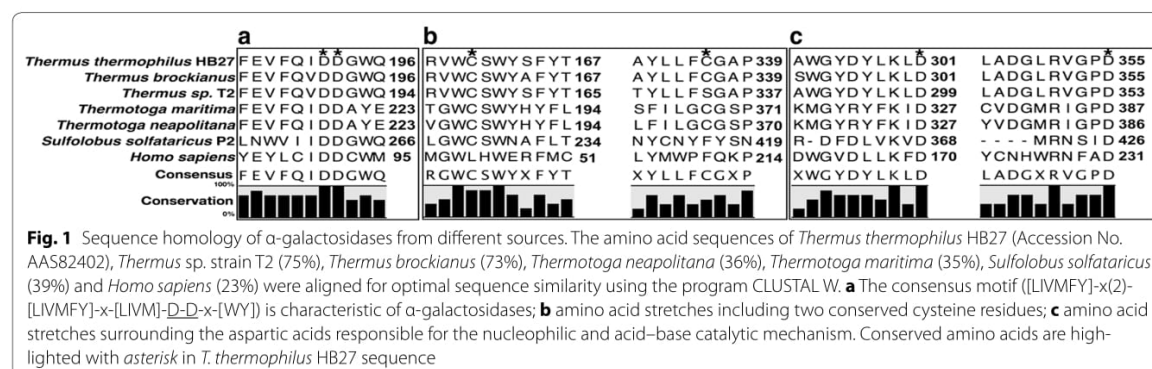


Fig. 1). At consensus level, whereas the motif including the catalytic nucleophile (D301) is fully conserved [K(Y/V/L/W)D], the A/B aspartic acid motif (D355) is more variable (RXXXD) (Fig. 1c). The co-presence of these two motifs defines the sub-group identity of GH36bt (where “bt” stands for bacterial thermophilic) [40] that also includes the thermophilic *Thermotoga* and *Thermus* α-galactosidases. Another characteristic of the GH36bt enzymes is the presence of two conserved cysteine residues (C161 and C336) (Fig. 1b) whose functional, structural and stabilization role is questioned.

The TTP0072 gene is located on the megaplasmid pTT27 upstream of a gene encoding for the galactose-1-phosphate uridylyltransferase gene (*galT*) and partially overlapping it. This operon-like structure closely resembles that found in other *Thermus* spp. [41], thus suggesting that their functional association might be important for galactose metabolism.

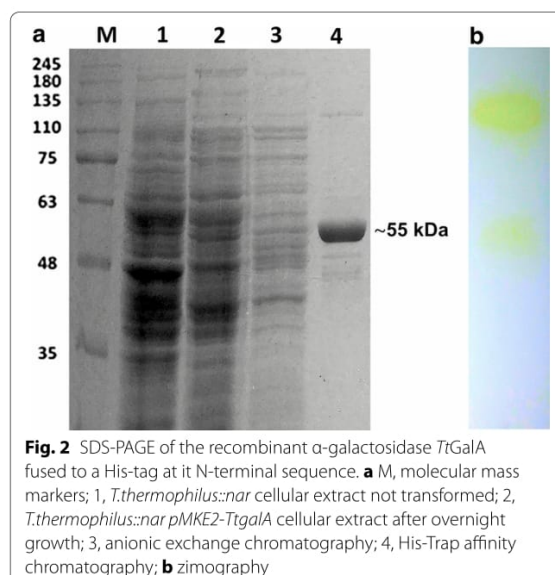
#### Cloning, expression and purification of *TtGalA*

The TTP0072 gene was cloned both in pET28(b) and in pMKE2 vectors to compare the expression levels of the N-terminal His-tagged enzymes *EcGalA* and *TtGalA* in the heterologous (*E. coli*) as well as in the homologous (*T. thermophilus* HB27::*nar*) hosts. In the case of *E. coli*, after a two-step purification procedure i.e. a thermal precipitation at 70 °C and an affinity chromatography through His-trap column, the final protein amount was very low (0.5 mg/L) (Fig. 2a) (Additional file 1: Table S1).

On the other hand, the enzyme *TtGalA* was expressed at higher level in *T. thermophilus* HB27::*nar* with a final amount of 5 mg/L (tenfold higher than *EcGalA*). Moreover, its specific activity (338 U/mg) was twofold higher than that of *EcGalA* (Additional file 1: Tables S1, S2). As previously observed, the over-production of soluble and active enzymes in mesophilic hosts is in some cases limited by: (1) differences in the codon usage [42]; (2) domain misfolding during protein synthesis at a

temperature (37 °C), which is far lower than the optimal growth temperature of the native host; (3) requirement of specific chaperone(s), cofactors, metals as well as genus- or species-specific post-translational modifications [27].

Given the significant higher amount of the soluble active enzyme produced by the thermophilic host, all the subsequent characterizations were performed on the *TtGalA* enzyme. The *nar* promoter, which drives the expression of the genes cloned in the pMKE2 vector, is induced by the combined action of nitrate and anoxia in the facultative anaerobic derivatives of *T. thermophilus* HB27 [34]. In our tested conditions, the biomass yield of the culture achieved under anaerobic growth was rather low, thus negatively affecting the amount of enzyme produced by the cells. To overcome



this limitation, the expression of *TtGalA* was carried out by growing *T. thermophilus* HB27::*nar* cells aerobically to reach an higher biomass yields. A total protein amount, similar to that of the cells cultured anaerobically, was achieved.

We resolved to set up a purification protocol from crude extracts of aerobically cultured cells based on anionic exchange followed by affinity His-trap chromatography. The recombinant enzyme purified to homogeneity displays a single band on SDS-PAGE with an estimated molecular weight (MW) of 55 kDa (Fig. 2a), which is consistent with the predicted MW of a his-tagged monomer (55.8 kDa). The identity of the recombinant *TtGalA* was verified by mass spectrometry (data not shown). It is important to note that the presence of the His-tag at the N-terminus of the recombinant enzyme ensures that the reported experiments are not affected by the presence of the endogenous enzyme. Furthermore, zymography revealed the presence of two bands with hydrolytic activity indicating that: (1) *TtGalA* adopts an oligomeric structure; (2) the oligomer is far more active than the monomer and (3) it is partially resistant to the denaturing conditions employed in the SDS-PAGE. These results prompted us to further investigate on the quaternary structure of *TtGalA* (Fig. 2b).

### Characteristics of the recombinant *TtGalA*

#### Determination of the molecular weight

To assess the quaternary structure, size-exclusion chromatography coupled with a triple-angle light scattering-QELS, was performed. This analysis showed a molecular weight of about 320 kDa  $\pm$  0.2% (RH = 8.1 nm  $\pm$  3%), thus indicating that *TtGalA* is a hexamer in solution. This oligomeric structure is in agreement with that of some previously characterised  $\alpha$ -galactosidases, which adopt dimeric (*Thermotoga maritima*) [43], trimeric (*Sulfolobus solfataricus*) [40], tetrameric (*T. Brockianus*) [39], octameric (*Thermus* sp. strain T2) structure [44]. This complex oligomeric state might correlate with the stability at higher temperature of *TtGalA*, as it was showed for *B. stearothermophilus*  $\alpha$ -galactosidases [45].

To understand if C161 and C336 had a structural role (Fig. 1b), the purified *TtGalA* was analysed on SDS-PAGE with and without a reducing agent. In the sample containing  $\beta$ -mercaptoethanol *TtGalA* is present mainly in monomeric form, while in the absence of this reducing agent the protein forms essentially high MW oligomers (data not shown). Indeed, the widespread stabilizing role of intracellular disulphide bonds in thermophiles and hyperthermophiles, has been already established as a strategy for protein stabilization [46].

### Catalytic and stability properties

*TtGalA* is able to hydrolyze *pNP*- $\alpha$ -D-galactopyranoside, but shows negligible activity on both *pNP*- $\alpha$ -substituted (D-glucose, D-mannose, L-rhamnose) and *pNP*- $\beta$ -substituted (D-galactose, D-glucose, and D-mannose) (Table 1). In particular, the enzyme has a barely detectable activity for  $\beta$  anomer of galactose (6.75 U/mg), which is 50-fold lower than activity over *pNP*- $\alpha$ -galactose (338.0 U/mg). Therefore, the kinetic enzymatic properties were determined, using *pNP*- $\alpha$ -D-galactopyranoside as substrate, at optimal pH and temperature (Table 2). *TtGalA* shows higher affinity towards its substrate ( $K_M$  = 0.69 mM) compared to  $\alpha$ -galactosidase from *Thermus* sp. strain T2 ( $K_M$  = 4.7 mM) [44] and *T. Brockianus* ( $K_M$  = 2.5 mM) [39]. However, comparing the kinetic parameters between the most known thermoactive ( $T_{opt}$  105 °C)  $\alpha$ -galactosidase of *Thermotoga neapolitana* (*TnGalA*) and the *TtGalA*, the  $K_M$  value is very similar. Interestingly, the different catalytic constant of 152.5/s towards 709.7/s, for *TnGalA* and *TtGalA* respectively [47] (Table 2) reflects a great efficiency of *TtGalA* on *pNP*- $\alpha$ -D-galactopyranoside substrate. This aspect constitutes an important criterion for employing different enzyme variants for industrial purposes. For instance, the high catalytic efficiency of *TtGalA* makes it a suitable candidate to enhance pulp bleachability in combination with other hemicellulases exhibiting different catalytic specificity [11].

*TtGalA* is among the most thermoactive and pH tolerant  $\alpha$ -galactosidases known so far. Indeed, when assayed at different pH and temperatures, it exhibited an optimal hydrolytic activity at 90 °C and pH 6.0 (Figs. 3, 4). As reported for an  $\alpha$ -galactosidase from

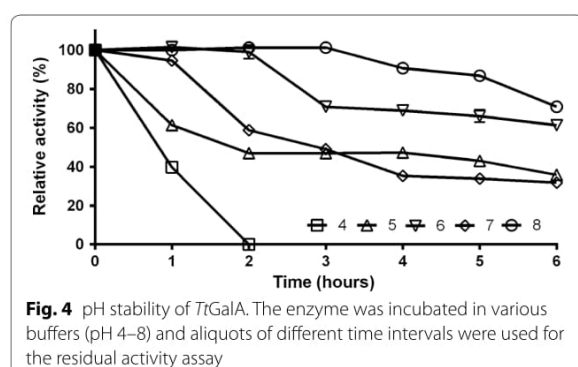
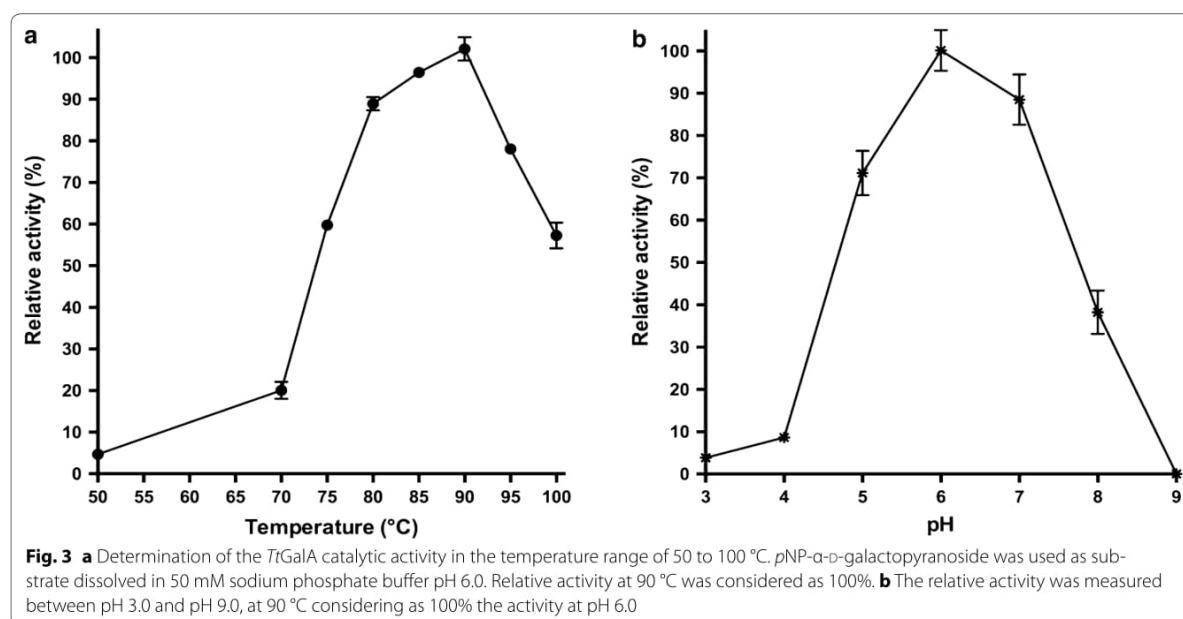
**Table 1 Substrate specificity of *TtGalA***

Substrate	Specific activity (U/mg)
<i>pNP</i> - $\alpha$ -D-mannose	0
<i>pNP</i> - $\beta$ -glucose	0.65
<i>pNP</i> - $\alpha$ -L-rhamnose	1.5
<i>pNP</i> - $\alpha$ -D-glucose	2.16
<i>pNP</i> - $\beta$ -galactose	6.75
<i>pNP</i> - $\beta$ -mannose	7.13
<i>pNP</i> - $\alpha$ -D-galactose	338.0

**Table 2 Kinetic parameters for the hydrolysis *pNPG* hydrolysis at 90 °C by the *TtGalA***

$K_M$ (mM)	$V_{max}$ (U/mg)	$k_{cat}$ (/s)	$k_{cat}/K_M$ (/s M)
0.69 $\pm$ 0.017	338.0 $\pm$ 7.9	709.7 $\pm$ 17.7	1.03 $\times 10^4 \pm 0.025 \times 10^4$





*Bacillus megaterium* VHM1 (optimal pH 7–7.5) [48], it is possible to foresee the employment of *TtGalA* for the removal of oligosaccharides from soya based foods, thus improving their nutritive value. Noteworthy, *TtGalA* might be a better catalyst for this process, since its pH optimum (pH 6.0) is even closer to that of the soymilk hydrolysis process (pH 6.2–6.4).

Interestingly, the retained activity was greater than 40% within the pH range from 5.0 to 8.0, which is a quite wide tolerance range compared to other characterised thermostable  $\alpha$ -galactosidases [40]. Therefore, pH shifts during on-going enzymatic reaction in industrial processes could have a minor impact on its activity (Fig. 3). The recombinant enzyme did not lose activity after 2 h of incubation at pH 6.0 and 8.0, and it retained up to 60% of

residual activity after 6 h (Fig. 4). Approximately 50–60% loss in activity was recorded on either side of the pH optimum after 6 h incubation, while at pH 4.0, the activity rapidly dropped, as expected from the pH-dependence data (Fig. 4). Because of its considerable tolerance towards neutral/slightly alkaline pH values, *TtGalA* could be employed in hydrothermal processing in which water in liquid phase or in vapour phase is used to pretreat lignocellulosic biomasses [49]. In this process, controlling the pH around neutral values minimizes the formation of fermentation inhibitors [50]. Typically, the optimal temperature for catalysis of thermophilic enzymes mirrors the growing temperature of the native host, like the  $\alpha$ -galactosidase from *Thermus* sp. strain T2 (75 °C) [44], whereas their activity is limited at lower temperatures. *TtGalA* is unusual since its optimum was set at 90 °C and its activity was lower at temperature  $\leq 70$  °C, which is the optimal growth temperature for most of *Thermus* species. Moreover, *TtGalA* is among the most thermophilic  $\alpha$ -galactosidases so far characterised, such as that of *T. neapolitana* (105 °C) [47], *T. Brockianus* (94 °C) and *T. maritima* (95 °C) [39, 43].

The thermal inactivation data indicate that the *TtGalA* has a half-life of 60 min (Fig. 5) at its optimal temperature (90 °C). Moreover, residual activity higher than 90% was detected up to 6 h of incubation at 70 °C (Fig. 5), retaining 50% of its activity after 30 h (not shown).

It has already been reported that previously characterised enzymes from *Thermus* species display in vitro an optimal catalytic temperature higher than the growing

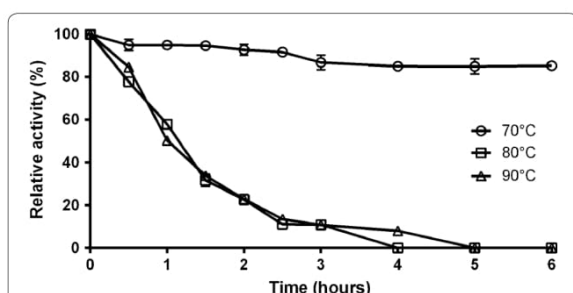


**Fig. 5** Thermal inactivation of *TtGalA*. The purified enzyme from *T. thermophilus* was incubated in 20 mM sodium-phosphate buffer pH 6.0 at 90, 80 and 70 °C for different period of time and then assayed for residual activity at 90 °C

temperature of the native host [51], thus making this microorganism a fruitful source of enzyme catalytically active at temperature above 70 °C. Due to the elevated temperatures used during some industrial applications (such as sugar manufacturing processes and/or raw material pretreatments in bioethanol production), stability at high temperatures is an important feature for the utilization of  $\alpha$ -galactosidases, since it prevents the loss of ternary/quaternary structures that leads to enzyme inactivation as for the mesophilic counterparts [36, 37].

#### Effect of metal ions

Metal ions can be released during processing of biomass as consequence of corrosion of pretreatment equipment, resulting in the liberation of heavy metal ions, which can be inhibitory to biocatalysts [52]. Moreover, other cations can derive from chemicals used to adjustment the pH. Noteworthy, several divalent cations are potent inhibitors of  $\alpha$ -galactosidases; therefore, we tested their effect on the enzyme activity over a range of concentration from 0.5 to 5 mM (Table 3). Interestingly, the enzyme turned to be slightly activated in the presence of  $\text{Co}^{+2}$ ,  $\text{Mn}^{+2}$ ,  $\text{Zn}^{+2}$  at 1 mM concentration suggesting that it is a metalloenzyme or requires divalent cations as cofactors. On

the other hand, this effect is negligible with monovalent cations (Table 3). The inhibition effect occurred only at the highest concentration of metal ions tested (5 mM). To further investigate on the possible role of metal ions, the enzyme activity was assayed in the presence of EDTA (5 mM) and a 20% reduction of its catalytic activity was observed. The inhibitory effect of EDTA was studied up to 40 mM concentration (not shown) resulting in a linear decrease of the enzymatic activity, thus indirectly confirming the role as cofactor of the metal ions ( $\text{Co}^{+2}$ ,  $\text{Mn}^{+2}$ ,  $\text{Zn}^{+2}$ ) (Table 3). Similar to these findings, EDTA slightly inhibited also the  $\alpha$ -galactosidase activity from *Lenzites elegans* [53], whereas it has no effect on the activity of  $\alpha$ -galactosidases from *B. megaterium* and *Ganoderma lucidum* [48, 54].

#### Inhibition of activity

Since detergents are reported to strongly inhibit the  $\alpha$ -galactosidase activity in *Glycine max* and *Penicillium griseoroseum* [55, 56], we assayed *TtGalA* in the presence of 5 mM detergents. The enzyme turned out to be very sensitive to the common anionic detergent SDS, which leads to a complete loss of function possibly due to the disruption of enzyme native structure. By contrast, the non-ionic detergents Tween 20 and Triton X-100 had a less marked effect with reduction of the enzyme activity to ~40 and ~19%, respectively (Table 4).

During pretreatment and saccharification of lignocellulosic biomasses, several sugars are released. These can inhibit the activity of glycoside hydrolases during the saccharification phase [49, 50]. Moreover, various sugars were also reported to inhibit the  $\alpha$ -galactosidase activity, for instance, an  $\alpha$ -galactosidase from *Aspergillus nidulans* is competitively inhibited by D-galactose and D-glucose [57]. Accordingly, the activity of *TtGalA* turned out to be inhibited by the presence of several saccharides, such as D-galactose, D-saccharose and D-arabinose (Table 4). Nevertheless, *TtGalA* might have a potential use in the sugar

**Table 3** Influence of metal ions on the relative activity of *TtGalA*

Metal ions	0.5 mM	1 mM	2.5 mM	5 mM
$\text{Mg}^{+2}$	99.3 $\pm$ 0.7	91.7 $\pm$ 0.3	89.9 $\pm$ 2.5	55.6 $\pm$ 0.5
$\text{Ca}^{+2}$	95.9 $\pm$ 0.7	95.8 $\pm$ 0.1	90.1 $\pm$ 2.4	27.8 $\pm$ 0.4
$\text{Cu}^{+2}$	87.7 $\pm$ 3.1	77.2 $\pm$ 1.6	63.9 $\pm$ 0.97	22.2 $\pm$ 0.3
$\text{Li}^{+}$	106.3 $\pm$ 0.5	113.9 $\pm$ 3.6	114.8 $\pm$ 3.1	93.6 $\pm$ 2.5
$\text{Zn}^{+2}$	100.6 $\pm$ 2.2	110.3 $\pm$ 0.6	70.4 $\pm$ 0.6	15.1 $\pm$ 0.3
$\text{Mn}^{+2}$	103.4 $\pm$ 1.0	128.5 $\pm$ 1.9	114.8 $\pm$ 3.0	20.2 $\pm$ 0.6
$\text{Co}^{+2}$	101.8 $\pm$ 2.6	136.2 $\pm$ 0.4	92.8 $\pm$ 0.9	30.1 $\pm$ 0.7

**Table 4** Influence of additives on the activity of *TtGalA*

Compound (5 mM)	Relative activity (%)
EDTA	79.9
D-Galactose	27.9
D-Saccharose	44.6
D-Arabinose	54.7
Urea	60.0
Guanidine chloride	36.8
SDS	1.6
Tween 20	39.8
Triton X100	18.8



beet industry for raffinose hydrolysis, because it retains 44.6% of its activity in presence of sucrose [10].

Finally, *TtGalA* was assayed in presence of caotropic agents such as urea and guanidine chloride. The partial reduction of the catalytic activity is in agreement with its intrinsic stability as thermozyme [20].

## Conclusions

In this work, we report the biochemical characterization of a thermoactive and thermostable  $\alpha$ -galactosidase from *T. thermophilus* HB27 (*TtGalA*). Moreover, the drawbacks of using a heterologous mesophilic host (*E. coli*) for the production of this thermozyme have been highlighted. Indeed, “hot” expression systems are in some cases indispensable to get functional thermozymes in reasonable amounts.

Interestingly, the long-term retained activity of *TtGalA* (30 h at 70 °C) might pave the way to its utilization after thermal pretreatment of lignocellulosic biomass (pre-saccharification), when the temperature is still too high for the fungal enzymes currently used for the hydrolysis of the biomass.

Despite its already interesting catalytic features, a fine-tuning of *TtGalA* enzymatic properties, through genetic engineering, will be attempted to make it even more suitable for industrial applications.

## Methods

### Bacterial strains and growth conditions

*Thermus thermophilus* HB27 strain was purchased from DSMZ. A frozen (−80 °C) stock culture was streaked on a *Thermus* Medium (TM) solidified by the addition of 0.8% Gelrite® (Sigma) and incubated at 70 °C overnight [58]. *T. thermophilus* HB27::nar strain, kindly provided by Prof. J. Berenguer (Universidad Autónoma de Madrid) was used for the homologous expression of *TtGalA*. *E. coli* strains were grown in Luria–Bertani (LB) medium at 37 °C with 50 µg/ml kanamycin, 33 µg/ml chloramphenicol as required. *E. coli* DH5 $\alpha$  and BL21-CodonPlus (DE3)-RIL (Stratagene, La Jolla, CA, USA) strains were used for DNA manipulations and for the heterologous expression of the recombinant  $\alpha$ -galactosidase, respectively.

### Cloning and sequencing of TTP0072 gene

A single colony of *T. thermophilus* HB27 was inoculated into TM liquid medium and genomic DNA was isolated using DNeasy® 124 Tissue kit, (Qiagen), according to the instruction manufacturer. TTP0072 gene, encoding for a putative  $\alpha$ -galactosidase, was amplified by PCR from *T. thermophilus* HB27 genomic DNA using the primers 5'GGAGGGCATATGAGGCTGAA3' (*Nde*I site underlined) and 5'CGGTGGAAGCTTTTATAGAAGG3' (*Hind*III site underlined) and Phusion Taq Polymerase (NEB).

The amplification was carried out at 94 °C for 1 min, 58 °C for 1 min and 72 °C for 1 min, for 35 cycles. The PCR product was purified with QIAquick PCR purification kit (Qiagen Spa, Milan, Italy) and cloned in pCR4-TOPO\_vector using the TOPO TA CLONING Kit (Invitrogen). The identity of the cloned DNA fragment was confirmed by DNA sequencing (BMR Genomics). Then, the insert was sub-cloned into the *Nde*I/*Hind*III digested pET28(b) and for pMKE2 [34] vectors for *E. coli* and *T. thermophilus* HB27::nar expression, respectively.

### Expression and purification of recombinant *EcGalA* and *TtGalA*

The recombinant  $\alpha$ -galactosidases expressed in *E. coli* (*EcGalA*) and *T. thermophilus* HB27::nar (*TtGalA*) bear an His-tag at their N-terminus. To express *EcGalA*, *E. coli* BL21-CodonPlus (DE3)-RIL was transformed with the recombinant plasmid pET28(b)-*EcgalA*. Protein expression was induced by adding 0.5 mM of isopropyl- $\beta$ -D-1-thiogalactopyranoside (IPTG) to exponentially growing cells (0.5 OD<sub>600</sub>) and culturing them for 12 h. Since *EcGalA* was poorly expressed, different approaches were attempted to achieve a sufficient amount of soluble recombinant protein: (1) varying the induction time (2, 4, 6, and 8 h and overnight induction); (2) lowering the temperature during induction (down to 20 °C); (3) decreasing the IPTG concentration (0.01–0.1 mM). At every conditions, the expression levels were monitored by SDS-PAGE and enzymatic assays. However, none of these strategies turned out to reasonably increase the final amount of the recombinant protein.

For the homologous expression 200 ng of pMKE2-*TtgalA* plasmid were added to exponentially growing (0.4 OD<sub>600nm</sub>) *T. thermophilus* HB27::nar cells and transformants were selected on TM plates at 70 °C containing 50 µg/ml kanamycin [59]. The induction of *TtGalA* expression was performed as previously described [34].

Crude extracts from both *E. coli* BL21-CodonPlus (DE3)-RIL and *T. thermophilus* HB27::nar cells were prepared following a similar procedure. Cell pellets were collected from 1-L cultures by centrifugation at 4000 $\times g$  for 15 min at 4 °C and resuspended in buffer A (50 mM Tris–HCl, pH 7.5 and 500 mM NaCl) for *EcGalA* and in buffer B (50 mM Tris–HCl, pH 7.5) for *TtGalA* purification, respectively. Protease inhibitor cocktail tablets (Roche) were added in both cases. The cells were homogenized by sonication (Sonicator:Heat System Ultrasonic, Inc.) for 5 min, alternating 30 s of pulse-on and 30 s of pulse-off and clarification of the cell extract was obtained by centrifugation at 40,000 $\times g$  for 20 min at 4 °C. Purification of *EcGalA* from the soluble fraction was performed through a two-step procedure, i.e. (1) thermal precipitation at



70 °C for 10 min followed by centrifugation at  $5000\times g$  for 20 min at 4 °C; (2) affinity chromatography on a His-Trap column (1 ml, GE Healthcare) connected to an AKTA Explorer system (GE Healthcare). The affinity chromatography was equilibrated with buffer A and the *EcGalA* was eluted with the same buffer A supplemented with a linear gradient of imidazole (0–250 mM).

*TtGalA* was purified through a similar procedure, except that the first thermal precipitation step was substituted with an anionic exchange chromatography on a Hi-trap Q HP column (5 ml, GE Healthcare). The column was equilibrated in buffer B and elution was performed in the same buffer through a linear gradient from 0 to 500 mM NaCl. The affinity chromatography was carried out under the same conditions described above. Protein identity was further verified by Western blot analysis using anti-His antibodies and LC–MS/MS analysis.

Protein concentration was estimated by using bovine serum albumin as standard according to Bradford [60]. Protein fractions displaying  $\alpha$ -galactosidase hydrolysing activity toward *p*-nitrophenyl- $\alpha$ -D-galactopyranoside (herein named *pNP*- $\alpha$ -D-galactopyranoside, Sigma) were pooled, dialyzed against 20 mM Tris–HCl pH 7.5 and analysed by 12% SDS-PAGE [61]. The *TtGalA* activity was detected through zymography in 12% SDS-PAGE under not reducing conditions. After electrophoresis, the gel was soaked in 2.5% Triton X-100 for 30 min at 4 °C and then was incubated with 20 mM of *pNP*- $\alpha$ -D-galactopyranoside solution at 90 °C for 10 min.

#### Molecular weight determination

The native molecular weight of the purified *TtGalA* was analysed by gel-filtration chromatography connected to Mini DAWN Treos light-scattering system (Wyatt Technology) equipped with a QELS (quasi-elastic light scattering) module mass value and hydrodynamic radius (*Rh*) measurements [62]. Five hundreds micrograms of protein (1 mg/ml) were loaded on a S200 column (16/60, GE Healthcare) with a flow-rate of 0.5 ml/min and equilibrated in buffer A. Data were analysed using Astra 5.3.4.14 software (Wyatt Technology).

#### Determination of the $\alpha$ -galactosidase activity

The *TtGalA* standard assay was performed by using *pNP*- $\alpha$ -D-galactopyranoside as substrate (2.0 mM) in 50 mM sodium phosphate buffer (pH 6.0) at 90 °C in 160  $\mu$ l of the reaction mixture using 50 ng of the enzyme. All assays were performed in triplicate in a 96-well microplate reader (Synergy H4, Biotek), on at least 3 different enzyme preparations. The reaction was stopped, after 10 min, by addition of 1 volume of cold 0.5 M  $\text{Na}_2\text{CO}_3$  and the concentration of the released *p*-nitrophenol (molar extinction coefficient, 18.5/mM cm) was determined by measuring  $A_{405\text{nm}}$ . One

unit of enzyme activity (U) was defined as the amount of enzyme required to release 1  $\mu$ mol *p*-nitrophenol per minute, under the above assay conditions.

#### Catalytic and stability properties

The optimal pH and temperature were determined by performing the *pNP*- $\alpha$ -D-galactopyranoside assay between pH 3.0–9.0 using the following buffers (each 50 mM): citrate phosphate (pH 3.0–5.0), sodium phosphate (pH 6.0–9.0). Thermal inactivation assays were performed by incubating 50 ng of enzyme at different temperatures (70, 80, 90 °C) in buffer sodium phosphate at pH 6.0 and taking aliquots at regular time intervals to measure the residual enzyme activity under standard assay conditions (90 °C for 10 min, pH 6.0). To test enzyme stability to pH, the assays were performed by incubating *TtGalA* at 70 °C in various buffers (pH 4.0–8.0). The residual activity was measured at different time intervals following the  $\alpha$ -galactosidase standard assay.

#### Inhibition of activity

The effect of  $\text{MgCl}_2$ ,  $\text{CaCl}_2$ ,  $\text{CuCl}_2$ ,  $\text{LiCl}$ ,  $\text{ZnSO}_4$ ,  $\text{MnCl}_2$ ,  $\text{CoSO}_4$  on the  $\alpha$ -galactosidase activity was studied over a range of concentrations (0.5–5.0 mM) by pre-incubating the enzyme (50 ng) for 5 min at room temperature with the specific metal ions and by measuring the residual activity under standard assay conditions.

The influence of reducing (DTT,  $\beta$ -mercaptoethanol) and chelating (EDTA) agents as well as of sugars (D-galactose, sucrose, L-arabinose, and D-fucose), each tested at 5 mM concentration, was studied under the same pre-incubation and assay conditions as above.

#### Substrate specificity

*TtGalA* was tested for the hydrolysis of *pNP*- $\alpha$ -substituted hexoses (D-glucose, D-mannose, L-rhamnose) and of *pNP*- $\beta$ -substituted hexoses (D-galactose, D-glucose, and D-mannose) at a concentration of 2 mM under standard conditions (90 °C and pH 6.0 for 10 min). The kinetic parameters were determined using different *pNP*- $\alpha$ -D-galactopyranoside concentration (ranging from 0.0125 to 2 mM) with 50 ng of *TtGalA* for 3 min. The Michaelis constant ( $K_M$ ) and  $V_{\text{max}}$  were calculated by non-linear regression analysis using GraphPad 6.0 Prism software.

#### Additional file

**Additional file 1: Table S1.** Purification table of *EcGalA*. **Table S2.** Purification table of *TtGalA*.

#### Abbreviations

bt: bacterial thermophilic; CAZy: carbohydrate-active enzymes; DTT: dithiothreitol; *EcGalA*: *Thermus thermophilus*  $\alpha$ -galactosidase expressed in *E. coli*; EDTA: ethylenediaminetetraacetic acid; GH: glycoside hydrolase; g: gravity;

h: hour(s); IPTG: isopropyl- $\beta$ -D-1-thiogalactopyranoside;  $k_{cat}$ : catalytic constant;  $K_M$ : Michaelis constant; LB: Luria-Bertani broth; LC–MS/MS: liquid chromatography–tandem mass spectrometry; pNP: p-nitrophenol; QELS: quasi-elastic light scattering; Rh: hydrodynamic radius; s: second(s); TM: thermus medium; TrGalA: *Thermotoga neapolitana*  $\alpha$ -galactosidase; TtGalA: *Thermus thermophilus*  $\alpha$ -galactosidase; SDS-PAGE: sodium dodecyl sulphate–polyacrylamide gel electrophoresis.

#### Authors' contributions

MA and SF performed experiments. SF, GF, DL, EP, SB and PC supervised the project. MA and PC drafted the manuscript. All authors read and approved the final manuscript.

#### Author details

<sup>1</sup> Dipartimento di Biologia, Università degli Studi di Napoli Federico II, Complesso Universitario Monte S. Angelo, Via Cinthia, 80126 Naples, Italy. <sup>2</sup> Division of Industrial Biotechnology, Department of Biology and Biological Engineering, Chalmers University of Technology, Gothenburg, Sweden.

#### Acknowledgements

We thank Dr. Andrea Carpentieri for performing the LC–MS/MS analysis and Prof. José Berenguer who kindly provided us with the pMKE2 plasmid.

#### Competing interests

The authors declare that they have no competing interests.

#### Availability of data and materials

Recombinant strains described in this work are made available upon request to the corresponding author. Data sharing not applicable to this article as no datasets were generated or analysed during the current study.

#### Funding

This work was supported by BIOPOLIS: PON03PE\_00107\_1 CUP: E48C14000030005.

Received: 22 September 2016 Accepted: 25 January 2017

Published online: 13 February 2017

#### References

- Pauly M, Keegstra K. Plant cell wall polymers as precursors for biofuels. *Curr Opin Plant Biol*. 2010;13:304–11.
- Malgas S, van Dyk JS, Pletschke BI. A review of the enzymatic hydrolysis of mannans and synergistic interactions between  $\beta$ -mannanase,  $\beta$ -mannosidase and  $\alpha$ -galactosidase. *World J Microbiol Biotechnol*. 2015;31:1167–75.
- Chauhan PS, Puri N, Sharma P, Gupta N. Mannanases: microbial sources, production, properties and potential biotechnological applications. *Appl Microbiol Biotechnol*. 2012;93:1817–30.
- Marraccini P, Rogers WJ, Cailliet V, Deshayes A, Granato D, Lausanne F, Lechat S, Pridmore D, Pétiard V. Biochemical and molecular characterization of  $\alpha$ -D-galactosidase from coffee beans. *Plant Physiol Biochem*. 2005;43:909–20.
- Pourcher T, Bassilana M, Sarkar HK, Kaback HR, Leblanc G. Melibiose permease and  $\alpha$ -galactosidase of *Escherichia coli*: identification by selective labeling using a T7 RNA polymerase/promoter expression system. *Biochemistry*. 1990;29:690–6.
- Yang D, Tian G, Du F, Zhao Y, Zhao L, Wang H, Ng TB. A fungal  $\alpha$ -galactosidase from *Pseudobalsamia microspora* capable of degrading raffinose family oligosaccharides. *Appl Biochem Biotechnol*. 2015;176:2157–69.
- Linthorst GE, Hollak CE, Donker-Koopman WE, Strijland A, Aerts JM. Enzyme therapy for Fabry disease: neutralizing antibodies toward agalactase  $\alpha$  and  $\beta$ . *Kidney Int*. 2004;66:1589–95.
- Lim HG, Kim GB, Jeong S, Kim YJ. Development of a next-generation tissue valve using a glutaraldehyde-fixed porcine aortic valve treated with decellularization,  $\alpha$ -galactosidase, space filler, organic solvent and detoxification. *Eur J Cardiothorac Surg*. 2015;48:104–13.
- Olsson ML, Hill CA, De La Vega H, Liu QP, Stroud MR, Valdinocci J, Moon S, Clausen H, Kruskall MS. Universal red blood cells—enzymatic conversion of blood group A and B antigens. *Transfus Clin Biol*. 2004;11:33–9.
- Linden JC. Immobilized  $\alpha$ -D-galactosidase in the sugar beet industry. *Enzym Microb Technol*. 1982;4:130–6.
- Clarke JH, Davidson K, Rixon JE, Halstead JR, Fransen MP, Gilbert HJ, Hazlewood GP. A comparison of enzyme-aided bleaching of softwood paper pulp using combinations of xylanase, mannanase and  $\alpha$ -galactosidase. *Appl Microbiol Biotechnol*. 2000;53:661–7.
- Pessela BC, Fernández-Lafuente R, Torres R, Mateo C, Fuentes M, Filho M, Vian A, García JL, Guisán JM, Carrascosa AV. Production of a thermoresistant  $\alpha$ -galactosidase from *Thermus* sp. strain T2 for food processing. *Food Biotechnol*. 2007;21:91–103.
- Prashanth SJ, Mulimani V. Soymilk oligosaccharide hydrolysis by *Aspergillus oryzae*  $\alpha$ -galactosidase immobilized in calcium alginate. *Process Biochem*. 2005;40:1199–205.
- Rosgaard L, Pedersen S, Langston J, Akerhielm D, Cherry JR, Meyer AS. Evaluation of minimal *Trichoderma reesei* cellulase mixtures on differently pretreated barley straw substrates. *Biotechnol Prog*. 2007;23:1270–6.
- Sun Y, Cheng J. Hydrolysis of lignocellulosic materials for ethanol production: a review. *Bioresour Technol*. 2002;83:1–11.
- Linares-Pastén JA, Andersson M, Karlsson NE. Thermostable glycoside hydrolases in biorefinery technologies. *Current Biotechnol*. 2014;3:26–44.
- Paës G, O'Donohue MJ. Engineering increased thermostability in the thermostable GH-11 xylanase from *Thermobacillus xylanilyticus*. *J Biotechnol*. 2006;125:338–50.
- Henne A, Brüggemann H, Raasch C, Wierze A, Hartsch T, Liesegang H, Johann A, Lienard T, Gohl O, Martínez-Arias R, et al. The genome sequence of the extreme thermophile *Thermus thermophilus*. *Nat Biotechnol*. 2004;22:547–53.
- Limauro D, D'Ambrosio K, Langella E, De Simone G, Galdi I, Pedone C, Pedone E, Bartolucci S. Exploring the catalytic mechanism of the first dimeric Bcp: functional, structural and docking analyses of Bcp4 from *Sulfolobus solfataricus*. *Biochimie*. 2010;92:1435–44.
- Contursi P, D'Ambrosio K, Pirone L, Pedone E, Aucelli T, She Q, De Simone G, Bartolucci S. C68 from the *Sulfolobus islandicus* plasmid-virus pSSVx is a novel member of the ABR-like transcription factor family. *Biochem J*. 2011;435:157–66.
- Prato S, Vitale RM, Contursi P, Lipps G, Saviano M, Rossi M, Bartolucci S. Molecular modeling and functional characterization of the monomeric primase–polymerase domain from the *Sulfolobus solfataricus* plasmid pIT3. *FEBS J*. 2008;275:4389–402.
- Fiorantino G, Del Giudice I, Bartolucci S, Durante L, Martino L, Del Vecchio P. Identification and physicochemical characterization of BldR2 from *Sulfolobus solfataricus*, a novel archaeal member of the MarR transcription factor family. *Biochemistry*. 2011;50:6607–21.
- Contursi P, Farina B, Pirone L, Fusco S, Russo L, Bartolucci S, Fattorusso R, Pedone E. Structural and functional studies of Stf76 from the *Sulfolobus islandicus* plasmid-virus pSSVx: a novel peculiar member of the winged helix-turn-helix transcription factor family. *Nucleic Acids Res*. 2014;42:5993–6011.
- Contursi P, Fusco S, Limauro D, Fiorentino G. Host and viral transcriptional regulators in *Sulfolobus*: an overview. *Extremophiles*. 2013;17:881–95.
- Francis DM, Page R. Strategies to optimize protein expression in *E. coli*. *Curr Protoc Protein Sci*. 2010;Chapter 5:Unit 5.24.21–9.
- Rosano GL, Ceccarelli EA. Recombinant protein expression in *Escherichia coli*: advances and challenges. *Front Microbiol*. 2014;5:172.
- Hidalgo A, Betancor L, Moreno R, Zafra O, Cava F, Fernández-Lafuente R, Guisán JM, Berenguer J. *Thermus thermophilus* as a cell factory for the production of a thermophilic Mn-dependent catalase which fails to be synthesized in an active form in *Escherichia coli*. *Appl Environ Microbiol*. 2004;70:3839–44.
- Contursi P, Cannio R, She Q. Transcription termination in the plasmid/virus hybrid pSSVx from *Sulfolobus islandicus*. *Extremophiles*. 2010;14:453–63.
- Fusco S, She Q, Bartolucci S, Contursi P. T(lys), a newly identified *Sulfolobus* spindle-shaped virus 1 transcript expressed in the lysogenic state, encodes a DNA-binding protein interacting at the promoters of the early genes. *J Virol*. 2013;87:5926–36.
- Contursi P, Fusco S, Cannio R, She Q. Molecular biology of fuselloviruses and their satellites. *Extremophiles*. 2014;18:473–89.

31. Prato S, Cannio R, Klenk HP, Contursi P, Rossi M, Bartolucci S. pIT3, a cryptic plasmid isolated from the hyperthermophilic crenarchaeon *Sulfolobus solfataricus* IT3. *Plasmid*. 2006;56(35–45):31.
32. Bartolucci S, Contursi P, Fiorentino G, Limauro D, Pedone E. Responding to toxic compounds: a genomic and functional overview of Archaea. *Front Biosci (Landmark Ed)*. 2013;18:165–89.
33. Suzuki H, Yoshida K-I, Ohshima T. Polysaccharide-degrading thermophiles generated by heterologous gene expression in *Geobacillus kaustophilus* HTA426. *Appl Environ Microbiol*. 2013;79:5151–8.
34. Moreno R, Haro A, Castellanos A, Berenguer J. High-level overproduction of His-tagged Tth DNA polymerase in *Thermus thermophilus*. *Appl Environ Microbiol*. 2005;71:591–3.
35. Wu WL, Liao JH, Lin GH, Lin MH, Chang YC, Liang SY, Yang FL, Khoo KH, Wu SH. Phosphoproteomic analysis reveals the effects of PilF phosphorylation on type IV pilus and biofilm formation in *Thermus thermophilus* HB27. *Mol Cell Proteomics*. 2013;12:2701–13.
36. Viikari L, Alapuranen M, Puranen T, Vehmaanperä J, Siika-Aho M. Thermostable enzymes in lignocellulose hydrolysis. *Adv Biochem Eng Biotechnol*. 2007;108:121–45.
37. Elleuche S, Schäfers C, Blank S, Schröder C, Antranikian G. Exploration of extremophiles for high temperature biotechnological processes. *Curr Opin Microbiol*. 2015;25:113–9.
38. Sarmiento F, Peralta R, Blamey JM. Cold and hot extremozymes: industrial relevance and current trends. *Front Bioeng Biotechnol*. 2015;3:148.
39. Fridjonsson O, Watzlawick H, Gehweiler A, Rohrhirsch T, Mattes R. Cloning of the gene encoding a novel thermostable alpha-galactosidase from *Thermus brockianus* IT1360. *Appl Environ Microbiol*. 1999;65:3955–63.
40. Brouns SJ, Smits N, Wu H, Snijders AP, Wright PC, de Vos WM, van der Oost J. Identification of a novel alpha-galactosidase from the hyperthermophilic archaeon *Sulfolobus solfataricus*. *J Bacteriol*. 2006;188:2392–9.
41. Fridjonsson O, Watzlawick H, Mattes R. The structure of the alpha-galactosidase gene loci in *Thermus brockianus* IT1360 and *Thermus thermophilus* TH125. *Extremophiles*. 2000;4:23–33.
42. Jenney FE, Adams MW. Hydrogenases of the model hyperthermophiles. *Ann NY Acad Sci*. 2008;1125:252–66.
43. Liebl W, Wagner B, Schellhase J. Properties of an  $\alpha$ -galactosidase, and structure of its gene galA, within an  $\alpha$ - and  $\beta$ -galactoside utilization gene cluster of the hyperthermophilic bacterium *Thermotoga maritima*. *Syst Appl Microbiol*. 1998;21:1–11.
44. Ishiguro M, Kaneko S, Kuno A, Koyama Y, Yoshida S, Park GG, Sakakibara Y, Kusakabe I, Kobayashi H. Purification and characterization of the recombinant *Thermus* sp. strain T2 alpha-galactosidase expressed in *Escherichia coli*. *Appl Environ Microbiol*. 2001;67:1601–6.
45. Gote M, Khan M, Gokhale D, Bastawde K, Khire J. Purification, characterization and substrate specificity of thermostable  $\alpha$ -galactosidase from *Bacillus stearothermophilus* (NCIM-5146). *Process Biochem*. 2006;41:1311–7.
46. Beeby M, O'Connor BD, Ryttersgaard C, Boutz DR, Perry LJ, Yeates TO. The genomics of disulfide bonding and protein stabilization in thermophiles. *PLoS Biol*. 2005;3:e309.
47. Duffaud GD, McCutchen CM, Leduc P, Parker KN, Kelly RM. Purification and characterization of extremely thermostable beta-mannanase, beta-mannosidase, and alpha-galactosidase from the hyperthermophilic eubacterium *Thermotoga neapolitana* 5068. *Appl Environ Microbiol*. 1997;63:169–77.
48. Patil A, Praveen Kumar S, Mulimani VH, Veeranagouda Y, Lee K.  $\alpha$ -Galactosidase from *Bacillus megaterium* VHM1 and its application in removal of flatulence-causing factors from soymilk. *J Microbiol Biotechnol*. 2010;20:1546–54.
49. Hu F, Ragauskas A. Pretreatment and lignocellulosic chemistry. *Bioenergy Research*. 2012;5:1043–66.
50. Jönsson LJ, Martín C. Pretreatment of lignocellulose: formation of inhibitory by-products and strategies for minimizing their effects. *Bioresour Technol*. 2016;199:103–12.
51. Blank S, Schröder C, Schirrmacher G, Reisinger C, Antranikian G. Biochemical characterization of a recombinant xylanase from *Thermus brockianus*, suitable for biofuel production. *JSM Biotechnol Biomed Eng*. 1027;2014:2.
52. Turner P, Mamo G, Karlsson EN. Potential and utilization of thermophiles and thermostable enzymes in biorefining. *Microb Cell Fact*. 2007;6:9.
53. Sampietro D, Quiroga E, Sgariglia M, Soberón J, Vattuone MA. A thermostable  $\alpha$ -galactosidase from *Lenzites elegans* (Spreng.) ex Pat. MB445947: purification and properties. Antonie Van Leeuwenhoek. 2012;102:257–67.
54. Sriputan T, Aoki K, Yamamoto K, Tongkao D, Kumagai H. Purification and characterization of thermostable  $\alpha$ -galactosidase from *Ganoderma lucidum*. *Biosci Biotechnol Biochem*. 2003;67:1485–91.
55. Falkoski DL, Guimarães VM, Callegari CM, Reis AP, de Barros EG, de Rezende ST. Processing of soybean products by semipurified plant and microbial alpha-galactosidases. *J Agric Food Chem*. 2006;54:10184–90.
56. Mi S, Meng K, Wang Y, Bai Y, Yuan T, Luo H, Yao B. Molecular cloning and characterization of a novel  $\alpha$ -galactosidase gene from *Penicillium* sp. F63 CGMCC 1669 and expression in *Pichia pastoris*. *Enzym Microb Technol*. 2007;40:1373–80.
57. Rios S, Pedregosa AM, Fernández Monistrol I, Laborda F. Purification and molecular properties of an alpha-galactosidase synthesized and secreted by *Aspergillus nidulans*. *FEMS Microbiol Lett*. 1993;112:35–41.
58. Del Giudice I, Limauro D, Pedone E, Bartolucci S, Fiorentino G. A novel arsenate reductase from the bacterium *Thermus thermophilus* HB27: its role in arsenic detoxification. *Biochim Biophys Acta Proteins Proteom*. 2013;1834:2071–9.
59. Koyama Y, Hoshino T, Tomizuka N, Furukawa K. Genetic transformation of the extreme thermophile *Thermus thermophilus* and of other *Thermus* spp. *J Bacteriol*. 1986;166:338–40.
60. Bradford MM. A rapid and sensitive method for the quantitation of microgram quantities of protein utilizing the principle of protein-dye binding. *Anal Biochem*. 1976;72:248–54.
61. Laemmli UK. Cleavage of structural proteins during the assembly of the head of bacteriophage T4. *Nature*. 1970;227:680–5.
62. Limauro D, De Simone G, Pirone L, Bartolucci S, D'Ambrosio K, Pedone E. *Sulfolobus solfataricus* thiol redox puzzle: characterization of an atypical protein disulfide oxidoreductase. *Extremophiles*. 2014;18:219–28.

Submit your next manuscript to BioMed Central and we will help you at every step:

- We accept pre-submission inquiries
- Our selector tool helps you to find the most relevant journal
- We provide round the clock customer support
- Convenient online submission
- Thorough peer review
- Inclusion in PubMed and all major indexing services
- Maximum visibility for your research

Submit your manuscript at  
[www.biomedcentral.com/submit](http://www.biomedcentral.com/submit)





## Manuscript 2-II:

### A thermophilic enzymatic cocktail for galactomannans degradation

Aulitto Martina\*, Fusco Francesca Anna\*, Fiorentino Gabriella, Bartolucci Simonetta, Contursi Patrizia<sup>#</sup>, Limauro Danila

Dipartimento di Biologia, Università degli Studi di Napoli Federico II, Naples, Italy

\*These authors equally contributed to the work

<sup>#</sup>Correspondence: [contursi@unina.it](mailto:contursi@unina.it)

#### Abstract

The full utilization of hemicellulose sugars (pentose and exose) present in lignocellulosic material, is required for an efficient bio-based fuels and chemicals production. Two recombinant thermophilic enzymes, an endo-1,4- $\beta$ -mannanase from *Dictyoglomus turgidum* (*Dtur*CelB) and an  $\alpha$ -galactosidase from *Thermus thermophilus* (*Tt*GalA), were assayed at 80°C, to assess their heterosynergistic association on galactomannans degradation, particularly abundant in hemicellulose. The enzymes were tested under various combinations simultaneously and sequentially, in order to estimate the optimal conditions for the release of reducing sugars. The results showed that the most efficient degree of synergy was obtained in simultaneous assay with a protein ratio of 25% of *Dtur*CelB and 75% of *Tt*GalA, using Locust bean gum as substrate. On the other hand, the mechanism of action was demonstrated through the sequential assays, i.e. when *Tt*GalA acting as first to enhance the subsequent hydrolysis performed by *Dtur*CelB. The synergistic association between the thermophilic enzymes herein described has an high potential application to pre-hydrolyse the lignocellulosic biomasses right after the pretreatment, prior to the conventional saccharification step.

Keywords: Synergy; *Dictyoglomus turgidum*; *Thermus thermophilus*; Thermophiles;  $\alpha$ -galactosidase; endo-1,4- $\beta$ -mannanase.

#### 1. Background:

Lignocellulose is the most abundant available feedstock produced every-day on the Earth and it is constituted by cellulose (35-50%), hemicellulose (26-35%) and lignin (14-21%), as well as by other minor components [1]. Lignin provides the structural integrity of the plant, encapsulating the microfibrils of hemicellulose and cellulose, to withstand the herbivores and pathogens attacks. Hemicellulose is the second most abundant biopolymer present in lignocellulosic-feedstocks [2]. Unlike cellulose, a linear homopolymer of  $\beta$ (1,4)-linked D-glucose residues, hemicellulose is a branched heteropolymer composed by pentoses (i.e. xylose and arabinose), hexoses (i.e. glucose, galactose, mannose) and also by sugars in acidified form (glucuronic acid and galacturonic acid) [3]. During the detrital food webs, the polysaccharides hydrolysis is carried out by saprophytes and detritivores, as the natural process for the deconstruction of biomasses [4]. Since lignocellulosic feedstock is clean and available in large amount, the biomass is currently used to produce value added-products such as bio-fuels and -chemicals [1, 5]. In the industrial processes, the deconstruction is performed using chemical and physical pretreatments upon which the lignin is disarrayed [6]. The resulting polysaccharides (i.e. cellulose and hemicellulose) are subsequently hydrolyzed by enzymatic mixture to produce fermentable sugars. This latter process, also named saccharification, involves an array of (hemi)cellulases, auxiliary enzymes and proteins to obtain an effective hydrolysis [7].

Mannans are the major source of secondary cell wall found in hemicellulose fraction of conifers (softwood) and leguminosae. On the basis of their sugars

components they are classified in: mannans, glucomannans, galactomannans and galactoglucomannans [8]. To achieve an efficient hydrolysis of galactoglucomannans, the presence of multiple hydrolases such as  $\beta$ -glucosidases (EC 3.2.1.21), endomannanases (EC 3.2.1.78), mannosidases (EC 3.2.1.25) and  $\alpha$ -galactosidases (EC 3.2.1.22), is needed [9]. Therefore, studies of synergistic association among these enzymes pave the way to establish an efficient enzymatic cocktail to achieve the complete hydrolysis of mannans. Since the pretreatment step is performed at high temperature (90°-120°C), the development of thermophilic enzymatic mixtures which could operate at high temperature is needed to reduce the whole process cost [10].

The main objective of this work has been to study the synergistic effect of the thermophilic endo-1,4- $\beta$ -mannanase (*DturCelB*) from *Dictyoglomus turgidum* and  $\alpha$ -1,6-galactosidase (*TtGalA*) from *Thermus thermophilus* on galactomannan substrates from Locust bean gum, Carob and Guar.

## **2. Methods**

### **2.1. Substrates**

Locust bean gum was purchased from Sigma-Aldrich. Galactomannans (Carob, Low viscosity and Guar, Medium viscosity) were purchased from Megazyme.

### **2.2 Expression and purification of recombinant enzymes**

*DturCelB* was expressed from a culture of *Escherichia coli* BL21 (DE3), transformed with the recombinant plasmid pET30b-*DturCelB* and purified by nickel affinity chromatography [18]. *T. thermophilus* HB27::nar strain transformed with the recombinant plasmid pMKE2-*TtGalA* was used for the homologous expression of *TtGalA* and the purification was performed according to Aulitto *et al* [11].

### **2.3 Substrate specificity determination of *DturCelB* and *TtGalA* towards galactose- containing-polymers**

*DturCelB* and *TtGalA* activities were determined using Locust bean gum, Carob and Guar as polymeric substrates. The reaction mixtures (1 mL) containing one of the purified enzymes (1  $\mu$ g) were assayed using 1 % galactomannan substrates dissolved in 50 mM citrate-phosphate buffer pH 6.0. The reaction was carried out at 80 °C for 30 min and the concentration of reducing ends was determined following the Nelson-Somogyi (NS) method, using mannose as standard [12]. All enzyme assays were performed in triplicate. One unit of enzyme activity was defined as the amount of enzyme required to release 1  $\mu$ mol of product per min, under the above assay conditions.

### **2.4 *DturCelB* and *TtGalA* synergistic action**

To evaluate the degree of synergy between *DturCelB* and *TtGalA* the enzymes were tested simultaneously and sequentially using 1.0 % of galactomannan substrates (Locust bean gum, Carob and Guar) dissolved in 50 mM citrate-phosphate buffer pH 6.0. For the simultaneous assay, various ratios of *DturCelB* and *TtGalA* were tested (50%*DturCelB*-50%*TtGalA*; 25%*DturCelB*-75%*TtGalA*; 75%*DturCelB* -25%*TtGalA*) for a total amount of 2  $\mu$ g. The assays were carried out as described above through NS.

For the sequential assay 1  $\mu$ g of *DturCelB* or *TtGalA* was incubated at 80°C for 30 min in the reaction mixture described above. Afterwards, the mixture was boiled for 10 min to inactivate the first enzyme. After ice-cooling, the second enzyme (1  $\mu$ g) was added to the mixture and the reaction was carried out under the same conditions (80°C for 30 min). Reactions containing only one of the heat-inactivated enzyme were used

as a negative control. All the samples were analyzed for the concentration of reducing ends by NS method using mannose as standard. All enzyme assays were run in triplicate.

## 2.5 Synergy studies

To investigate the interaction between two or more enzymes, synergism is calculated as ratio between the observed activity of the enzyme mixture and the theoretical sum of individual specific activity of the same enzymes. The degree of synergy (DS), between *DturCelB* and *TtGalA*, was determined by the following equation:

$$DS = \frac{Y_{1+2}}{(Y_1 + Y_2)}$$

where  $Y_{1+2}$ , indicates the yield ( $\mu\text{g}$ ) of reducing sugars achieved by the two enzymes working simultaneously or sequentially,  $Y_1$  and  $Y_2$  indicate the yields ( $\mu\text{g}$ ) of reducing sugars achieved by each enzyme when working separately.

## 3. Results and discussion

In nature plant biomass degradation is accomplished by the complex action of various glycosyl hydrolases (GH) enzymes. Therefore, the optimization of enzymatic mixtures to improve the conversion of biomasses into fermentable sugars is needed for biorefinery purposes. Nevertheless, a major issue in this context is to set up the right reaction conditions to achieve a synergistic interaction among enzymes that act on the same complex substrate. Moreover, enzymes belonging to diverse families can display synergistic and/or antis synergistic interaction due to their own substrate specificities. A synergistic association between two or more enzymes is present when the degree of synergy (DS) is greater than 1.0 and therefore produces a degradation yield greater than those obtained from enzymes acting separately. Synergy among mannanolytic enzymes is classified in two types: i) homosynergy between two main-chain enzymes or two side-chain enzymes; ii) heterosynergy between side- and main-chain enzymes [8].

Previous studies showed that galactomannans could be effectively degraded by the combined action of a main-chain-cleaving mannanase and a side-chain-cleaving galactosidase compared to when mannanases or galactosidases were used alone [13]. However, knowledge about thermophilic enzymatic cocktails is scarce. Therefore, it is interesting to study the synergistic action of enzymes derived from different “hot” sources that can be employed in biomasses hydrolysis right after the pretreatment.

### 3.1 Determination of specific activity of *DturCelB* and *TtGalA* on different galactomannans

The recombinant enzymes *DturCelB* and *TtGalA* were previously characterized for their biochemical catalytic features [18, 21]. In this study, the hydrolytic endomannanase activity of *DturCelB* was assayed at 80°C and pH 6.0 towards Locust bean gum (44.0 U  $\text{mg}^{-1}$ ), Carob (40.3 U  $\text{mg}^{-1}$ ) and Guar (2.8 U  $\text{mg}^{-1}$ ) (Tab.1).



Substrate	<i>DturCelB</i> Specific activity (U · mg <sup>-1</sup> )	<i>TtGalA</i> Specific activity (U · mg <sup>-1</sup> )
Locust bean gum (G/M:1/4)	44.0	4.4
Carob (G/M:1/3.5)	40.3	1.4
Guar (G/M:1/2)	2.8	0.33

**Table 1.** Specific activity of *DturCelB* and *TtGalA* on different galactomannan substrates. Abbreviations: Galactose (G) and Mannose (M).

The different catalytic efficiency can be explained by the increasing number of galactose residues (Guar > Carob > Locust bean gum) branching out from the linear mannan backbones and causing steric hindrance to the enzyme (Fig.1).

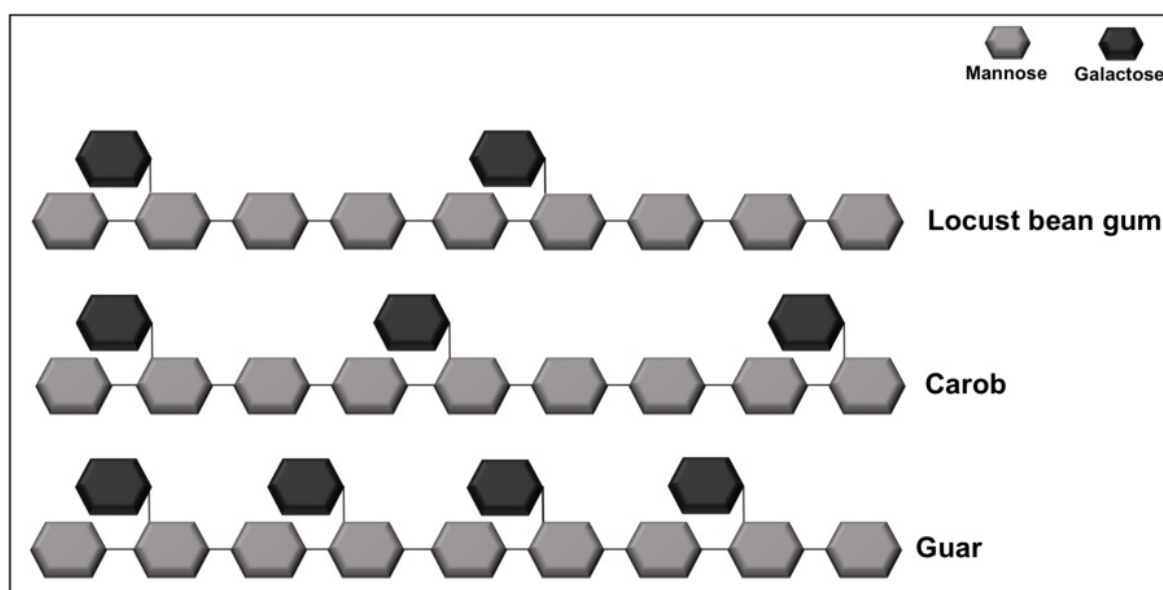


**Figure 1.** Graphical representation of the galactomannans used in this study: Locust bean gum, Carob and Guar.

A similar behaviour was also demonstrated for *Clostridium thermocellum* Man5A [14]. Therefore, one way to improve the *DturCelB* hydrolysis of galactomannans is to combine its catalytic activity with an  $\alpha$ -galactosidase acting on the branched glycosidic 1,6- $\alpha$ -bounds between galactose and mannose. As potential partner, it was chosen *TtGalA*, an  $\alpha$ -galactosidase from *Thermus thermophilus* performing its highest catalytic activity at 90°C and pH 6.0 on pNPG synthetic substrate [11]. Assays conditions for the two enzymes were set at 80°C and pH 6.0 because *TtGalA* retained 98% of its catalytic activity at 80°C. In this work *TtGalA* was assayed towards Locust bean gum (4.4 U mg<sup>-1</sup>), Carob (1.4 U mg<sup>-1</sup>) and Guar (0.33 U mg<sup>-1</sup>) galactomannans and displayed a specific activity lower than that detected on pNPG substrate (338 U mg<sup>-1</sup>). The different specific activities are in agreement with the preference of *TtGalA* towards galactose-oligosaccharides over -polysaccharides, as for other GH36 members [13]. Nevertheless *TtGalA* catalytic activity on polymeric substrates is not negligible (Tab. 1), indeed it is higher if compared to that of a GH36 AgIC (1.0 U mg<sup>-1</sup>) from *Aspergillus niger* and very similar to that of a GH27 Aga27A from *Cyamopsis tetragonolobus* (3.7 U mg<sup>-1</sup>) [13]. Therefore, the synergistic association between these two thermophilic enzymes might be functional to improve the hydrolysis of hemicellulose as already demonstrated in other systems [8, 13].

### 3.2 Synergistic studies of *TtGalA* and *DturCelB* towards three galactose containing-polymers

The aim of this study was centred on the setting up of reaction conditions suitable to achieve heterosynergy between *TtGalA* and *DturCelB* to ameliorate the galactomannans hydrolysis. The synergistic interaction between the recombinant enzymes was assessed through the quantification of the reducing sugars released during the degradation of the three galactomannan substrates. These contained a different ratio of galactose- versus mannose- residues to assess how the activity and synergistic interactions of *TtGalA* and *DturCelB* were influenced by the extent of galactose substitution on the mannan backbone (Figure 1). In simultaneous assays the enzymes were added to the reaction mixture at the same time, varying their relative ratio (50%*TtGalA* -50%*DturCelB*; 75%*DturCelB*-25%*TtGalA* and 25%*DturCelB*-75%*TtGalA*), while in sequential assays it was used the same ratio (50%*DturCelB* -50%*TtGalA*).

Locust bean gum is the most important galactomannan used as stabilizing agent in food and non-food industries [15], it is purified from endosperm of carob tree seeds [16] and is the lowest galactose containing polymer (G/M: 1/4) among the substrates tested (Figure 1). All the conditions led to an increase of the release of reducing sugars compared to that achieved by the two enzymes alone (Figure 2).

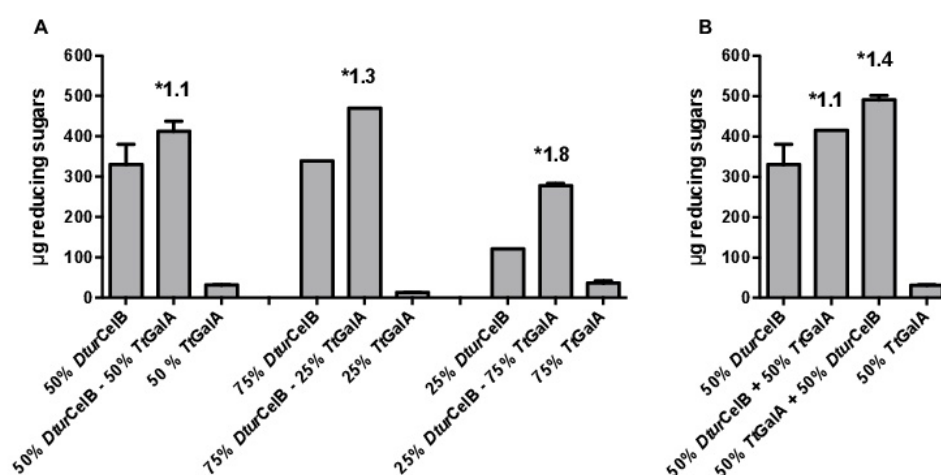


**Figure 2.** Simultaneous (A) and sequential (B) assays of *TtGalA* and *DturCelB* using 1 % Locust bean gum. Various combinations of recombinant enzymes were tested and protein ratio was expressed in percentage form. The degree of synergy is highlighted with an asterisk. Values were presented as mean values  $\pm$  S.D. ( $n = 3$ ).

Using this substrate, the enzymes exhibited synergism under all combinations with a DS of 1.8, 1.3 and 1.1 using a ratio of 25%*DturCelB*-75%*TtGalA*, 75%*DturCelB*-25%*TtGalA* and 50%*DturCelB*-50%*TtGalA*, respectively (Figure 2A). To get further insight into the observed synergistic action, we performed sequential assays. When *DturCelB* was added as first, the DS=1.1-turned out to be identical to that obtained with simultaneous assays (Figure 2A). Conversely, the DS raised up to 1.4 when *TtGalA* was added as first (Figure 2B). These results demonstrate that *TtGalA* significantly supported *DturCelB* activity by removing galactose branches on the polymer that would have sterically hindered *DturCelB*.

Locust bean gum and Carob are both isolated from *Ceratonia siliqua*. These galactomannan polymers display different chemical and rheological properties depending on their geographic origin [17]. The reported G/M ratio of Carob is slightly lower (1/3.5) than Locust bean gum (Figure 1) and our data indicate that the specific



activity of *TtGalA* on Carob is 30% of that on Locust bean gum (Table 1). Therefore, we resolved to perform a comparative synergy study of the two thermophilic enzymes also using this substrate. In fact, when *DturCelB* and *TtGalA* were assayed in combination of 50%-50% no synergy was exhibited (DS=0.8) (Figure 3A).

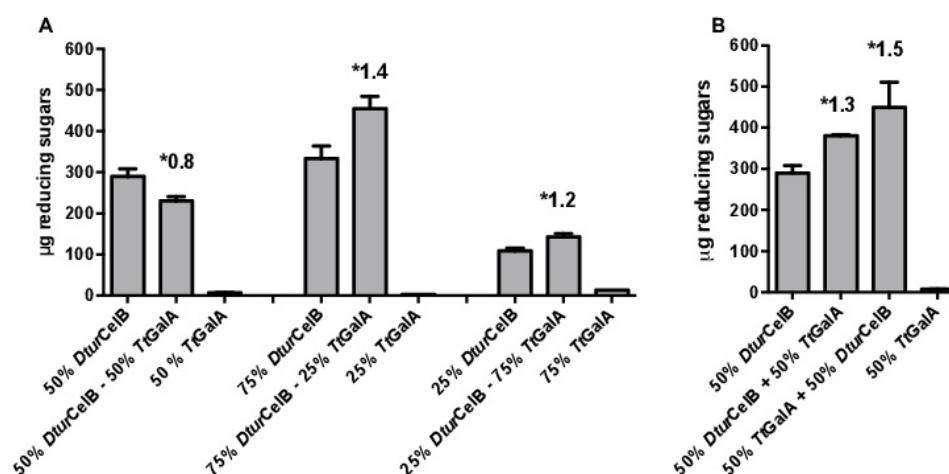


**Figure 3.** Simultaneous (A) and sequential (B) assays of *TtGalA* and *DturCelB* using 1% Carob. Various combinations of recombinant enzymes were tested and protein ratio was expressed in percentage form. The degree of synergy is highlighted with an asterisk. Values were presented as mean values  $\pm$  S.D. ( $n = 3$ ).

This result might be explainable with a complex nature of the Carob substrate (purity degree, extent of galactose ramifications) that renders the binding of *TtGalA* not completely productive, thus in turn inhibiting the *DturCelB* hydrolysis when they are present in the enzymatic mixture in a similar amount. However, a similar degree of synergy (DS=1.4 on Carob vs DS=1.3 on Locust bean gum) was achieved when the enzymes were assayed simultaneously, with a protein ratio of *DturCelB* to *TtGalA* 75%-25% and the total amount of reducing sugars released was also comparable (467  $\mu$ g vs 454  $\mu$ g) (Figure 3A and 2A). Yet, the highest DS obtained on Carob (DS=1.4) was indeed lower than that measured on Locust bean gum (Figure 2A, DS=1.8), indicating that the two enzymes performed their synergistic catalytic activity, less efficiently on this substrate (Figure 2A and 1A). This result can be only explained by the low specific activity of *TtGalA* on Carob, since the affinity of *DturCelB* on Carob and Locust bean gum is almost the same (Table 1). Our data highlighted the role of *TtGalA*, that plays a major function in enhancing the *DturCelB* activity, improving the linear mannan chain accessibility. Accordingly, results from the sequential assay show clearly that also on Carob the synergistic association, between the two enzymes, benefits (DS=1.5) by the previous action of the debranching enzyme.

The Guar backbone is composed of a linear chain of mannose residues (Figure 1), where the galactose residues branch at every second mannose residue. The specific activity of *DturCelB* and *TtGalA* on Guar was lower than that obtained on Locust bean gum (Table 1), due to the higher extent of galactose substitutions (Figure 1). Accordingly, the total yield of reducing sugars obtained on this substrate was much lower than that on Locust bean gum and Carob (Figure 2, 3 and 4).

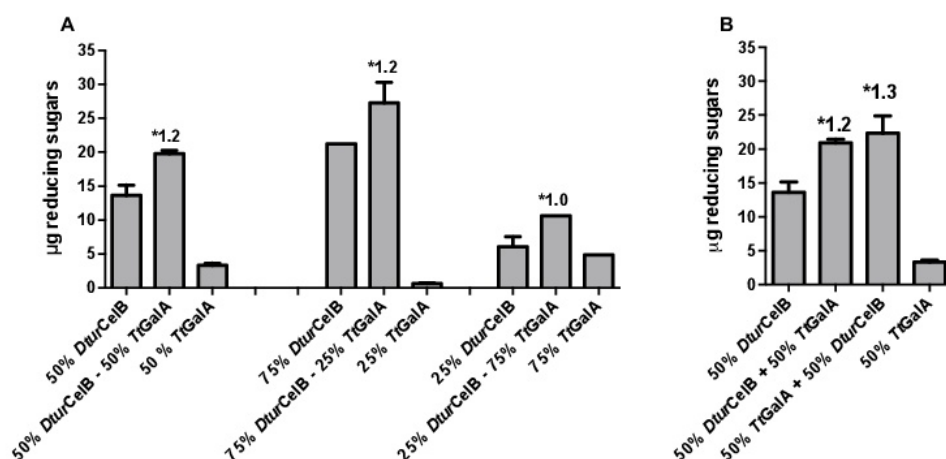


**Figure 4.** Simultaneous (A) and sequential (B) assays of *TtGalA* and *DturCelB* using 1% Guar. Various combinations of recombinant enzymes were tested and protein ratio was expressed in percentage form. The degree of synergy is highlighted with an asterisk. Values were presented as mean values  $\pm$  S.D. ( $n = 3$ ).

Nevertheless, in simultaneous assays our data clearly indicate that the synergistic interaction between the two enzymes occurred also using Guar as substrate (i.e.  $DS \geq 1.0$ ) under all the conditions tested (Figure 4A). The sequential assays further confirmed that the prior action of *TtGalA* by removing galactose substituents, increases the release of reducing sugar by *DturCelB* (Figure 4).

## 4.0 Conclusions

One of the major factor contributing to increase the yield of the efficient lignocellulose biomass conversion yield, resides in understanding how different enzymes may cooperate to degrade complex polymeric substrates. Both the new isolated thermophilic *DturCelB* and *TtGalA* enzymes performed a better catalytic activity working in synergy rather than alone, preferring the low galactose-polysaccharides than the highly galactose decorated polymers used in this study. In fact, a good degree of heterosynergy relationship with each other on galactomannan degradation was clearly demonstrated on all the substrate tested at high temperature (80°C) and in a relatively short time (30 min) compared to other studies [13]. Based on the sequential assays, the synergy was a result of *TtGalA* activity, which removes galactose branches from the galactomannan polymers, then improving the accessibility of the linear mannan backbone to *DturCelB*. Our finding also revealed that the 75%-25% ratio of *DturCelB* and *TtGalA* is the best combination to attain a compromise between a good degree of synergy and the highest yield of reducing sugars released. The strength point of this enzymatic cocktail resides in the thermophilicity and thermostability of both the *TtGalA* and *DturCelB* enzymes [11] that allows to foresee their employment during the gradual cooling right after the pretreatment of lignocellulosic material. The addition of thermophilic enzymes earlier in this step would result in time savings and improved conversion efficiency of the whole process, compared to the use of mesophilic/moderate thermophilic enzyme cocktails.

## Acknowledgements

The authors thank prof. José Berenguer, Centro de Biología Molecular Severo Ochoa, Universidad Autónoma de Madrid, Spain, for generously providing *Thermus thermophilus* HB27::nar strain and pMKE2 vector.

## Funding

This research was carried out in the frame of Programme STAR, financially supported by UniNA and Compagnia di San Paolo (16-CSP-UNINA-007). The work was also financially supported by Ministero dell'Istruzione, dell'Università e della Ricerca (IT); BIOPOLIS (PON03PE\_00107\_1 CUP: E48C14000030005).

## References:

1. Arevalo-Gallegos A, Ahmad Z, Asgher M, Parra-Saldivar R, Iqbal HM: **Lignocellulose: A sustainable material to produce value-added products with a zero waste approach—A review.** *International Journal of Biological Macromolecules* 2017.
2. Pérez J, Muñoz-Dorado J, de la Rubia T, Martínez J: **Biodegradation and biological treatments of cellulose, hemicellulose and lignin: an overview.** *International Microbiology* 2002, **5**:53-63.
3. Saha BC: **Hemicellulose bioconversion.** *J Ind Microbiol Biotechnol* 2003, **30**:279-291.
4. Cragg SM, Beckham GT, Bruce NC, Bugg TD, Distel DL, Dupree P, Etxabe AG, Goodell BS, Jellison J, McGeehan JE: **Lignocellulose degradation mechanisms across the Tree of Life.** *Current Opinion in Chemical Biology* 2015, **29**:108-119.
5. Anwar Z, Gulfranz M, Irshad M: **Agro-industrial lignocellulosic biomass a key to unlock the future bio-energy: a brief review.** *Journal of radiation research and applied sciences* 2014, **7**:163-173.
6. Hu F, Ragauskas A: **Pretreatment and lignocellulosic chemistry.** *Bioenergy Research* 2012, **5**:1043-1066.
7. Keshk SM: **Cellulase Application in Enzymatic Hydrolysis of Biomass.** 2016.
8. Malgas S, van Dyk JS, Pletschke BI: **A review of the enzymatic hydrolysis of mannans and synergistic interactions between  $\beta$ -mannanase,  $\beta$ -mannosidase and  $\alpha$ -galactosidase.** *World Journal of Microbiology and Biotechnology* 2015, **31**:1167-1175.
9. Malherbe AR, Rose SH, Viljoen-Bloom M, van Zyl WH: **Expression and evaluation of enzymes required for the hydrolysis of galactomannan.** *J Ind Microbiol Biotechnol* 2014, **41**:1201-1209.
10. Van Dyk J, Pletschke B: **A review of lignocellulose bioconversion using enzymatic hydrolysis and synergistic cooperation between enzymes—factors affecting enzymes, conversion and synergy.** *Biotechnology advances* 2012, **30**:1458-1480.
11. Aulitto M, Fusco S, Fiorentino G, Limauro D, Pedone E, Bartolucci S, Contursi P: ***Thermus thermophilus* as source of thermozymes for biotechnological applications: homologous expression and biochemical characterization of an  $\alpha$ -galactosidase.** *Microbial Cell Factories* 2017, **16**:28.
12. Nelson N: **A photometric adaptation of the Somogyi method for the determination of glucose.** *Journal of biological chemistry* 1944, **153**:375-380.

13. Malgas S, van Dyk SJ, Pletschke BI:  **$\beta$ -Mannanase (Man26A) and  $\alpha$ -galactosidase (Aga27A) synergism—A key factor for the hydrolysis of galactomannan substrates.** *Enzyme and microbial technology* 2015, **70**:1-8.
14. Mizutani K, Fernandes VO, Karita S, Luís AS, Sakka M, Kimura T, Jackson A, Zhang X, Fontes CM, Gilbert HJ: **Influence of a mannan binding family 32 carbohydrate binding module on the activity of the appended mannanase.** *Applied and environmental microbiology* 2012, **78**:4781-4787.
15. Wielinga W, Maehall A: **Handbook of Hydrocolloids.** Phillips G O, Williams PA, eds. Boca Raton: CRC Press 2000, **200**:137-154.
16. Yousif AK, Alghzawi H: **Processing and characterization of carob powder.** *Food chemistry* 2000, **69**:283-287.
17. Bouzouita N, Khaldi A, Zgoulli S, Chebil L, Chekki R, Chaabouni M, Thonart P: **The analysis of crude and purified locust bean gum: A comparison of samples from different carob tree populations in Tunisia.** *Food chemistry* 2007, **101**:1508-1515.
18. Fusco FA, Ronca R, Fiorentino G, Pedone E, Contursi P, Bartolucci S, Limauro D: **Biochemical characterization of a thermostable endomannanase/endoglucanase from *Dictyoglomus turgidum*.** Accepted.



## Paper 2-III:

Extremophiles (2015) 19:539–546  
DOI 10.1007/s00792-014-0717-y

### METHOD PAPER

# A standardized protocol for the UV induction of *Sulfolobus* spindle-shaped virus 1

Salvatore Fusco · Martina Aulitto ·  
Simonetta Bartolucci · Patrizia Contursi

Received: 29 September 2014 / Accepted: 26 November 2014 / Published online: 6 December 2014  
© Springer Japan 2014

**Abstract** The *Fuselloviridae* prototype member *Sulfolobus* spindle-shaped virus 1 is a model of UV-inducible viruses infecting *Crenarchaeota*. Previous works on SSV1 UV induction were based on empirically determined parameters that have not yet been standardized. Thus, in many peer reviewed literature, it is not clear how the fluence and irradiance have been determined. Here, we describe a protocol for the UV induction of SSV1 replication, which is based on the combination of the following instrumentally monitored parameters: (1) the fluence; (2) the irradiance; (3) the exposure time, and (4) the exposure distance. With the aim of finding a good balance between the viral replication induction and the host cells viability, UV-irradiated cultures were monitored for their ability to recover in the aftermath of the UV exposure. This UV irradiation procedure has been set up using the well-characterized *Sulfolobus solfataricus* P2 strain as model system to study host–virus interaction.

**Keywords** *Sulfolobus* spindle-shaped virus · UV induction · Irradiation protocol · *Fuselloviridae* · Viral titre · Plaque assay · Fluence · Irradiance

## Introduction

*Sulfolobus* spindle-shaped virus 1 (SSV1), isolated from the native host *Sulfolobus shibatae* in Beppu (Japan), is the prototype and the best characterized member of the *Fuselloviridae* family (Prangishvili 2013; Martin et al. 1984). SSV1 can propagate only in few hosts (Ceballos et al. 2012), among which a strain of *S. solfataricus* isolated from the solfataric field of Pisciarelli near Naples (Italy), turned out to be suitable for carrying out genetic (Stedman et al. 1999; Clore and Stedman 2007; Iverson and Stedman 2012), biochemical (Kraft et al. 2004a, b; Menon et al. 2008; Zhan et al. 2012; Eilers et al. 2012) and physiological studies (Reiter et al. 1987; Schleper et al. 1992; Zillig et al. 1980; Fröls et al. 2007a; Fusco et al. 2013).

The genome of SSV1 is a double-stranded DNA molecule of 15 Kbp, which has been found both as integrated (provirus) and as episomal form into the host cells (Schleper et al. 1992; Yeats et al. 1982). Its complete sequence has been determined (Palm et al. 1991), and as for other fuselloviruses (Stedman et al. 2003; Wiedenheft et al. 2004; Redder et al. 2009; Contursi et al. 2007, 2010, 2014a), it encodes for a number of quasi-orphan proteins, which do not have detectable homologues in the databases other than in related hyperthermophilic viral genomes (Contursi et al. 2013). This has led to the necessity of performing structural and functional analyses to unravel their functions. For instance, the structure of several SSV1 transcription factors (TFs) has been solved revealing that, despite the lack of homology, most of these viral TFs are bacterial like (Kraft et al. 2004a, b; Menon et al. 2008; Zhan et al. 2012; Eilers et al. 2012; Contursi et al. 2013; 2011; 2014b).

Insights about the role of some SSV1 proteins have been derived from genetic analyses that revealed some of the

Communicated by L. Huang.

**Electronic supplementary material** The online version of this article (doi:10.1007/s00792-014-0717-y) contains supplementary material, which is available to authorized users.

S. Fusco · M. Aulitto · S. Bartolucci · P. Contursi (✉)  
Dipartimento di Biologia, Università degli Studi di Napoli  
Federico II, Complesso Universitario Monte S. Angelo,  
Via Cinthia, 80126 Naples, Italy  
e-mail: contursi@unina.it

essential SSV1 genes (Stedman et al. 1999; Iverson and Stedman 2012). Furthermore, its genome has been used as template for the construction of replicative and expression vectors, which have been employed for heterologous gene expression as well as for studying viral ORFs essentiality (Contursi et al. 2014a; Stedman et al. 1999; Iverson and Stedman 2012; Jonuscheit et al. 2003; Albers et al. 2006; Cannio et al. 1998; Cannio et al. 2001).

Pioneering studies on SSV1 helped shedding light on how gene expression is regulated in *Archaea*. In particular, the elucidation of the SSV1 transcriptional map as well as the identification of all the transcriptional start sites (TSSs) (Reiter et al. 1987; Fröls et al. 2007a; Fusco et al. 2013), led to the discovery of two conserved sequence motifs that resemble those of the eukaryotic basal gene promoters recognized by the RNA polymerase II (Reiter et al. 1988). Therefore, the bacterial-like transcription regulators encoded by *Archaea* operate in a eukaryal-like transcriptional context (Contursi et al. 2013).

Upon infection, one copy of the viral genome site specifically integrates into the host chromosome at an arginyl-tRNA gene (Schleper et al. 1992), whereas the episomal form (~5 copies per cell) is maintained in host cells in three isoforms, i.e. (1) as positively or negatively supercoiled and (2) as relaxed double-stranded DNA (Snyder et al. 2003). Intriguingly, so far SSV1 is the only member of the *Fusell-oviridae* family that shows an UV-inducible life cycle. Upon UV light exposure a well-characterized gene expression pattern is triggered and involves the expression of a short UV-inducible transcript, namely  $T_{ind}$ , followed by: (1) the time-coordinated expression of all the other viral transcripts, (2) the induction of the SSV1 genome replication (Fröls et al. 2007a) and (3) a steep increase of the viral titre. Only recently efforts have been made to get insights into the molecular switch from the lysogenic state to the replication induction (Fusco et al. 2013). Nevertheless, mechanisms underpinning these processes are still murky.

So far, in peer reviewed published literature, it is not clear how the fluence (or UV dose) and the irradiance have been measured. Indeed, the fluence ( $J\ m^{-2}$ ) administered to the cells has been only empirically determined and no attention has been paid to monitoring the irradiance ( $J\ m^{-2}\ s^{-1}$ ) (Martin et al. 1984; Reiter et al. 1987; Schleper et al. 1992; Fröls et al. 2007a). Furthermore, the negative effect on the host viability, that the UV treatment implies, has been underestimated. Since an essential parameter such as the irradiance has not been taken into account elsewhere (Martin et al. 1984; Reiter et al. 1987; Schleper et al. 1992; Fröls et al. 2007a) and the nomenclature may be misleading, important definitions need to be discussed. The irradiance is a proper term used when a surface is irradiated by UV light coming from all directions above the aforementioned surface. Indeed, the irradiance is the total radiant power incident from

all upward directions on an infinitesimal element of surface having area  $dA$  and containing the point under consideration divided by  $dA$ , as defined by Bolton (Bolton and Linden 2003). When the irradiance is constant (as herein described), the fluence is derived multiplying the irradiance by the exposure time (in seconds). The term UV dose, so far used to refer to the fluence, is confusing since the word “dose” describes a total energy adsorbed by a surface (e.g. the skin). In UV irradiation of microbial suspensions, the major amount of the incident UV light crosses the sample with only a small percentage being adsorbed by the cells. For this reason, fluence is a much more appropriated term since it is related to the incident UV energy, rather than to the adsorbed fraction (Bolton and Linden 2003).

Herein, we describe a protocol that has been developed with the purpose of: (1) standardizing all the parameters needed for performing an UV induction experiment on SSV1 lysogens and (2) finding a good balance between the viral induction and the host viability. Indeed, we show that by tuning fluence and irradiance, cells viability can be improved and, in turn, the viral induction reaches highest values determined so far.

## Materials and methods

### Growth conditions and UV irradiation

Cells of the *S. solfataricus* P2 lysogenic strain (SSV1-P2) were revitalized by depositing few microliters of culture onto the soft layer of an SCVYU-Gelrite plate and incubating at 75 °C for 3–5 days, as described elsewhere (Contursi et al. 2006). Subsequently, local growth areas (spots) were inoculated into 50 ml of SCVY medium, i.e. a glycine-buffered Brock's basal salt solution, supplemented with 0.2 % sucrose (wt/vol), 0.2 % casamino acids (wt/vol),  $1 \times$  vitamins (Wolin et al. 1963) and 0.005 % yeast extract (wt/vol); the pH was adjusted to 3.5 with concentrated  $H_2SO_4$ . Cells cultivation was conducted in a 250-ml Erlenmeyer flask with a long neck, at 75 °C with a shaking rate of 180 rpm using a MaxQ™ 4000 Benchtop Orbital Shaker (Thermo Scientific). The cell growth was spectrophotometrically monitored at 600 nm ( $OD_{600}$ ) by means of a Varian Cary® 50 Bio UV/Visible Spectrophotometer (McKinley Scientific). Once the culture reached the logarithmic phase of growth (0.4–0.6  $OD_{600}$ ), it was diluted to a value of 0.05  $OD_{600}$  in 50 ml of fresh SCVY medium and let to grow up to 0.8  $OD_{600}$ .

Before performing UV irradiations, the SSV1-P2 culture was diluted in 400 ml of SCVY medium to 0.08  $OD_{600}$  into a 1-L Erlenmeyer flask and let to grow up to the mid-logarithmic growth phase (0.5  $OD_{600}$ ). Aliquots of this culture were then UV-irradiated or mock treated. In detail, 40 ml of



culture was transferred into a 150 × 25-mm Petri plate (BD Falcon™) and UV irradiation was carried out at room temperature in a dark room under red light, by carefully hand shaking the plate under a germicidal lamp G15T8 (254 nm, 15 W, Sankyo Denki). Differently from previous reports (Martin et al. 1984; Reiter et al. 1987; Schleper et al. 1992; Fröls et al. 2007a), the fluence and the irradiance were instrumentally measured by means of a Quantum-photo-radiometer HD9021, equipped with an LP9021 UVC probe (Delta Ohm). The fluence was of 30, 45 and 60 J m<sup>-2</sup> (with an irradiance of 1.0 J m<sup>-2</sup> s<sup>-1</sup>) or of 45, 60 and 75 J m<sup>-2</sup> (with an irradiance of 0.5 J m<sup>-2</sup> s<sup>-1</sup>) (Fig. 1). The irradiance was tuned by changing the exposure distance, which was of 70 cm (for an irradiance of 0.5 J m<sup>-2</sup> s<sup>-1</sup>) or of 50 cm (for an irradiance of 1.0 J m<sup>-2</sup> s<sup>-1</sup>), whereas the desired fluence was achieved by changing the exposure time to the UV light source. As control, a mock-treated sample was subjected to the same procedure except for the UV light exposure. Treated samples were separately collected in 250-ml Erlenmeyer flasks, which were wrapped with aluminium foil to protect the culture from further light exposure, and incubated at 75 °C with a shaking rate of 180 rpm.

To check cells viability immediately after the treatment, serial dilutions of the cultures were plated on SCVYU-Gelrite and incubated at 75 °C for 7–10 days. Colonies were counted (100–300 cells per plate) and a survival percentage was calculated. Moreover, cell growth was spectrophotometrically monitored throughout the post-treatment incubation and samples were taken after 8 and 24 h, because a peak in the amount of SSV1 DNA and in the viral titre was expected, respectively (our unpublished data). Cellular pellets as well as cell-free supernatants were obtained through centrifugation at 3,000×g for 15 min using the Centrifuge 5810R (Eppendorf). The procedure was carried out in triplicate and average (Avg) as well as standard deviation (SD) were calculated for the data reported below.

#### Quantitative plaque assay

SSV1 viral titre was determined for cell-free supernatants by quantitative plaque assays using the uninfected *S.*

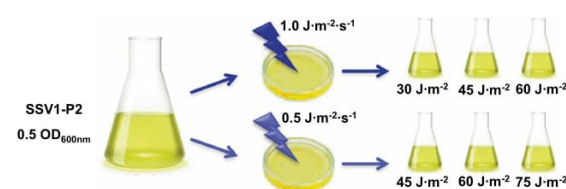


**Fig. 1** Schematic illustration of the UV irradiation procedure. Cells were grown exponentially until 0.5 OD<sub>600</sub> before being irradiated with an irradiance of 0.5 or 1.0 J m<sup>-2</sup> s<sup>-1</sup>

*solfataricus* strain P2, as lawn. This strain was first revitalized on SCVY-plate and then transferred into 50 ml of SCVYU medium, as described above. Cell density was monitored spectrophotometrically at 600 nm until the late logarithmic phase of growth (0.6 OD<sub>600</sub>).

Lower layers of SCVY-Gelrite were prepared by pouring, in 100 × 15 mm plastic plates (Falcon), 30 ml of 1 × SCVY mixed with Gelrite® (Sigma Aldrich) at the final concentration of 0.8 % (w/v). Subsequently, 100 μl of serial dilutions (from 10<sup>-4</sup> to 10<sup>-8</sup>) of cell-free supernatants (containing SSV1 viral particles) were added to a mix composed of: (1) 1 × SCVY medium, (2) Gelrite® at the final concentration of 0.4 % (w/v) and (3) 0.5 ml of the 0.6 OD<sub>600</sub> *S. solfataricus* P2 culture (about 0.5 × 10<sup>8</sup> cells). Each mix (the upper layer) was poured onto the lower layer of a pre-warmed SCVY-Gelrite plate. After a short incubation at room temperature to allow gelification of the upper layers, plates were transferred to 75 °C for 5–7 days. Growth inhibition areas (turbid halos), which appeared onto the upper layer as consequence of local growth retardation, were counted (up to 100 plaques per plate) and the viral titre (PFU/ml) was calculated considering the dilution factor.

Although quantitative plaque assay of SSV1 viral particles is notoriously challenging, we have noticed that a critical point for obtaining clearer halos depends on the physiological state as well as on the number of the cells used as lawn. Indeed, when about 0.5 × 10<sup>8</sup> cells of a not-freshly diluted culture are used, clear halos appear on the plate surface upon infection (Supplementary material, S1). Conversely, if the culture is freshly diluted with pre-warmed medium before plating, halos appear turbid and difficult to be counted.

#### Semi-quantitative PCR analysis

SSV1-P2 pellets, collected 8 h post-irradiation, were treated for total DNA extraction using the DNeasy tissue kit (Qiagen), following the manufacturer's instructions. The concentration of the DNA samples was spectrophotometrically measured by means of a Nanodrop 2000 Spectrophotometer (Thermo Scientific). To detect variations of the viral DNA content, total DNA samples from mock-treated and UV-irradiated cells were analysed by semi-quantitative PCR assays. With this aim, two primer couples were designed (Fusco et al. 2013) using Primer3 software (available at the website: <http://bioinfo.ut.ee/primer3-0.4.0/>), to amplify: (1) a 155-bp region of the SSV1 single-copy gene *vp2* and (2) a 108-bp region of the host single-copy gene *orc1* (Table 1). A PCR master mix was prepared as follows: 1 × Taq buffer, 2.5 mM MgCl<sub>2</sub>, 0.2 mM dNTP mix (Thermo Scientific), 0.6 μM *orc1*-fw, 0.6 μM *orc1*-rv, 0.6 μM *vp2*-fw, 0.6 μM *vp2*-rv and 0.1U/μl of Taq DNA Polymerase (Thermo Scientific). Aliquots of the master mix (60 μl each) were dispensed into 200-μl tubes (Eppendorf) and 100 ng of total DNA from

**Table 1** Sequences of oligonucleotides used for the semi-quantitative PCR assays

Name	Sequence (5'-3')	Length (nt)
<i>orc1-fw</i>	TATAAATTGTTATAGACATAGAACGCTGTA	30
<i>orc1-rv</i>	TTAAATACTTCTGTGCGGATAGTCC	26
<i>vp2-fw</i>	GGAGGGTACATCGCTACCTTATGA	24
<i>vp2-rv</i>	CAGTAGGGCTGACAGTAAACTACG	24

mock-treated or UV-irradiated cells were added. Each aliquot was then split into three sub-aliquots (20  $\mu$ l each), to collect the tubes at the 20th, 25th and 30th cycle of amplification. The thermal cycling protocol was carried out into a Mastercycler Personal (Eppendorf®) as follows: an initial denaturation step of 5 min at 95 °C, followed by 30 cycles of 40 s at 95 °C, 40 s at 62 °C, and 1 min at 72 °C. After collecting the samples at the 30th cycle, a final step at 72 °C has been carried out for 10 min. PCR products were run on a 2 % agarose gel in 1  $\times$  TAE buffer (40 mM Tris, 20 mM acetic acid and 1 mM EDTA) for 1 h. Pictures were taken by means of a Gel Doc XR System (Biorad) and DNA bands quantified using the Quantity One Software (Biorad).

## Results

The UV irradiation has a dose-dependent effect on the host cell viability

The UV irradiation not only induces the viral replication in SSV1-lysogens, but affects metabolism and survival of the host as well. In fact, major changes in growth rate and gene expression have been observed in the aftermath of UV irradiation of *S. solfataricus* cells.

Nevertheless, discrepant data have been produced about the UV-dependent gene regulation in this crenarchaeon, probably because the equipment and the procedure used, have not been standardized (Fröls et al. 2007b, 2009; Götz et al. 2007; Salerno et al. 2003).

Likewise most of the bacteriophages and viruses known, the SSV1 development seems to be sensitive to the physiological state of the host (Prangishvili 2013; Contursi et al. 2006; Bondy-Denomy and Davidson 2014). Therefore, a suitable protocol for SSV1 induction requires taking into account the host response in regard of cell viability and ability to recover upon UV exposure.

With the aim of setting up the best conditions for the induction of the SSV1 replication, cells were UV-irradiated by combining a set of different parameters: (1) the fluence ranging from 30 to 75 J m<sup>-2</sup>, (2) the irradiance of 0.5 or 1.0 J m<sup>-2</sup> s<sup>-1</sup>, (3) the exposure times ranging from 30 to 150 s, and (4) the exposure distance of 50 or 70 cm.

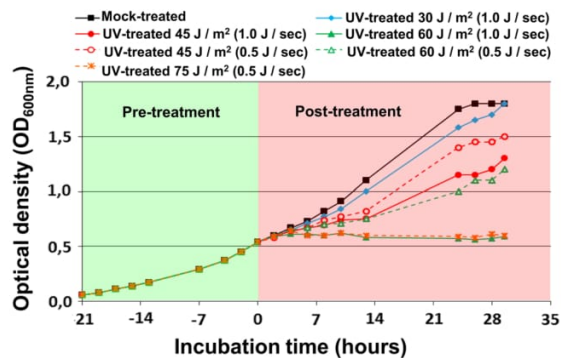


**Fig. 2** Growth curves of SSV1-P2 pre- and post-UV treatment. The OD<sub>600nm</sub> values were measured over a time window of ~55 h. Cells were grown exponentially until 0.5 OD<sub>600nm</sub> value (21st h of incubation) before being mock or UV treated (green area of the graph). Afterwards, the samples were split into seven flasks, incubated back to 75 °C and further monitored (red area of the graph). The growth retardation is related to the fluence and irradiance administered

As shown in Fig. 2, cell growth is slowed down by the treatment with a dose-dependent trend. The highest UV fluency levels, i.e. 60 J m<sup>-2</sup> and 75 J m<sup>-2</sup>, resulted in heavy growth retardation, probably as consequence of an impaired activation of the DNA lesions repairing system(s). Conversely, cell growth was only partially delayed when the fluence and irradiance were progressively reduced down (Fig. 2). Furthermore, cells viability determined by plating aliquots of the cultures, revealed that the survival percentage upon UV irradiation gradually increased by reducing both the fluence and irradiance (Table 2). To compensate for effects related to temperature changes, control cultures were subjected to the same procedure except for the UV irradiation.

Interestingly, our data indicate that the fluence (J m<sup>-2</sup>) is not the only parameter affecting the cell survival (Table 2) and their ability to recover after the treatment (Fig. 1). Indeed, the irradiance (J m<sup>-2</sup> s<sup>-1</sup>) is crucial to preserve cells viability. In fact, using a milder irradiance reduces cells lethality and, in turn, improves the viral replication (see below), which relies on the host machinery. Indeed, the same fluence provided with two values of irradiance (0.5 or 1.0 J m<sup>-2</sup> s<sup>-1</sup>) led to different percentage of viability. For all the values of fluence tested, the percentage of survival cells is higher when they are treated with a lower irradiance (0.5 J m<sup>-2</sup> s<sup>-1</sup>; Table 2).

A suitable UV fluence for the induction of the SSV1 replication

The effect of UV irradiation on the SSV1 replication has been evaluated by monitoring the relative amount of the SSV1 DNA in the mock-treated and UV-irradiated cultures



**Table 2** Cells viability after UV treatment

Total fluence (J m <sup>-2</sup> )	CFU/ml Avg $\pm$ SD ( <i>n</i> = 3)	Survival percentage (%) <sup>a</sup>
0	$8.63 \times 10^7 \pm 0.26 \times 10^7$	100
30 <sup>b</sup>	$6.07 \times 10^7 \pm 0.30 \times 10^7$	70.33
45 <sup>c</sup>	$3.17 \times 10^7 \pm 0.08 \times 10^7$	36.73
45 <sup>b</sup>	$1.87 \times 10^7 \pm 0.08 \times 10^7$	21.67
60 <sup>c</sup>	$0.60 \times 10^7 \pm 0.06 \times 10^7$	6.95
60 <sup>b</sup>	$0.23 \times 10^7 \pm 0.02 \times 10^7$	2.67
75 <sup>c</sup>	$0.51 \times 10^6 \pm 0.01 \times 10^6$	0.59

<sup>a</sup> Survival percentages calculated considering the mock-treated sample as 100 %

<sup>b</sup> Cells irradiated with an irradiance of 1.0 J m<sup>-2</sup> s<sup>-1</sup>

<sup>c</sup> Cells irradiated with an irradiance of 0.5 J m<sup>-2</sup> s<sup>-1</sup>

by semi-quantitative PCR assays. Cells were irradiated with a set of different conditions as described above and collected 8 h post-irradiation. Two single-copy genes on the host and viral chromosomes (*orc1* and *vp2*, respectively) were chosen to provide an estimation of the viral genome content under all the conditions tested. As shown, the PCR products were analysed for each sample on agarose gel at the 20th, 25th and 30th cycle of amplification (Fig. 3).

Densitometric analysis, performed by means of the software Quantity One (BioRad), revealed that the *vp2/orc1* fluorescence ratio increases in all the UV-irradiated samples compared to the mock-treated ones (when the same amplification cycle is considered). Notably, the highest value was detected for the sample treated with an irradiance of 0.5 J m<sup>-2</sup> s<sup>-1</sup> and a fluence of 45 J m<sup>-2</sup>, which, therefore, is the most suitable condition among the several tested (Fig. 3). For this latter sample, the fluorescence intensity of *vp2* at the 20th amplification cycle is comparable to its intensity at the 25th amplification cycle of the mock-treated sample (lysogenic culture). Under the best conditions, at each amplification cycle the amount of a specific amplicon

increases by a factor of 2<sup>*n*</sup>, where *n* is the number of cycle. Since the same amount of *vp2* (fluorescence intensity) is reached 5 cycles in advance in the irradiated sample, the copy number of SSV1 in this latter is ~32-fold higher (2<sup>5</sup>) than in the mock-treated one. Being the SSV1 copy number ~5 episomes per cell, the total viral amount reaches 160 copies per cell.

Worth of note is that, using the QIAprep Spin Miniprep Kit (Qiagen), about 20 µg of SSV1 DNA (~1.2 × 10<sup>12</sup> SSV1 episomal genomes) were isolated from independent preparations, by processing 50-ml pellets of cells harvested 8 h post-irradiation (0.75 OD<sub>600</sub>). If it is assumed that 1 OD<sub>600</sub> culture contains about 2 × 10<sup>8</sup> cells/ml (as calculated by plate efficiency), 50 ml of a 0.75 OD<sub>600</sub> culture contains ~7.5 × 10<sup>9</sup> cells. According to the data already measured by the densitometric analysis, the initial SSV1 copy number increases of 32-fold.

The SSV1 viral particles accumulate in the culture supernatant after the irradiation

Performing quantitative plaque assay to determine the SSV1 viral titre is notoriously challenging. However, we have noticed that using a not-freshly diluted culture as lawn, the resulted halos appeared clearer and easier to be counted than those obtained when a freshly diluted culture was plated. Therefore, the growth retardation induced by SSV1 infection is more pronounced when the culture is harvested from an exhausted medium.

Viral titre was determined for the culture supernatants harvested at the 8th and the 24th h post-irradiation. These two time points were chosen because after 8 h of incubation the amount of viral DNA in the cells reaches its maximum, while subsequently decreases (10–24 h), probably as consequence of the viral particles extrusion into the culture medium (our unpublished data). The highest amount of viral particles (5 × 10<sup>9</sup> PFU/ml) was produced from cells treated with a fluence of 45 J m<sup>-2</sup> (irradiance of

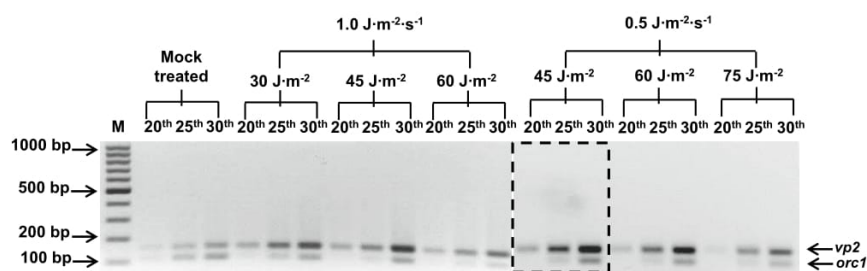


**Fig. 3** Semi-quantitative PCR analysis on DNA from mock- and UV-treated SSV1 -P2 cultures. Agarose gel electrophoresis of PCR products collected at the 20th, 25th and 30th amplification cycle. *Black-straight arrows* point out to molecular weight markers as well as to host

(*orc1* = 108 bp) and viral (*vp2* = 155 bp) PCR products. Densitometric analysis detected a maximum amount of SSV1 DNA for the sample irradiated with a fluence of 45 J m<sup>-2</sup> and an irradiance of 0.5 J m<sup>-2</sup> s<sup>-1</sup> (*dashed frame*)

0.5 J m<sup>-2</sup> s<sup>-1</sup>) and harvested 24 h post-irradiation. Whilst, the same fluence (45 J m<sup>-2</sup>), provided using an irradiance of 1.0 J m<sup>-2</sup> s<sup>-1</sup>, led to a lower viral titre (6 × 10<sup>8</sup> PFU/ml). This difference is due to the fact that, in the former case, a larger fraction of the cell population is viable (37 vs 22 %, Table 2), thus better supporting viral replication and virions extrusion.

## Discussion

Three decades have passed since the discovery of SSV1 and it still represents a valid model to study the host–virus interaction in harsh environments (Martin et al. 1984; Ceballos et al. 2012; Schleper et al. 1992; Fröls et al. 2007a; Fusco et al. 2013). Moreover, so far it is the only member of the *Fuselloviridae* family showing a UV-inducible life cycle (Prangishvili 2013; Contursi et al. 2014a). Interestingly, the first proof of the existence of a UV-specific response in *Sulfolobus* was just derived from the transcription analysis of SSV1. In particular, the primary reaction after UV treatment of the host cells is the expression of a small transcript T<sub>ind</sub>, which either acts as primer for viral replication and/or encodes for a UV-responsive transcription factor (Fröls et al. 2007a).

However, the UV irradiation exerts effect not only on the SSV1 induction but also on the host metabolism and vitality as well. Indeed, the transcriptional response in *Sulfolobus* cells is paralleled by a phase of marked growth retardation with DNA replication and cell division slowing down (Fröls et al. 2009). Exposure of cells to UV light causes the formation of two prevalent DNA lesions, i.e. cyclobutane pyrimidine dimers (CPDs) and 6–4 photoproducts, the former of which has been detected in UV-irradiated cells of *S. solfataricus* (Salerno et al. 2003). The best characterized UV-damage repair system is the nucleotide excision repair (NER) pathway. Noteworthy, the genome of *S. solfataricus* encodes for homologues of the eukaryal NER system, which were found to be transcriptionally

up-regulated upon UV irradiation (Salerno et al. 2003). In *Eukarya* the contribution of the NER pathway to the removal of UV-induced DNA lesions is dependent on the magnitude of the UV exposure used, i.e. on irradiance and fluence (Lee et al. 2004). Similarly, it has been shown that these two parameters represent key factors in the activation of the c-Jun N-terminal kinase (JNK), which is mediated by DNA lesions in mammalian cells. In particular, a prolonged activation of JNK was revealed when the UV fluence was administered using a lower irradiance (Adler et al. 1996). Notably, studies on UV response in *Eukarya* have evidenced that conflicting data are produced when different experimental procedures are used (Lee et al. 2004). Similar discrepancies in *S. solfataricus* (Fröls et al. 2007b, 2009; Götz et al. 2007; Salerno et al. 2003) might be attributed to the lack of a standardized protocol. Indeed, in previous literature the fluence has been only empirically determined, whilst the irradiance has not been taken into account (Martin et al. 1984; Reiter et al. 1987; Schleper et al. 1992; Fröls et al. 2007a).

In this manuscript, we describe a suitable UV irradiation procedure, which is based on instrumentally measured parameters, i.e. the fluence and irradiance. A clear dose–response relationship between the UV irradiation and the host survival percentage is shown. Interestingly, cells lethality was significantly reduced through the tuning of the irradiance (0.5 or 1.0 J m<sup>-2</sup> s<sup>-1</sup>) (Table 2). By analogy with eukaryal systems, this effect might be due to an improved functionality and/or activation of the DNA-damage repair systems (Lee et al. 2004; Adler et al. 1996).

A fluence of 45 J m<sup>-2</sup>, in combination with an irradiance of 0.5 J m<sup>-2</sup> s<sup>-1</sup>, turned out to be not only suitable to preserve host viability, but also to lead to the highest accumulation of viral DNA and of viral particles (Fig. 2; Table 3). Indeed, densitometric analysis of the PCR products showed an increase of the SSV1 copy number of about 32-fold, i.e. of ~160 viral genome copies per cell in the irradiated culture collected 8 h post-irradiation. Moreover, the viral titre determined under the same irradiation conditions (about

**Table 3** Viral titre at 8th and 24th hours after UV treatment

Total fluence (J m <sup>-2</sup> )	PFU/ml 8th Avg ± SD (n = 3)	PFU/ml 24th Avg ± SD (n = 3)	PFU/ml fold of increase 8th/24th
0	2.10 × 10 <sup>7</sup> ± 0.12 × 10 <sup>7</sup>	2.45 × 10 <sup>7</sup> ± 0.18 × 10 <sup>7</sup>	1.17
30 <sup>a</sup>	2.03 × 10 <sup>7</sup> ± 0.16 × 10 <sup>7</sup>	8.26 × 10 <sup>7</sup> ± 0.13 × 10 <sup>7</sup>	4.07
45 <sup>b</sup>	2.31 × 10 <sup>8</sup> ± 0.25 × 10 <sup>8</sup>	4.91 × 10 <sup>9</sup> ± 0.11 × 10 <sup>9</sup>	21.26
45 <sup>a</sup>	3.85 × 10 <sup>7</sup> ± 0.15 × 10 <sup>7</sup>	6.35 × 10 <sup>8</sup> ± 0.20 × 10 <sup>8</sup>	16.49
60 <sup>b</sup>	3.92 × 10 <sup>7</sup> ± 0.11 × 10 <sup>7</sup>	5.03 × 10 <sup>8</sup> ± 0.13 × 10 <sup>7</sup>	12.83
60 <sup>a</sup>	1.76 × 10 <sup>7</sup> ± 0.16 × 10 <sup>7</sup>	3.68 × 10 <sup>7</sup> ± 0.17 × 10 <sup>7</sup>	2.09
75 <sup>b</sup>	1.81 × 10 <sup>7</sup> ± 0.08 × 10 <sup>7</sup>	2.94 × 10 <sup>7</sup> ± 0.16 × 10 <sup>7</sup>	1.62

<sup>a</sup> Cells irradiated with an irradiance of 1.0 J m<sup>-2</sup> s<sup>-1</sup>

<sup>b</sup> Cells irradiated with an irradiance of 0.5 J m<sup>-2</sup> s<sup>-1</sup>



5  $10^9$  PFU/ml, Table 3), was one order of magnitude higher than previously reported for *S. solfataricus* (Schleper et al. 1992). Therefore, the enhanced viability of the cell population affects viral replication and virions extrusion, thus influencing the increase of both copy number and viral titre.

Altogether these data highlight the necessity of standardizing the irradiation procedure to better compare results from different research groups.

Moreover, the establishment of a standardized protocol for SSV1 induction might have biotechnological potentialities since it allows the isolation of a huge amount of viral DNA as well as of viral particles to be employed for genetic manipulation and nanoparticles production, respectively. In this regard, viral particles from hyperthermophilic *Archaea* have been demonstrated to be exploitable for the fabrication of new nanoparticles. In particular, the rod-shaped virus SIRV2 (*Sulfolobus islandicus* rod-shaped virus 2) has been referred as a novel nanobuilding block (Evans 2009). Similarly, the virion of SSV1 can be considered, by its nature, a stable nanoparticle that is resistant to low pH and high temperature, and is, therefore, a good candidate for future biotechnological applications.

**Acknowledgments** Research in the authors' laboratories is supported by the grant "Programma F.A.R.O. IV tornata", founded by Università Federico II di Napoli and "Compagnia di San Paolo" (Naples Laboratory). We thank Dr Maria Ciaramella for providing us with the equipment for the UV irradiation.

## References

- Adler V, Polotskaya A, Kim J, Dolan L, Davis R, Pincus M, Ronai Z (1996) Dose rate and mode of exposure are key factors in JNK activation by UV irradiation. *Carcinogenesis* 17:2073–2076
- Albers SV, Jonuscheit M et al (2006) Production of recombinant and tagged proteins in the hyperthermophilic archaeon *Sulfolobus solfataricus*. *Appl Environ Microbiol* 72:102–111
- Bolton JR, Linden KG (2003) Standardization of methods for fluence (UV Dose) determination in bench-scale UV experiments. *J Environ Eng* 129:209–215
- Bondy-Denomy J, Davidson AR (2014) When a virus is not a parasite: the beneficial effects of prophages on bacterial fitness. *J Microbiol* 52:235–242
- Cannio R, Contursi P, Rossi M, Bartolucci S (1998) An autonomously replicating transforming vector for *Sulfolobus solfataricus*. *J Bacteriol* 180:3237–3240
- Cannio R, Contursi P, Rossi M, Bartolucci S (2001) Thermoadaptation of a mesophilic hygromycin B phosphotransferase by directed evolution in hyperthermophilic *Archaea*: selection of a stable genetic marker for DNA transfer into *Sulfolobus solfataricus*. *Extremophiles* 5:153–159
- Ceballos RM, Marceau CD, Marceau JO, Morris S, Clore AJ, Stedman KM (2012) Differential virus host-ranges of the *Fuselloviridae* of hyperthermophilic *Archaea*: implications for evolution in extreme environments. *Front Microbiol* 3:295
- Clore AJ, Stedman KM (2007) The SSV1 viral integrase is not essential. *Virology* 361:103–111
- Contursi P, Jensen J, Aucelli T, Rossi M, Bartolucci S, She Q (2006) Characterization of the *Sulfolobus* host-SSV2 virus interaction. *Extremophiles* 10:615–627
- Contursi P, Cannio R, Prato S, She Q, Rossi M, Bartolucci S (2007) Transcriptional analysis of the genetic element pSSVx: differential and temporal regulation of gene expression reveals correlation between transcription and replication. *J Bacteriol* 17:6339–6350
- Contursi P, Cannio R, She Q (2010) Transcription termination in the plasmid/virus hybrid pSSVx from *Sulfolobus islandicus*. *Extremophiles* 14:453–463
- Contursi P, D'Ambrosio K, Pirone L, Pedone E, Aucelli T, She Q, De Simone G, Bartolucci S (2011) C68 from the *Sulfolobus islandicus* plasmid-virus pSSVx is a novel member of the AbrB-like transcription factor family. *Biochem J* 435:157–166
- Contursi P, Fusco S, Limauro D, Fiorentino G (2013) Host and viral transcriptional regulators in *Sulfolobus*: an overview. *Extremophiles* 17:881–895
- Contursi P, Fusco S, Cannio R, She Q (2014a) Molecular biology of fuselloviruses and their satellites. *Extremophiles* 3:473–489
- Contursi P, Farina B, Pirone L, Fusco S, Russo L, Bartolucci S, Fattorusso R, Pedone E (2014b) Structural and functional studies of Stf76 from the *Sulfolobus islandicus* plasmid-virus pSSVx: a novel peculiar member of the winged helix-turn-helix transcription factor family. *Acids Res, Nucl.* doi:10.1093/nar/gku215
- Eilers BJ, Young MJ, Lawrence CM (2012) The structure of an archaeal viral integrase reveals an evolutionarily conserved catalytic core yet supports a mechanism of DNA cleavage in trans. *J Virol* 86:8309–8313
- Evans DJ (2009) Exploitation of plant and archaeal viruses in bionanotechnology. *Biochem Soc Trans* 37:665–670
- Fröls S, Gordon PM, Panlilio MA, Schleper C, Sensen CW (2007a) Elucidating the transcription cycle of the UV-inducible hyperthermophilic archaeal virus SSV1 by DNA microarrays. *Virology* 365:48–59
- Fröls S, Gordon PM, Panlilio MA, Duggin IG, Bell SD, Sensen CW, Schleper C (2007b) Response of the hyperthermophilic archaeon *Sulfolobus solfataricus* to UV damage. *J Bacteriol* 189:8708–8718
- Fröls S, White MF, Schleper C (2009) Reactions to UV damage in the model archaeon *Sulfolobus solfataricus*. *Biochem Soc Trans* 37:36–41
- Fusco S, She Q, Bartolucci S, Contursi P (2013) T(lys), a newly identified *Sulfolobus* spindle-shaped virus 1 transcript expressed in the lysogenic state, encodes a DNA-binding protein interacting at the promoters of the early genes. *J Virol* 87:5926–5936
- Götz D, Paytubi S, Munro S, Lundgren M, Bernander R, White MF (2007) Responses of hyperthermophilic crenarchaea to UV irradiation. *Genome Biol* 8:R220
- Iverson E, Stedman K (2012) A genetic study of SSV1, the prototypical fusellovirus. *Front Microbiol* 3:200
- Jonscheit M, Martusewitsch E, Stedman KM, Schleper C (2003) A reporter gene system for the hyperthermophilic archaeon *Sulfolobus solfataricus* based on a selectable and integrative shuttle vector. *Mol Microbiol* 48:1241–1252
- Kraft P, Kummel D, Oeckinghaus A, Gauss GH, Wiedenheft B, Young M, Lawrence CM (2004a) Structure of D-63 from *Sulfolobus* spindle-shaped virus 1: surface properties of the dimeric four-helix bundle suggest an adaptor protein function. *J Virol* 78:7438–7442
- Kraft P, Oeckinghaus A, Kummel D, Gauss GH, Gilmore J, Wiedenheft B, Young M, Lawrence CM (2004b) Crystal structure of F-93 from *Sulfolobus* spindle-shaped virus 1, a winged-helix DNA-binding protein. *J Virol* 78:11544–11550
- Lee DF, Drouin R, Pitsikas P, Rainbow AJ (2004) Detection of an involvement of the human mismatch repair genes *hMLH1* and *hMSH2* in nucleotide excision repair is dependent on UVC fluence to cells. *Cancer Res* 64:3865–3870

- Martin A, Yeats S, Janekovic D, Reiter WD, Aicher W, Zillig W (1984) SAV1, a temperate UV-inducible DNA virus-like particle from the archaeobacterium *Sulfolobus acidocaldarius* isolate B12. *EMBO J* 3:2165–2168
- Menon SK, Maaty WS, Corn GJ, Kwok SC, Eilers BJ, Kraft P, Gilitzer E, Young MJ, Bothner B, Lawrence CM (2008) Cysteine usage in *Sulfolobus* spindle-shaped virus 1 and extension to hyperthermophilic viruses in general. *Virology* 376:270–278
- Palm P, Schleper C, Grampp B, Yeats S, McWilliam P, Reiter WD, Zillig W (1991) Complete nucleotide sequence of the virus SSV1 of the archaeobacterium *Sulfolobus shibatae*. *Virology* 185:242–250
- Prangishvili D (2013) The wonderful world of archaeal viruses. *Annu Rev Microbiol* 8:565–585
- Redder P, Peng X, Brugger K, Shah SA, Roesch F, Greve B, She Q, Schleper C, Forterre P, Garrett RA, Prangishvili D (2009) Four newly isolated fuselloviruses from extreme geothermal environments reveal unusual morphologies and a possible interval recombination mechanism. *Environ Microbiol* 11:2849–2862
- Reiter WD, Palm P, Yeats S, Zillig W (1987) Gene expression in archaeobacteria: physical mapping of constitutive and UV-inducible transcripts from the *Sulfolobus* virus-like particle SSV1. *Mol Gen Genet* 209:270–275
- Reiter WD, Palm P, Zillig W (1988) Analysis of transcription in the archaeobacterium *Sulfolobus* indicates that archaeobacterial promoters are homologous to eukaryotic pol II promoters. *Nucleic Acids Res* 16:1–19
- Salerno V, Napoli A, White MF, Rossi M, Ciaramella M (2003) Transcriptional response to DNA damage in the archaeon *Sulfolobus solfataricus*. *Nucleic Acids Res* 31:6127–6138
- Schleper C, Kubo K, Zillig W (1992) The particle SSV1 from the extremely thermophilic archaeon *Sulfolobus* is a virus: demonstration of infectivity and of transfection with viral DNA. *Proc Natl Acad Sci USA* 89:7645–7649
- Snyder JC, Stedman K, Rice G, Wiedenheft B, Spuhler J, Young MJ (2003) Viruses of hyperthermophilic *Archaea*. *Res Microbiol* 154:474–482
- Stedman KM, Schleper C, Rumpf E, Zillig W (1999) Genetic requirements for the function of the archaeal virus SSV1 in *Sulfolobus solfataricus*: construction and testing of viral shuttle vectors. *Genetics* 152:1397–1405
- Stedman KM, She Q, Phan H, Arnold HP, Holz I, Garrett RA, Zillig W (2003) Relationships between fuselloviruses infecting the extremely thermophilic archaeon *Sulfolobus*: SSV1 and SSV2. *Res Microbiol* 154:295–302
- Wiedenheft B, Stedman KM, Roberto F, Willits D, Gleske AK, Zoeller L, Snyder J, Douglas T, Young M (2004) Comparative genomic analysis of hyperthermophilic archaeal *Fuselloviridae* viruses. *J Virol* 78:1954–1961
- Wolin EA, Wolin MG, Wolfe RS (1963) Formation of methane by bacterial extracts. *J Biol Chem* 238:2882–2886
- Yeats S, McWilliam P, Zillig W (1982) A plasmid in the archaeobacterium *Sulfolobus acidocaldarius*. *EMBO J* 1:1035–1038
- Zhan Z, Ouyang S, Liang W, Zhang Z, Liu ZJ, Huang L (2012) Structural and functional characterization of the C-terminal catalytic domain of SSV1 integrase. *Acta Cryst D* 68:659–670
- Zillig W, Stetter KO, Wunderl S, Schulz W, Priess H, Scholz I (1980) The *Sulfolobus*–“Caldariella” group: taxonomy on the basis of the structure of DNA-dependent RNA polymerases. *Arch Microbiol* 125:259–269





# CHAPTER III





## Chapter III:

### Industrial application of thermophilic and cellulolytic lactic acid producer, *Bacillus coagulans*

---

Lignocellulosic materials are indispensable for the carbon cycle and require numerous time-consuming processes, including mechanical, chemical, thermal, and biological treatments. In natural environments, the biodegradation of waste proceeds exclusively through biological processes and involves microbial communities, that produce a series of enzymes for the bioconversion process. In this context, the isolation of new microorganisms from agricultural waste represents a reservoir of hydrolytic enzymes, as well as a potential source of cell factories to be exploited in several industrial processes.

The paper 3-I “***Bacillus coagulans* MA-13: a promising thermophilic and cellulolytic strain for the production of lactic acid from lignocellulosic hydrolysate**” describes the isolation of a novel thermophilic and cellulolytic strain MA-13 from canned beans manufacturing residues. MA-13 is a facultative anaerobic bacterium with an optimal temperature of growth at 55°C, able to secrete soluble endo-1,4-β-glucanase enzymes into the culture supernatant. MA-13 was also characterized for the production of lactic acid from lignocellulose-derived sugars and in presence of lignocellulose hydrolysate inhibitors. For this reason, the manuscript 3-II “**Seed culture pre-adaptation improves lactic acid production of *Bacillus coagulans* MA-13 in Simultaneous Saccharification and Fermentation**” illustrates the setting up of simultaneous saccharification and fermentation (SSF) process based on the MA-13.

RESEARCH

Open Access



# *Bacillus coagulans* MA-13: a promising thermophilic and cellulolytic strain for the production of lactic acid from lignocellulosic hydrolysate

Martina Aulitto<sup>1,2†</sup>, Salvatore Fusco<sup>1,2†</sup> , Simonetta Bartolucci<sup>1</sup>, Carl Johan Franzén<sup>2\*</sup> and Patrizia Contursi<sup>1\*</sup>

## Abstract

**Background:** The transition from a petroleum-based economy towards more sustainable bioprocesses for the production of fuels and chemicals (circular economy) is necessary to alleviate the impact of anthropic activities on the global ecosystem. Lignocellulosic biomass-derived sugars are suitable alternative feedstocks that can be fermented or biochemically converted to value-added products. An example is lactic acid, which is an essential chemical for the production of polylactic acid, a biodegradable bioplastic. However, lactic acid is still mainly produced by *Lactobacillus* species via fermentation of starch-containing materials, the use of which competes with the supply of food and feed.

**Results:** A thermophilic and cellulolytic lactic acid producer was isolated from bean processing waste and was identified as a new strain of *Bacillus coagulans*, named MA-13. This bacterium fermented lignocellulose-derived sugars to lactic acid at 55 °C and pH 5.5. Moreover, it was found to be a robust strain able to tolerate high concentrations of hydrolysate obtained from wheat straw pre-treated by acid-catalysed (pre-)hydrolysis and steam explosion, especially when cultivated in controlled bioreactor conditions. Indeed, unlike what was observed in microscale cultivations (complete growth inhibition at hydrolysate concentrations above 50%), *B. coagulans* MA-13 was able to grow and ferment in 95% hydrolysate-containing bioreactor fermentations. This bacterium was also found to secrete soluble thermophilic cellulases, which could be produced at low temperature (37 °C), still retaining an optimal operational activity at 50 °C.

**Conclusions:** The above-mentioned features make *B. coagulans* MA-13 an appealing starting point for future development of a consolidated bioprocess for production of lactic acid from lignocellulosic biomass, after further strain development by genetic and evolutionary engineering. Its optimal temperature and pH of growth match with the operational conditions of fungal enzymes hitherto employed for the depolymerisation of lignocellulosic biomasses to fermentable sugars. Moreover, the robustness of *B. coagulans* MA-13 is a desirable trait, given the presence of microbial growth inhibitors in the pre-treated biomass hydrolysate.

**Keywords:** Lactic acid, *Bacillus coagulans*, Thermophilic, Fermentation, Robustness, Cellulolytic enzymes, Wheat straw hydrolysate, Enzymes secretion

\*Correspondence: franzen@chalmers.se; contursi@unina.it

<sup>†</sup>Martina Aulitto and Salvatore Fusco contributed equally to the work

<sup>1</sup> Dipartimento di Biologia, Università degli Studi di Napoli Federico II, Naples, Italy

<sup>2</sup> Division of Industrial Biotechnology, Department of Biology and Biological Engineering, Chalmers University of Technology, 412 96 Gothenburg, Sweden



© The Author(s) 2017. This article is distributed under the terms of the Creative Commons Attribution 4.0 International License (<http://creativecommons.org/licenses/by/4.0/>), which permits unrestricted use, distribution, and reproduction in any medium, provided you give appropriate credit to the original author(s) and the source, provide a link to the Creative Commons license, and indicate if changes were made. The Creative Commons Public Domain Dedication waiver (<http://creativecommons.org/publicdomain/zero/1.0/>) applies to the data made available in this article, unless otherwise stated.

## Background

Given the finite nature of fossil-derived fuels and chemicals as well as their negative impact on the environment, it is important to develop technologies for the use of alternative and more eco-friendly feedstocks [1]. For instance, lignocellulosic biomasses from municipal, agricultural and forestry origins are continuously being generated by several anthropic activities [2]. Therefore, they are relatively inexpensive and abundant carbon sources that can be exploited for the production of biofuels and biochemicals, without giving a net contribution to the emissions of CO<sub>2</sub> into the atmosphere. Conversely, they can negatively contribute to the environmental pollution if not properly disposed of, recycled or valorised [3].

Currently, the global renewable biochemicals market is growing in size and importance, with polylactic acid (PLA) being one of the main shares among bioplastics [4]. PLA is a polymer of D- and L-lactic acid (LA), the latter of which can be obtained by fermentation of renewable feedstocks [5, 6]. Currently, several carbohydrates and nitrogenous materials are commercially used for the production of lactic acid, e.g. sucrose-containing syrups, juices and molasses; lactose from whey, maltose, glucose and mannitol [7]. Moreover, several *Lactobacillus* species have been recently employed for the production of LA from starch-containing materials. However, the use of such biomasses may compete with the supply of foods and feeds [8]. To overcome this conflict, non-food sources of fermentable sugars, i.e. lignocellulosic biomasses, are suitable alternatives [9]. The major component of these residues is cellulose (35–50%), which occurs together with hemicellulose (20–40%) and lignin (10–30%) at varying compositions that depend on the plant source [10]. Cellulose is a homopolymer consisting of  $\beta$ -1,4-linked D-glucose monomers. Unlike starch, it is not directly accessible as a carbon and energy source for the majority of microorganisms.

In nature, biodegradation of lignocellulose is an extremely slow and complex process that involves the concerted action of many microbial decomposers [11]. However, a more effective deconstruction process has been set up at industrial scale and includes three steps: (1) pre-treatment [12]; (2) enzymatic or chemical saccharification and (3) fermentation [13]. In this context, a major bottleneck is represented by the formation of toxic compounds during chemical and thermal pre-treatments [14]. These inhibitory compounds are classified into three major groups: furaldehydes (e.g. furfural and 5-hydroxymethylfurfural), weak acids (e.g. acetic acid, formic acid and levulinic acid) and phenolics (e.g. vanillin, syringaldehyde and coniferyl aldehyde) [15]. Such chemicals hamper microbial growth and affect the fermentation fitness, thus profoundly impacting the economy of the

whole process [16]. One strategy to remove the inhibitors is to include a detoxification step [17] but that, in turn, can lead to an increase of production costs [18]. In order to overcome this drawback, an alternative approach is to exploit the natural and/or induced tolerance of fermenting microorganisms (bacteria and yeasts) [16, 19]. In this perspective, it is important to isolate and characterise robust microorganisms for the production of eco-friendly chemicals, such as lignocellulose-based LA for PLA manufacturing [9, 20].

Besides being employed for fermentation, some fungal and bacterial strains are also sources of carbohydrate-active enzymes [21]. The use of biocatalysts for the saccharification of lignocellulosic biomass represents a more sustainable approach than the chemical counterparts [22]. Moreover, if the reaction conditions of both pre-treatment and saccharification are taken into account (i.e. temperature, pH, pressure and presence of inhibitory chemicals), thermostable enzymes are appropriate candidates [23]. Indeed, their operational stability at high temperature allows reducing the enzymes loading for the saccharification and, in turn, makes the production process more economically feasible [24]. In this regard, bacteria of the genus *Bacillus* are well-known to secrete various hydrolytic enzymes such as proteases, amylases and cellulases [25–27]. Therefore, thermophilic *Bacillus* strains might represent reservoirs of novel and robust cellulolytic enzymes.

The saccharification and fermentation phases can be carried out sequentially in a set-up known as separate hydrolysis and fermentation (SHF). Here, the plant cell wall polymers are first hydrolysed by lignocellulolytic enzymes to monomeric sugars which are then fermented by the microbial cells in a separate process [28]. However, the enzymes can be inhibited by the high concentrations of the hydrolysed products (monomeric sugars) achieved during saccharification [29]. For this reason, simultaneous saccharification and fermentation (SSF) has been developed to combine these two processes in the same batch, in order to alleviate the enzymatic inhibition [30]. Recently, consolidated bioprocessing (CBP), a one-step conversion of lignocellulosic biomass into the desired final product, is becoming a commercially attractive alternative [31]. In CBP, a native or genetically engineered microbial strain is used both for enzyme production, leading to hydrolysis of the complex carbohydrates, and at the same time, for fermentation of the released sugars into valued-added products [31, 32].

Here, we report the isolation and characterisation of a new thermophilic and cellulolytic *Bacillus coagulans* strain (MA-13), which is able to (1) secrete cellulolytic enzymes, (2) ferment lignocellulose-derived sugars to lactic acid and (3) withstand the toxicity of inhibitors



present in the liquid fraction (hydrolysate) of wheat straw pre-treated by acid-catalysed hydrolysis and steam explosion. The above-mentioned features, together with the possibility to implement new traits through genetic engineering of *B. coagulans* [33], make this microorganism a potential workhorse for the production of lactic acid from lignocellulosic raw materials.

## Methods

### Isolation and screening of cellulolytic microorganisms

The biological sample used in this study was in the form of an agricultural residue from a canned beans manufacturing process. In order to isolate cellulolytic microorganisms, a few grams of this waste residue were resuspended in 100 ml of sterile double-distilled water (ddH<sub>2</sub>O), placed in a 250-ml Erlenmeyer flask with a long neck and incubated at 60 °C with a shaking rate of 180 rpm for 30 min, using a MaxQTM 4000 Benchtop Orbital Shaker (Thermo Scientific). The waste suspension was serially diluted (tenfold) using sterile ddH<sub>2</sub>O and 150 µl from each dilution was spread on plates of solid carboxymethyl-cellulose (CMC; Sigma-Aldrich) containing screening medium (CMC-SM, Additional file 1: Table S1). After overnight incubation at 60 °C in a dry oven, microbial colonies appeared on the surface of the plates. Hundreds of these colonies were picked using sterile needles, transferred into tubes containing liquid CMC-SM and incubated at 60 °C with a shaking rate of 180 rpm. Microbial growth was spectrophotometrically monitored at an optical density of 600 nm (OD<sub>600</sub>) over a time span of 18 h. Only the colonies able to propagate in this liquid medium were also tested for the capability to metabolise filter paper (FP), using the screening medium FP-SM (Additional file 1: Table S1). To test if modifications of the FP texture could occur only as consequence of the stirring and high temperature applied, a control flask containing FP-SM without cells was incubated for the same time span at 60 °C.

### Identification, physiological characterisation and phylogenetic analysis of a new cellulolytic *Bacillus coagulans* strain

The best-performing isolate was identified as a strain of *B. coagulans* by 16S rRNA-encoding gene sequencing and cellular fatty acid analysis performed by a certified laboratory (DSMZ), and it is hereafter referred to as *B. coagulans* MA-13. Furthermore, the 16S sequence (GenBank accession number; MF373392) was used to search the GenBank database by means of BLASTn [34]. 16S rRNA sequences of several representative *B. coagulans* strains were retrieved, aligned with T-COFFEE and a phylogenetic tree (1000 bootstrap replicates) was constructed with the MEGA6 software using the Maximum

Likelihood method based on the Tamura–Nei model [35]. The 16S sequence from *Bacillus circulans* strain 5S5 was used as an outgroup to root the tree.

To further characterise this strain, standard physiological and biochemical tests were performed including: (1) motility assay; (2) Gram staining; (3) the Voges–Proskauer (VP) test; (4) catalase, oxidase, lecithinase, phenylalanine deaminase and arginine dihydrolase activity assays; (5) nitrate reduction test; (6) indole production; (7) citrate and propionate utilisation as well as (8) organic acids and gas production from glucose. Additionally, the strain was tested for its ability to hydrolyse different biopolymers, such as casein, gelatine, starch and Tween 80.

### Determination of the optimal temperature of growth

To assess the effect of the temperature on the growth of *B. coagulans* MA-13, a pre-culture was cultivated using LB medium in a 250-ml Erlenmeyer flask at 60 °C and shaking speed of 180 rpm for 4 h (up to an OD<sub>600</sub> value of 1.5). This latter was used to seed 50-ml aliquots of CMC-SM medium (Additional file 1: Table S1) at an initial OD<sub>600</sub> of 0.08. These cultures were then incubated at 37, 50, 55 and 60 °C, in 250-ml Erlenmeyer flasks with a long neck (to avoid evaporation) in a rotary shaker at 180 rpm. Optical density was measured regularly over a time span of 15 h. The steepest part of the ln (OD<sub>600</sub>) curves, assessed by at least four measurement points, was used to calculate both the maximum specific growth rates ( $\mu_{\max}$ ) and the coefficient of determination ( $R^2$ ). Three independent replicates of the experiment were performed using different precultures.

### Determination of endoglucanase activity in the culture supernatant and soluble proteins detection

The strain *B. coagulans* MA-13 was cultivated in liquid CMC-SM (Additional file 1: Table S1) at 55 °C up to the stationary phase (about 15 h) and harvested by centrifugation at 3000×g for 15 min. Proteins secreted by *B. coagulans* MA-13 were precipitated by gradually adding (NH<sub>4</sub>)<sub>2</sub>SO<sub>4</sub> into the cell-free culture supernatant, reaching a final concentration of 90% (w/v). After stirring for 1 h, the supernatant was centrifuged at 5000×g for 15 min (4 °C) and the obtained protein pellet was resuspended and dialysed in 50 mM Tris–HCl pH 7.0 (AppliChem). Protein concentration was determined according to Bradford assay [36], using serial dilutions of bovine serum albumin as standards. A preliminary detection of endoglucanase enzymes in the cell-free culture supernatant was performed by means of the CMC-hydrolysis spot assay. The concentrated and dialysed culture supernatant was spotted (5 µg of total proteins) on agar plates containing 1% (w/v) CMC and incubated at 55 °C for 30 min. In parallel, a positive control of degradation

was performed, by spotting the same amount of a commercially available enzyme solution (Cellulases from *Trichoderma reesei* ATCC 26921; Sigma-Aldrich). After staining with 0.1% (w/v) Congo Red (Sigma-Aldrich), degradation haloes were revealed by washing the plate surface with 1 M NaCl (AppliChem) and fixing with 5% (v/v) acetic acid (Carlo Erba).

To confirm the presence of soluble proteins, the concentrated and dialysed cell-free culture supernatant was subjected to a two-step purification procedure through cation-exchange and size-exclusion chromatography. To achieve this aim, the sample was loaded onto a 1-ml cation-exchange Resource S column (GE Healthcare) connected to a fast-performance liquid chromatography system (ÄKTA Explorer; GE Healthcare). The column was equilibrated with 50 mM Tris-HCl pH 7.0 and the elution was performed with a linear gradient of NaCl from 0 to 800 mM. Chromatography fractions were tested for endo-1,4- $\beta$ -glucanase activity, using Azo-CMC as substrate (Megazyme) and following the supplier's instructions. All positive fractions were pooled together in the same tube, dialysed against 50 mM Tris-HCl and 200 mM NaCl, pH 7.0 and concentrated to a final volume of approximately 0.2 ml, using a Centricon® membrane with a 3-kDa cut-off (Millipore). The concentrated sample was subjected to size-exclusion chromatography using a Superdex PC75 column (3.2 by 30 cm; GE Healthcare) equilibrated with 50 mM Tris-HCl pH 7.0 and eluted at a flow rate of 0.04 ml/min. Protein fractions displaying Azo-CMC activity were pooled and analysed by 12% SDS-PAGE [37].

#### Time course of the enzyme secretion into the culture supernatant

To set up a cultivation medium for the induction of enzymes secretion, *B. coagulans* MA-13 was grown at 55 °C in media containing: (1) glycine-buffered Brock's basal salt solution [38–41]; (2) 0.2% (w/v) nitrogen source [either (NH<sub>4</sub>)<sub>2</sub>HPO<sub>4</sub>, tryptone or yeast extract] and (3) 0.5% (w/v) CMC. Among the nitrogen sources, tryptone was found to better induce the secretion of enzymes and the corresponding medium was named carboxymethyl-cellulose induction medium (CMC-IM, Additional file 1: Table S1). CMC-IM was used to investigate if *B. coagulans* MA-13 was able to secrete endoglucanases at a lower temperature, by performing a time course analysis at 37 °C. In particular, 50 ml of CMC-SM was seeded with a glycerol stock of *B. coagulans* MA-13 and incubated under constant shaking (180 rpm) at 55 °C for 4 h (up to 1.5 OD<sub>600</sub>). This pre-culture was then used to inoculate a 50-ml aliquot of CMC-IM at an initial OD<sub>600</sub> of 0.08. This second phase of cultivation was carried out at 37 °C and 180 rpm. In parallel, LB medium was used as a

negative control of enzyme secretion. Aliquots were regularly withdrawn to measure the optical density as well as to obtain cell-free supernatants through centrifugation at 4000×g for 10 min. Endo-1,4- $\beta$ -glucanase activity of the cell-free supernatants was assayed at three different temperatures (37, 50 and 60 °C), using Azo-CMC as substrate (Megazyme) and following supplier's instructions. Three independent replicates of this experiment were carried out using different precultures.

#### Comparison of *Bacillus coagulans* MA-13 growth on different sugars and hydrolysate concentrations

The growth of *B. coagulans* MA-13 was monitored in microscale conditions (145  $\mu$ l) at 55 °C and pH 5.5, using the Bioscreen C MBR equipment (Oy Growth Curves Ab Ltd). Although the bacterium shows an optimal growth at pH 6.0, it is also able to propagate well at pH 5.5 (Additional file 1: Figure S1). Therefore, subsequent characterisations were carried out at pH 5.5, since acidic conditions are commonly used for the microbial production of LA at industrial scale. To test lignocellulose-derived sugars utilisation, media supplemented with trace metals and vitamins [42] and containing different sugars were used (Additional file 1: Table S1).

The strain robustness was tested by cultivations in the liquid fraction (hydrolysate) of a wheat straw slurry, pretreated by sulfuric acid-catalysed hydrolysis and steam explosion as described elsewhere [43] and containing inhibitors such as 3.8 g/l of acetic acid, 4.0 g/l of furfural and 1.4 g/l of 5-hydroxymethylfurfural (HMF); concentrations were determined by HPLC (see below). The pH of the hydrolysate was adjusted to 5.5 using concentrated NaOH, before being mixed with the above-mentioned medium and molasses as a source of sucrose [43] to achieve concentrations of hydrolysate ranging from 10 to 80% (v/v). Prior to microscale cultivations, *B. coagulans* MA-13 was grown into the stationary phase in LB medium at 55 °C and shaking speed of 180 rpm. To remove nutrients leftover from the LB medium, the culture was centrifuged at 3000×g for 10 min at room temperature and the cell pellet was resuspended in 1% (w/v) NaCl to an OD<sub>600</sub> value of about 3.0. This suspension was used to seed each well of the Bioscreen C plate at an initial OD<sub>600</sub> of about 0.1. To avoid sample evaporation, the multi-well plate was sealed with a transparent adhesive tape. Then, it was placed into a Bioscreen C MBR apparatus set at high amplitude and fast speed. At 20-min intervals, mixing was stopped for 5 s prior to each optical measurement (OD<sub>600</sub>).

The recorded cell density values were converted to equivalent OD<sub>600</sub> using the following Eq. (1):

$$\text{OD}_{\text{observed}} = \frac{\text{OD}_{\text{bioscreen}}}{\text{Pathlength (cm)} \times 1.32} \quad (1)$$



The non-linear correlation between optical density and cell density was corrected using Eq. (2) [40]:

$$\text{OD}_{\text{corrected}} = \text{OD}_{\text{observed}} + 0.449 \times \text{OD}_{\text{observed}}^2 + 0.191 \times \text{OD}_{\text{observed}}^3 \quad (2)$$

The steepest part of the  $\ln(\text{OD}_{\text{corrected}})$  curve, using 12 measurement points, was used to calculate both the maximum specific growth rate ( $\mu_{\text{max}}$ ) and the coefficient of determination ( $R^2$ ). For each experimental condition, a minimum of nine technical replicates were included in the plate. Moreover, two independent replicates were carried out using different starting seed cultures (for a total of 18 replicates).

### Fermentation

Fermentations were performed in 3.6 l bioreactor vessels (INFORS HT), autoclaved at 121 °C for 20 min before usage. Inoculum cultures were grown in 500 ml of LB medium in a 2.0 l flask at 55 °C and shaking speed of 180 rpm for 3–4 h (up to an  $\text{OD}_{600}$  value of about 1.0–1.3). Culture aliquots (about 100 ml) were centrifuged at  $4000 \times g$  for 10 min and the obtained bacterial pellets were resuspended using 20 ml of sterile medium collected from each bioreactor vessel. Fermentations were initiated by inoculating the cell suspension into the bioreactors through a sterile rubber septum at an initial  $\text{OD}_{600}$  of about 0.1. The composition of the batch fermentation media is reported in the Additional file 1: Table S1. Each batch fermentation was carried out in 1 l medium at 55 °C at a stirring speed of 500 rpm, until complete sucrose consumption. Nitrogen was sparged at 1 VVM (volume of gas/volume of medium/minute), and pH was kept at 5.5 by adding 3 M NaOH. Antifoam 204 (Sigma-Aldrich) was added as required. Optical density

was spectrophotometrically measured at 600 nm and the steepest part of the  $\ln(\text{OD}_{600})$  curves, estimated by linear regression over five points, was used to calculate both the maximum specific growth rates ( $\mu_{\text{max}}$ ) and the coefficient of determination ( $R^2$ ). The concentrations of sucrose and fermentation products (lactate, acetate and acetoin) were determined by HPLC analysis of the culture supernatant, as described below.

### HPLC analysis

Culture samples were centrifuged at  $4000 \times g$  for 5 min and supernatants were filtered using 0.2  $\mu\text{m}$  sterile filters (VWR®). High-performance liquid chromatography (HPLC) and quantification of sucrose, lactate, acetate and acetoin was performed by means of an UltiMate 3000 HPLC system equipped with a variable wavelength absorbance detector set at 210 nm (Dionex) and an IR-101 refractive index detector (Shodex), using a Rezex ROA column (Phenomenex). The analysis was carried out at a column temperature of 80 °C, using 5 mM  $\text{H}_2\text{SO}_4$  as the mobile phase at a flow rate of 0.8 ml/min throughout the analysis.

## Results

### Isolation, identification and characterisation of a new *Bacillus coagulans* strain

Hundreds of colonies from CMC-SM plates, seeded with an agricultural waste suspension, were tested for the ability to grow in liquid medium. In this condition, only five isolates could propagate in CMC-SM, thus confirming their ability to metabolise the polymeric carboxymethyl-cellulose substrate. These cellulolytic isolates were cultivated also in liquid FP-SM medium (Fig. 1a). Among these, the one named MA-13 achieved the highest optical density ( $\text{OD}_{600}$ ) in a time span of 24 h, when cultivated in

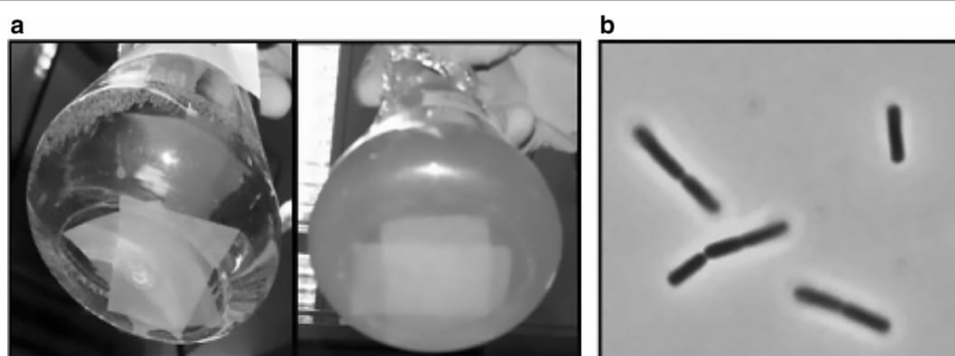


**Fig. 1** Isolation of the cellulolytic strain MA-13. **a** *Bacillus coagulans* MA-13 culture after overnight growth in FP-SM (right side) and negative control without cells (left side). **b** Light microscope observation of *B. coagulans* MA-13 cells when cultivated in CMC-SM (Additional file 1: Table S1)



both CMC-SM and FP-SM media. Subsequently, MA-13 was identified as a strain of *B. coagulans* through 16S rRNA-encoding gene sequencing and cellular fatty acids profiling (DSMZ). The phylogenetic tree based on 16S rRNA sequences showed two main branches (Group I and Group II) that included a similar number of *B. coagulans* strains. Although *B. coagulans* MA-13 clustered in Group I, it appears more phylogenetically distant from the other members of the same branch, similarly to the strain ATCC7050 (Fig. 2).

*Bacillus coagulans* MA-13 turned out to be a facultative anaerobic, spore-forming, Gram-positive, motile, rod-shaped bacterium (Fig. 1b; Table 1), which hydrolyses biopolymers such as gelatine, starch and casein (Table 1). Moreover, like other *Bacillus* species, MA-13 is capable of denitrification, the respiratory reduction of nitrate and nitrite to  $N_2O$  (Table 1). To assess its optimal temperature of growth, *B. coagulans* MA-13 was cultivated in liquid CMC-SM at different temperatures (Fig. 3a) and it showed the highest relative growth rate at 55 °C (Fig. 3b).

### *Bacillus coagulans* MA-13 secretes cellulases into the culture supernatant

The ability of *B. coagulans* MA-13 to utilise both CMC and FP as carbon sources suggested that this bacterium might produce cellulolytic enzymes for the hydrolysis of these substrates. To understand whether these enzymes were secreted into the medium, the cellulolytic activity of the cell-free supernatant was assayed. To this end, *B. coagulans* MA-13 was cultivated at 55 °C in liquid CMC-SM for 15 h, and the concentrated cell-free supernatant was spotted on CMC-agar plates. The appearance of a degradation halo after Congo Red staining proved the presence of cellulases in the culture supernatant (Fig. 4a). To further confirm the secretion of soluble enzymes, the concentrated cell-free supernatant was dialysed and partially purified through cation-exchange and size-exclusion chromatography. All the fractions were assayed for endo-1,4- $\beta$ -glucanase activity and the positive ones were pooled, concentrated and analysed on SDS-PAGE (Fig. 4b). Although several protein bands were visible on the gel, the predominant one migrated in the range

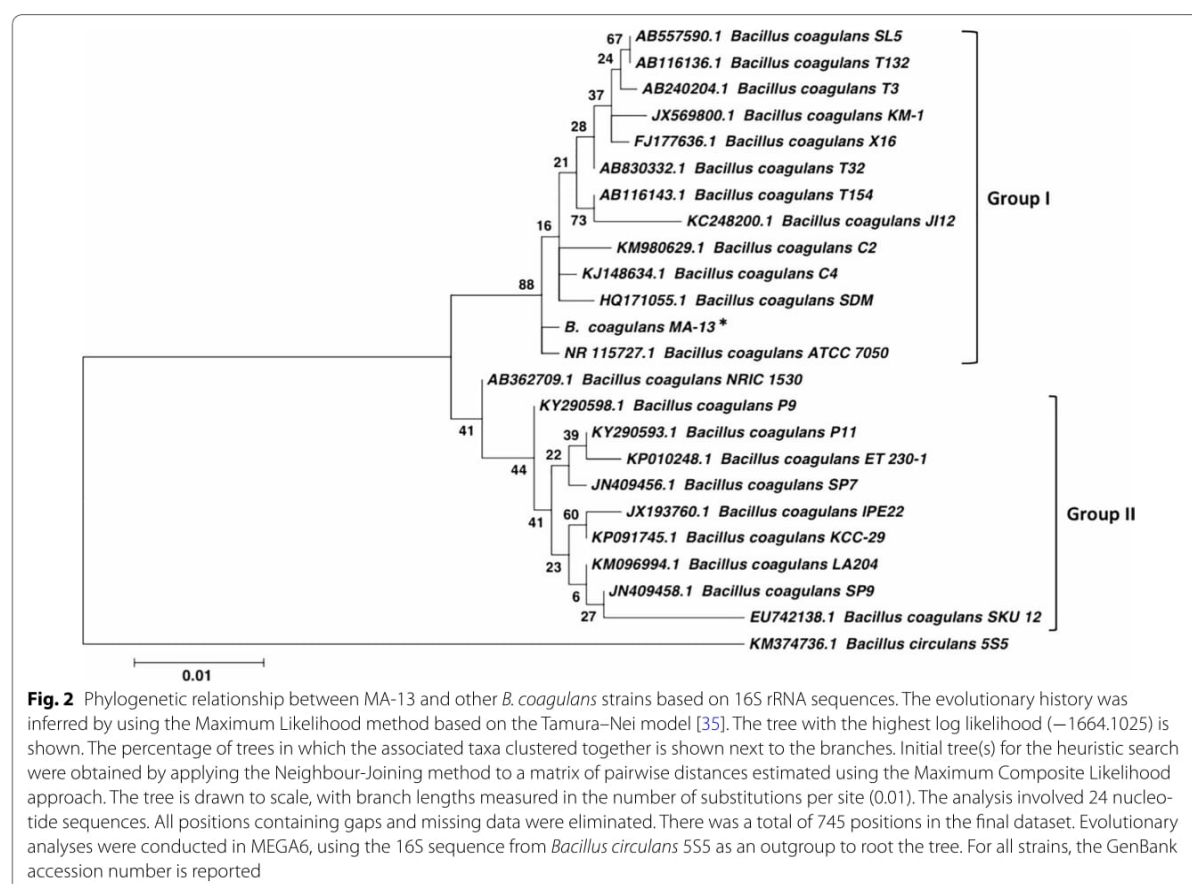


**Table 1 Physiological and biochemical properties of *Bacillus coagulans* MA-13**

Features	Reaction	Carried out
Gram staining	+	by DSMZ
Voges–Proskauer reaction	—	by DSMZ
Gas from glucose	—	by DSMZ
Spores	+	by DSMZ
Motility	+	by DSMZ
Denitrification		
$\text{NO}_3^- \rightarrow \text{NO}_2^-$	+	by DSMZ
Indol reaction	—	by DSMZ
Oxidase	—	by DSMZ
Growth		
30 °C	+	by DSMZ
37 °C	+	in this work
40 °C	+	by DSMZ
50 °C	+	by DSMZ and in this work
55 °C	+	in this work
60 °C	+	in this work
Growth in medium pH 4.5	+	in this work
pH 5.0	+	in this work
pH 5.5	+	in this work
pH 5.7	+	by DSMZ
pH 6.0	+	in this work
pH 7.0	+	in this work
NaCl 2%	+	by DSMZ
NaCl 5%	—	by DSMZ
Lysozyme-broth	+	by DSMZ
Aerobic	+	in this work
Anaerobic	+	by DSMZ and in this work
Acid fermentation of		
D-glucose	+	by DSMZ and in this work
D-mannose	+	in this work
D-galactose	—	in this work
D-arabinose	—	by DSMZ and in this work
L-arabinose	—	in this work
D-xylose	—	by DSMZ and in this work
D-mannitol	—	by DSMZ
D-fructose	+	by DSMZ and in this work
D-melibiose	+	in this work
D-cellobiose	+	in this work
Lactose	+	in this work
Hydrolysis of		
Casein	+	by DSMZ
Gelatine	+	by DSMZ
Starch	+	by DSMZ
Carboxymethyl-cellulose	+	in this work
Filter paper	+	in this work
Tween 80	—	by DSMZ
Enzymes production		
Phenylalanine deaminase	—	by DSMZ
Arginine dihydrolase	—	by DSMZ

**Table 1 continued**

Features	Reaction	Carried out
Lecithinase	—	by DSMZ
Catalase	+	by DSMZ
Endo-1,4-β-glucanase	+	in this work

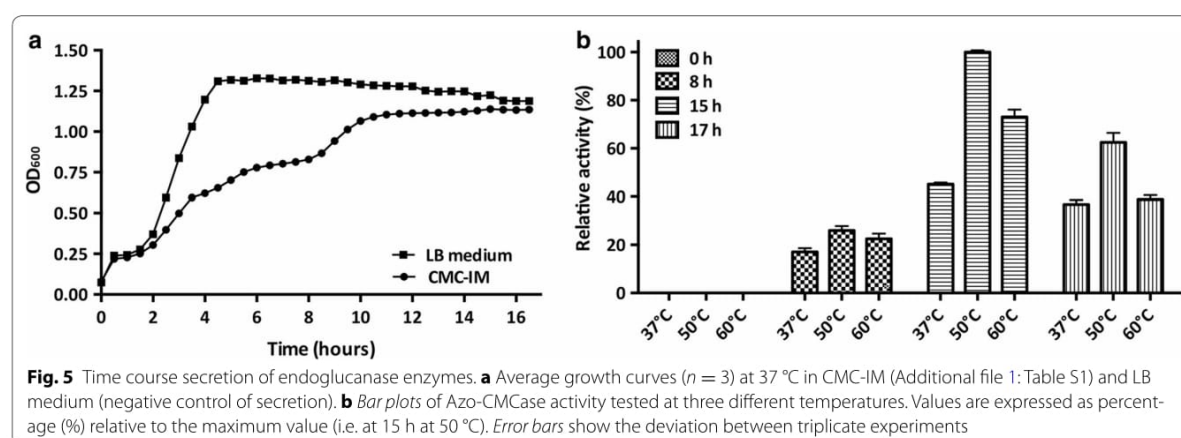
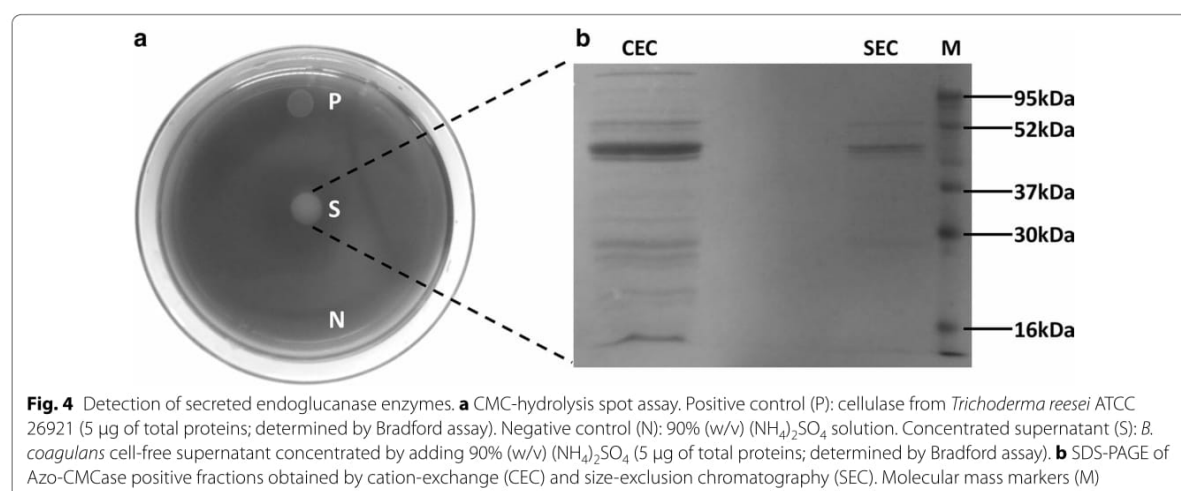
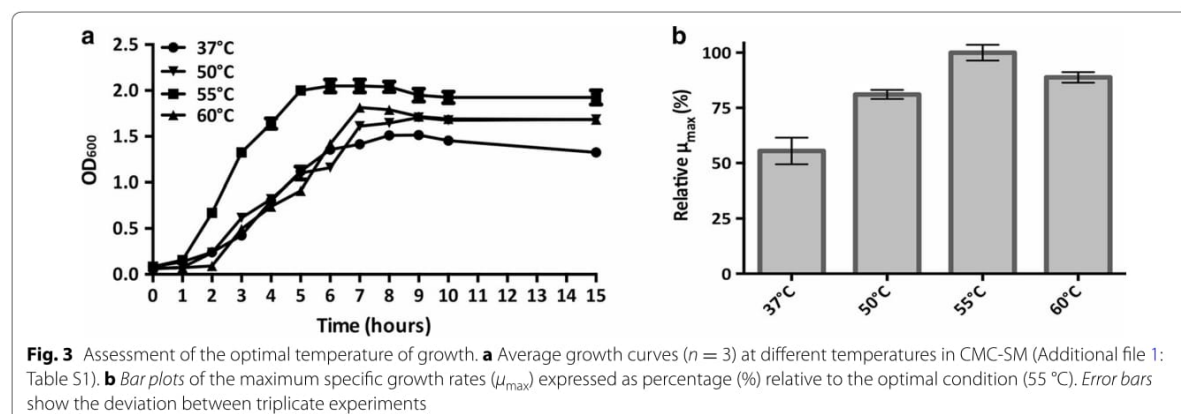
+, positive reaction; —, negative reaction

of 40–50 kDa, which is consistent with the molecular weight of other bacterial cellulases [29, 45, 46].

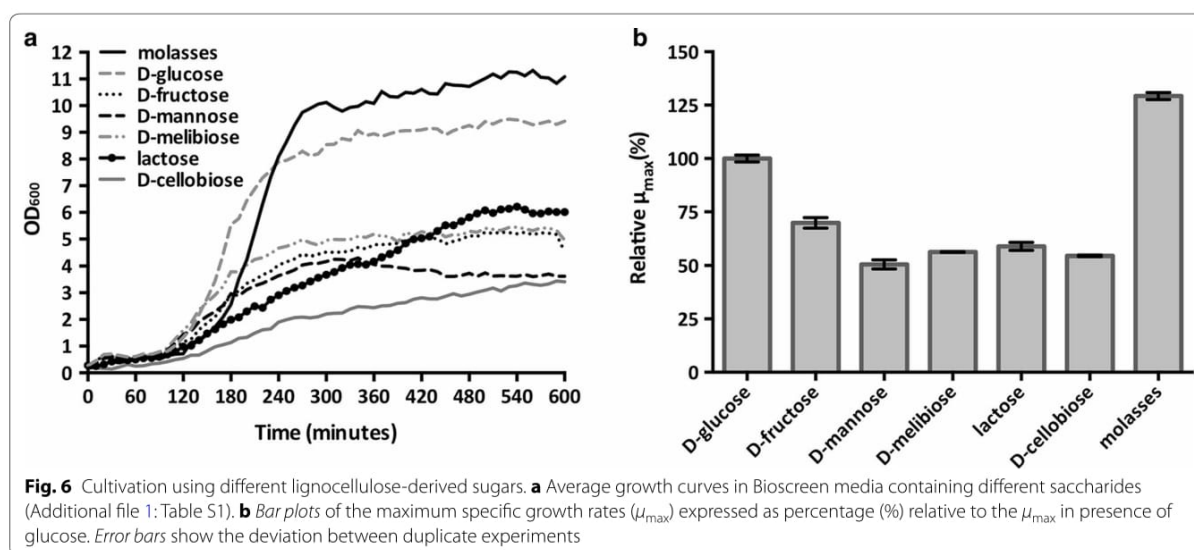
To assess the production of enzymes at a lower temperature, *B. coagulans* MA-13 was cultivated at 37 °C in both CMC-IM and in LB medium; this latter as a negative control of secretion (Fig. 5a). As expected, the LB medium culture supernatant did not show any endo-1,4-β-glucanase activity when tested by Azo-CMC assay (data not shown). When the bacterium was grown in CMC-IM, no Azo-CMC activity was detected during the first 7 h of cultivation (data not shown). Nevertheless, after a short stationary phase (Fig. 5a, 6–8 h), endo-1,4-β-glucanase activity was observed in the culture supernatant (Fig. 5b, 8 h). The enzymes secretion was accompanied by the onset of an additional short exponential growth phase (Fig. 5a, 8–10 h) and the highest enzymatic activity was detected after 15 h of cultivation (Fig. 5b). Furthermore, the enzymes in the supernatant were found to be active at three different temperatures (i.e. 37, 50 and 60 °C), although they performed better at 50 °C (Fig. 5b). Interestingly, when *B. coagulans* MA-13 was cultivated at its optimal temperature of growth (55 °C), the secretion of enzymes into the culture supernatant was comparable to that of cells cultivated at 37 °C (data not shown).

#### ***Bacillus coagulans* MA-13 is able to metabolise lignocellulose-derived sugars**

Several Gram-positive bacteria are able to ferment sugars to a wide palette of organic acids [47]; among these, *B. coagulans* is a well-known LA producer [9, 24, 48, 49]. For this reason, the ability of the strain MA-13 to utilise different sugars and to produce LA was tested. In particular, this bacterium was cultivated on several lignocellulose-derived monosaccharides (D-glucose, D-mannose, D-fructose, L-arabinose, D-xylose and D-galactose) and disaccharides (D-melibiose, D-cellobiose and lactose). Except for D- and L-arabinose, D-xylose and D-galactose, *B. coagulans* MA-13 was found to grow using all the sugars tested (Fig. 6a). Since glucose was the preferred carbon source, yielding the highest maximum specific growth rate ( $\mu_{\max}$ ), it was used as reference (100%) to calculate the relative  $\mu_{\max}$  for the other saccharides. Compared to D-glucose, the  $\mu_{\max}$  for D-fructose was about 30% lower, whereas for D-mannose, D-melibiose,







D-cellobiose and lactose it was reduced by about 50% (Fig. 6b). *B. coagulans* MA-13 was also cultivated using the commonly used and relatively inexpensive carbon source, molasses, which contains primarily sucrose [43]. Interestingly, in this case, the relative  $\mu_{\max}$  was even higher than that showed for D-glucose (Fig. 6b).

To assess the presence of organic compounds typically produced either aerobically (acetate and acetoin) or anaerobically (lactate), an end-point HPLC analysis was carried out for all the tested conditions. However at rather low concentration these compounds were produced from all the sugars analysed (Additional file 1: Table S2), except for D-cellobiose that yielded only acetate and acetoin. The lack of control over important parameters such as aeration, pH and proper mixing under microscale conditions can explain the low concentration of the organic compounds. On the other hand, their concomitant presence can be accounted to the microaerophilic environment of the plate, which may allow both aerobic and anaerobic metabolism.

#### The new isolate is tolerant to a steam-exploded wheat straw hydrolysate

The microscale cultivation at increasing concentration of steam-exploded wheat straw hydrolysate [43] was performed to test the inhibitory effect on the bacterium propagation (Fig. 7a) and on the production of LA (Additional file 1: Table S3). The relative  $\mu_{\max}$  was reduced compared to the control, but in a non-linear fashion (Fig. 7b). Only a slight reduction of the relative  $\mu_{\max}$  to about 80% was observed at low hydrolysate concentrations (10 and 20%, Fig. 7b). However, at both 30 and 40% concentrations of

hydrolysate, a drop in the  $\mu_{\max}$  by about 50% was detected (Fig. 7b). Only a further 10% reduction of the  $\mu_{\max}$  was observed at 50% hydrolysate (Fig. 7b), whilst the growth was completely inhibited at 60% hydrolysate (data not shown). Moreover, the end-point HPLC analysis showed that the production of lactate was negatively affected by the presence of hydrolysate (Additional file 1: Table S3).

#### *Bacillus coagulans* MA-13 is less inhibited by the hydrolysate in a controlled batch fermentation set-up

Although microscale cultivation using Bioscreen C allows assessing several conditions simultaneously, this system suffers from the lack of regulation of crucial parameters such as aeration and pH control. For this reason, both bacterial growth and lactic acid production were studied in controlled bioreactor conditions (Fig. 8). When anaerobically cultivated in a hydrolysate-free medium (Fig. 8a), *B. coagulans* MA-13 consumed all the sucrose in 16 hours, with a yield of  $0.92 \text{ g}_{\text{lactate}}/\text{g}_{\text{sucrose}}$ . The average and maximum volumetric productivities of LA were 1.40 and 2.55 g/l/h, respectively, whereas the average and maximum specific productivities were 0.28 and 0.50 g/l/h/OD, respectively (Table 2).

Unlike what was observed in microscale cultivations (Fig. 7b), the  $\mu_{\max}$  was only slightly reduced in 30 and 50% hydrolysate media (Table 2) when grown under controlled bioreactor conditions (Fig. 8b–d). Interestingly, the microbial growth was never completely inhibited, but was only reduced by about 40% even at the highest hydrolysate concentration (Table 2). On the other hand, the increase in the hydrolysate concentration in the fermentation medium was accompanied by

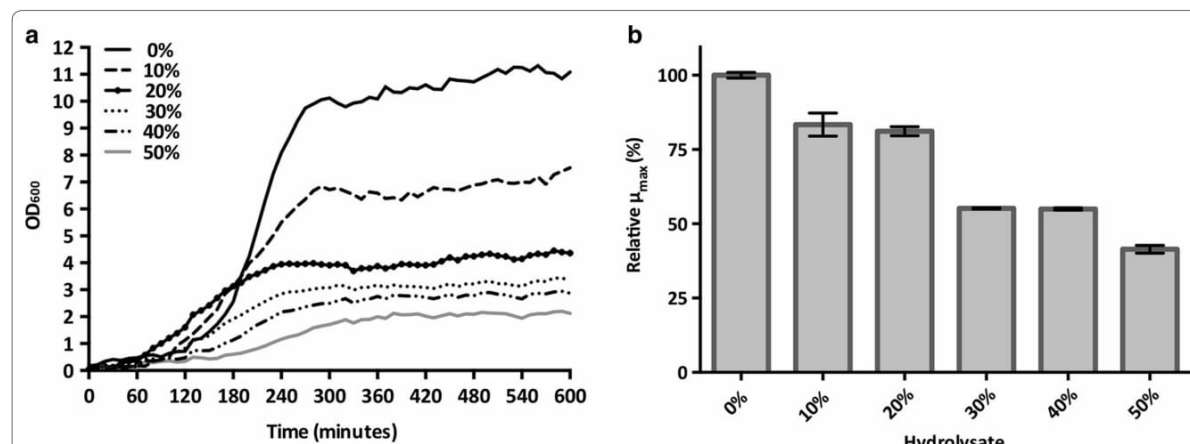


**Fig. 7** Effect of the steam-exploded wheat straw hydrolysate on the growth of *B. coagulans* MA-13. **a** Average growth curves in Bioscreen media containing different concentrations of hydrolysate (Additional file 1: Table S1). **b** Maximum specific growth rates ( $\mu_{max}$ ) expressed as percentage (%) relative to the rate in the absence of hydrolysate (0%). Error bars show the deviation between duplicate experiments

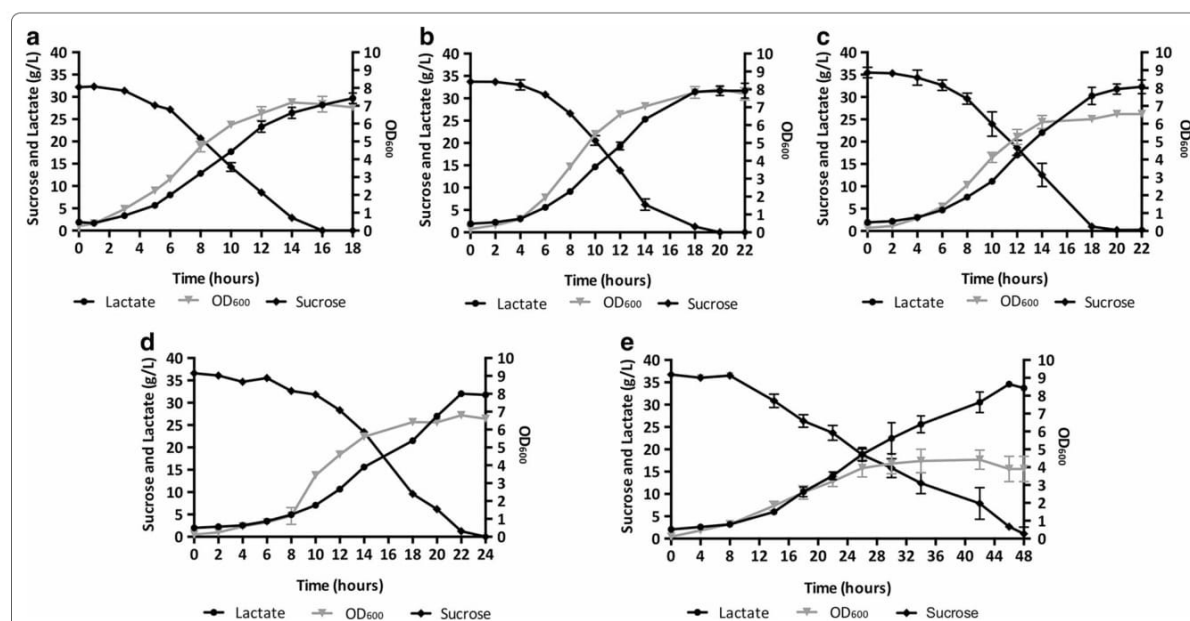


**Fig. 8** *B. coagulans* anaerobic batch fermentations. Growth and fermentation profiles in hydrolysate-free (**a**) as well as in hydrolysate-containing media: 30% (**b**), 50% (**c**), 70% (**d**) and 95% (**e**). For the composition of fermentation media see Additional file 1: Table S1. Error bars show the deviation between duplicate experiments

decreased average and maximum volumetric LA productivities (Table 2). Although this had an effect on the process time, the variation of the LA yield appeared to be negligible. Interestingly, both the average and maximum biomass-specific LA productivities increased proportionally to the hydrolysate concentration in the medium (Table 2).

## Discussion

Lignocellulosic biomasses, such as municipal, agricultural and forestry residues, are attractive renewable sources for the eco-friendly production of biofuels and chemicals. Nevertheless, to be sustainably used they need to be processed in order to release monomeric sugars that can be fermented or otherwise converted to

**Table 2 Effect of the hydrolysate on the growth and lactic acid production of *B. coagulans* MA-13**

Batch name	$\mu_{max}$ (h <sup>-1</sup> )	Relative $\mu_{max}$ (%)	Final LA concentration (g/l)	LA maximum volumetric productivity (g/l/h)	LA maximum specific productivity (g/l/h/OD)	LA average volumetric productivity (g/l/h)	LA average specific productivity (g/l/h/OD)	LA yield (g/g)	Fermentation time (h)
Hydrolysate-free	0.44	100	29.70	2.55	0.50	1.40	0.28	0.92	18
30% hydrolysate	0.37	84	32.05	2.70	0.42	1.25	0.23	0.95	22
50% hydrolysate	0.35	78	32.30	2.40	0.54	1.38	0.30	0.91	22
70% hydrolysate	0.30	67	31.77	1.81	0.63	1.24	0.30	0.91	24
95% hydrolysate	0.26	58	33.71	1.18	0.99	0.59	0.38	0.92	48



value-added products [2]. In this context, microorganisms represent both reservoirs of hydrolytic enzymes [21, 22] as well as potential cell factories for several bioconversion processes [47]. In nature, decomposition of lignocellulosic materials requires complex processes, with the participation of several lignocellulolytic microorganisms. The best biological niches for the isolation of such microorganisms are those where cellulose-containing substrates are present [50]. Therefore, thermophilic and cellulolytic microorganisms were isolated from an agricultural residue, and were screened for their ability to grow at high temperature using FP and CMC as carbon sources (Figs. 1a, 3a). The isolate *B. coagulans* MA-13 stood out for its rapid utilisation of these complex substrates, and when tested at different temperatures in a CMC-containing medium, 55 °C was found to be its optimal temperature of growth (Fig. 3).

The ability of several *Bacillus* species to secrete a wide range of hydrolytic enzymes [51, 52], together with the evidence that the strain MA-13 metabolises both CMC and FP, suggests that this bacterium might secrete lignocellulolytic enzymes. Moreover, thermophilic microorganisms are of huge interest since they are endowed with more stable enzymes [23]. For these reasons, the presence of soluble cellulases in the cell-free culture supernatant of *B. coagulans* MA-13 was preliminary tested by CMC-hydrolysis spot assay. Interestingly, the resulting degradation halo was comparable to that generated by a commercially available enzyme cocktail (Fig. 4a). Besides being tested by spot assay, the occurrence of cellulolytic enzymes in the bacterial supernatant was confirmed by partial purification (Fig. 4b) and Azo-CMC assay. To test if *B. coagulans* MA-13 could be a source of endoglucanases, even when cultivated at lower temperature, the time course of secretion was investigated at 37 °C. In the presence of CMC this bacterium showed a biphasic growth curve, with enzymes secretion occurring only after a first short stationary phase (Fig. 5a, 6–8 h), hinting that the shortage of some nutrients in the medium might trigger the production of cellulases. It is worth noting that, despite the low temperature of cultivation (37 °C), the secreted enzymes performed better at 50 °C (Fig. 5b), which overlaps the optimal operational temperature of commercial hydrolytic enzyme cocktails (50–55 °C) used for the saccharification of lignocellulosic biomasses [24]. Unlike the *B. coagulans* strain PFH N7 that showed a decreased enzyme secretion at temperatures higher than 37 °C [53], the secretion of endo-1,4- $\beta$ -glucanase enzymes by the strain MA-13 appears not to be influenced by the temperature of growth. Indeed, the enzyme activity in the supernatant was comparable when this bacterium was cultured at both 37 and 55 °C (data not shown).

Many strains of *B. coagulans* are generally regarded as safe (i.e. GRAS) by the U.S. Federal Drug Administration (FDA) [54–56]. Therefore, besides being used as a chemical for PLA manufacturing, the LA produced by this bacterium might be potentially used as an additive in pharmaceutical and cosmetic applications as well as in food industries [7]. Moreover, *B. coagulans* is one of the model organisms used for the production of LA from lignocellulose biomasses [8, 23, 45, 46]. For this reason, the strain M-13 was tested for the consumption and fermentation of different cellulose- and hemicellulose-derived sugars. Since *B. coagulans* MA-13 was selected for its capability to degrade cellulose, it was not surprising to observe that, besides D-mannose, it could not metabolise other hemicellulose-derived sugars (i.e. D- and L-arabinose, D-xylose and D-galactose). On the other hand, the utilisation of cellulose-derived sugars was expected (Fig. 6; D-glucose and D-cellobiose). The highest relative  $\mu_{\max}$  was observed when molasses was provided as carbon source (Fig. 6b). This is of particular interest because molasses is a renewable, easily available and relatively inexpensive source of sugars that is often used at industrial scale [57, 58]. The improved growth in molasses has already been observed for other *Bacillus* species [59, 60] and might be related to the presence of growth promoters such as vitamins, organic compounds and minerals.

Another desirable feature of microorganisms employed for the production of eco-friendly fuels and chemicals is the tolerance towards inhibitors released during the pretreatment of the lignocellulosic biomass [14–16]. To this end, the robustness of *B. coagulans* MA-13 was investigated by cultivation in the liquid fraction (hydrolysate) of an acid and steam-exploded wheat straw slurry [43]. Cell growth in media containing 10 and 20% hydrolysate was only slightly affected compared to the growth in hydrolysate-free medium, but the relative  $\mu_{\max}$  dropped significantly at 30–50% of hydrolysate (Fig. 7). Cell growth was completely inhibited at concentrations above 50%. Interestingly, these data show that *B. coagulans* MA-13 is indeed a robust bacterium able to withstand hydrolysate concentrations higher than those tolerated in batch cultivations by *Saccharomyces cerevisiae* using the same hydrolysate [43], i.e. a model organism widely used for lignocellulosic ethanol production. Moreover, *B. coagulans* MA-13 appears to better tolerate furfural than what is shown for the thermophilic *Bacillus* spp. IFA 119. Indeed, whereas in microscale cultivation MA-13 showed a 60% reduction of its relative  $\mu_{\max}$  in the medium containing 50% hydrolysate (about 2.0 g/l of furfural), the growth of the strain IFA 119 was inhibited by 96% when cultivated in a medium containing only 0.8 g/l of furfural [61]. On the other hand, the growth of *B. coagulans* MXL-9 was not inhibited by furfural up to 2.5 g/l [62], although its

behaviour was never tested in the presence of a complex mixture of inhibitors, such as the acid and steam-exploded wheat straw hydrolysate used in this work.

To study the behaviour of *B. coagulans* MA-13 in a more controlled experimental set-up, batch fermentations were carried out in high-performance bioreactors using hydrolysate-free medium as well as at concentrations of hydrolysate exceeding those tolerated in the microscale cultivations. Under strict anaerobic conditions the bacterium produced only LA, thus confirming its homo-fermentative nature. Moreover, the better mixing, together with stringent anaerobic condition and pH control throughout the cultivation in bioreactors, alleviated the detrimental effect of the hydrolysate inhibitors on the bacterial growth. In fact, compared to what was observed in a hydrolysate-free medium, in the presence of 95% hydrolysate the bacterial growth was reduced only by about 50% (Fig. 8; Table 2). This indicates that *B. coagulans* MA-13 is more robust than *B. coagulans* IPE22 (Fig. 2, Group II), the growth of which was reduced by about 75% when cultivated in a medium containing only furfural (3.0 g/l) as inhibitory compound [49]. Therefore, MA-13 might be an even more suitable strain for lignocellulosic LA production (Fig. 8; Table 2) than previously indicated by the microscale cultivation data (Fig. 7). Concerning the fermentation performance, it is noteworthy that the LA yield was similar in all the tested conditions. In contrast, the volumetric productivities were reduced in the hydrolysate-containing media (Table 2). These results show that the inhibitory compounds present in the hydrolysate [43] had no effect on the final lactate yield, whilst they affected the bacterial growth and, in turn, the volumetric LA productivities (Table 2). These data suggest that the fermentation rate is linked to the bacterial growth. Indeed, the time to complete the fermentation was extended from 18 h in the hydrolysate-free medium to 48 h in the 95%-hydrolysate-containing medium (Table 2). However, the specific LA productivities increased with the hydrolysate concentration (Table 2). This can be explained by a higher cellular requirement of energy to be used in stress responses and for detoxification of inhibitors at increased hydrolysate concentrations. Since sugar fermentation is the only way to produce energy (i.e. reducing power and ATP) in anaerobic conditions, this will in turn stimulate the production of LA.

Interestingly, once again, *B. coagulans* MA-13 was shown to be more robust than other strains such as *B. coagulans* JI12 (Fig. 2, Group I) and NL01; in fact, these latter showed a fermentation time of 48 h at lower concentration of furfural (1.4 and 0.18 g/l) and HMF (0.3 and 0.37 g/l), respectively [63, 64]. Altogether the features displayed by *B. coagulans* MA-13, i.e. (1) the

secretion of thermophilic cellulases; (2) the utilisation of lignocellulose-derived sugars and (3) the tolerance towards lignocellulose hydrolysate inhibitors, make this bacterium an appealing candidate for the production of LA from lignocellulosic biomasses. Nonetheless, given the presence of 20–40% of hemicellulose in lignocellulosic biomass, further development of the MA-13 strain is required to provide this strain with the ability to ferment hemicellulose-derived sugars (e.g. xylose). Indeed, this is a desirable trait for LA production strains, since it allows exploiting the full polysaccharide composition of the biomass and, in turn, to increase the final LA titre. Moreover, the future design of a consolidated bioprocess, via genetic and evolutionary engineering of MA-13, can be envisaged since genetic accessibility has already been reported for *B. coagulans* [33].

## Conclusions

In the present work, a novel thermophilic and cellulolytic strain of *B. coagulans* MA-13 was isolated from canned beans manufacturing residues for its ability to metabolise both CMC and FP. MA-13 is a facultative anaerobic bacterium showing an optimal temperature of growth of 55 °C, which is able to secrete soluble endo-1,4- $\beta$ -glucanase enzymes into the culture supernatant, even when cultivated at a lower temperature (37 °C). Although the secreted enzymes are active in a wide range of temperature (37–60 °C), they perform better at 50 °C. MA-13 was also characterised for the production of lactic acid in media containing a hydrolysate derived from the pre-treatment of wheat straw by acid-catalysed hydrolysis and steam explosion. Whereas the fermentation process was completed within 18 h in a hydrolysate-free medium, the process time was extended to 48 h at the highest hydrolysate concentration tested (95% v/v). However, the lactic acid yield was always higher than 0.9 g/g and was not influenced by the hydrolysate concentration in the fermentation medium. The secretion of cellulolytic enzymes and the ability to ferment lignocellulose-derived sugars to lactic acid in the presences of inhibitors make this bacterium a suitable starting point for the development of a consolidated bioprocess for the production of lactic acid from lignocellulosic biomass.

## Additional file

**Additional file 1: Table S1.** Media composition. CMC= carboxymethyl-cellulose; SM= Screening Medium; FP= Filter Paper; IM= Induction Medium; BM= Bioscreen Medium; FM= Fermentation Medium. **Figure S1.** Assessment of the optimal pH of growth. **Table S2.** HPLC analysis of filtered microscale cultures with different sugars. **Table S3.** HPLC analysis of filtered microscale cultures in the presence of hydrolysate from acid and steam-exploded wheat straw.sssss



## Abbreviations

CBP: consolidated bioprocessing; CMC: carboxymethyl-cellulose; ddH<sub>2</sub>O: double-distilled water; FP: filter paper; HMF: 5-hydroxymethylfurfural; IM: induction medium; LA: lactic acid; OD: optical density; PLA: polylactic acid; SHF: separate hydrolysis and fermentation; SM: screening medium; SSF: simultaneous saccharification and fermentation.

## Authors' contributions

All authors contributed to the conception and planning of the study. MA and SF performed experiments and drafted the manuscript. CJF and PC supervised the experimental work. SB, CJF and PC reviewed the manuscript. All authors read and approved the final manuscript.

## Competing interests

The authors declare that they have no competing interests.

## Availability of data and materials

The datasets used and/or analysed during the current study are available from the corresponding authors on reasonable request.

## Consent for publication

Not applicable.

## Ethics approval and consent to participate

Not applicable.

## Funding

This research was carried out in the frame of Programme STAR, financially supported by UniNA and Compagnia di San Paolo (16-CSP-UNINA-007). The work was also financially supported by Ministero dell'Istruzione, dell'Università e della Ricerca (IT); BIOPOLIS (PON03PE\_00107\_1 CUP: E48C14000030005). A travel grant for MA from The Foundation Blanceflor Boncompagni Ludovisi, née Bildt, is gratefully acknowledged. The funding bodies had no influence on the design of the study and were involved neither in the collection, analysis and interpretation of data, nor in the writing of the manuscript.

## Publisher's Note

Springer Nature remains neutral with regard to jurisdictional claims in published maps and institutional affiliations.

Received: 23 June 2017 Accepted: 28 August 2017

Published online: 07 September 2017

## References

- Bilal M, Asgher M, Iqbal HM, Hu H, Zhang X. Biotransformation of lignocellulosic materials into value-added products—A review. *Int J Biol Macromol*. 2017;98:447–58.
- Arevalo-Gallegos A, Ahmad Z, Asgher M, Parra-Saldivar R, Iqbal HM. Lignocellulose: a sustainable material to produce value-added products with a zero waste approach—A review. *Int J Biol Macromol*. 2017;99:308–18.
- Ko C-H, Chairapat S, Kim L-H, Hadi P, Hsu S-C, Leu S-Y. Carbon sequestration potential via energy harvesting from agricultural biomass residues in Mekong River basin, Southeast Asia. *Renew Sustain Energy Rev*. 2017;68:1051–62.
- Komesu A, de Oliveira JAR, da Silva Martins LH, Maciel MRW, Maciel Filho R. Lactic acid production to purification: a review. *BioResour*. 2017;12:4364–83.
- Abdel-Rahman MA, Tashiro Y, Sonomoto K. Lactic acid production from lignocellulose-derived sugars using lactic acid bacteria: overview and limits. *J Biotechnol*. 2011;156:286–301.
- John RP, Nampoothiri KM, Pandey A. Fermentative production of lactic acid from biomass: an overview on process developments and future perspectives. *Appl Microbiol Biotechnol*. 2007;74:524–34.
- Narayanan N, Roychoudhury PK, Srivastava A. L (+) lactic acid fermentation and its product polymerization. *Electr J Biotechnol*. 2004;7:167–78.
- Hofvendahl K, Hahn-Hägerdal B. Factors affecting the fermentative lactic acid production from renewable resources 1. *Enzyme microb technol*. 2000;26:87–107.
- Ou MS, Ingram LO, Shanmugam K. L (+)-Lactic acid production from non-food carbohydrates by thermotolerant *Bacillus coagulans*. *J Ind Microbiol Biotechnol*. 2011;38:599–605.
- Bajpai P. Structure of lignocellulosic biomass. In: Pretreatment of lignocellulosic biomass for biofuel production. Berlin: Springer; 2016. p. 7–12.
- de Sousa G, dos Santos VC, de Figueiredo Gontijo N, Constantino R, e Silva GdOP, Bahia AC, Gomes FM, de Alcantara Machado E. Morphophysiological study of digestive system litter-feeding termite *Cornitermes cumulans* (Kollar, 1832). *Cell Tissue Res*. 2017;368:1–12.
- Kumar P, Barrett DM, Delwiche MJ, Stroeve P. Methods for pretreatment of lignocellulosic biomass for efficient hydrolysis and biofuel production. *Ind Eng Chem Res*. 2009;48:3713–29.
- Chundawat SP, Beckham GT, Himmel ME, Dale BE. Deconstruction of lignocellulosic biomass to fuels and chemicals. *Ann Rev Chem Biomol Eng*. 2011;2:121–45.
- Alvira P, Tomás-Pejó E, Ballesteros M, Negro M. Pretreatment technologies for an efficient bioethanol production process based on enzymatic hydrolysis: a review. *Bioresour Technol*. 2010;101:4851–61.
- Parawira W, Tekere M. Biotechnological strategies to overcome inhibitors in lignocellulose hydrolysates for ethanol production: review. *Crit Rev Biotechnol*. 2011;31:20–31.
- Klinke HB, Thomsen A, Ahring BK. Inhibition of ethanol-producing yeast and bacteria by degradation products produced during pre-treatment of biomass. *Appl Microbiol Biotechnol*. 2004;66:10–26.
- Zhang J, Zhu Z, Wang X, Wang N, Wang W, Bao J. Biotransformation of toxins generated from lignocellulose pretreatment using a newly isolated fungus, *Amorphotheca resinae* ZN1, and the consequent ethanol fermentation. *Biotechnol Biofuels*. 2010;3:26.
- Almeida JR, Bertilsson M, Gorwa-Grauslund MF, Gorsich S, Lidén G. Metabolic effects of furaldehydes and impacts on biotechnological processes. *Appl Microbiol Biotechnol*. 2009;82:625–38.
- Almeida JR, Modig T, Petersson A, Hahn-Hägerdal B, Lidén G, Gorwa-Grauslund MF. Increased tolerance and conversion of inhibitors in lignocellulosic hydrolysates by *Saccharomyces cerevisiae*. *J Chem Technol Biotechnol*. 2007;82:340–9.
- Keating JD, Panganiban C, Mansfield SD. Tolerance and adaptation of ethanologenic yeasts to lignocellulosic inhibitory compounds. *Biotechnol Bioeng*. 2006;93:1196–206.
- El Kaoutari A, Armougom F, Gordon JJ, Raoult D, Henricsson B. The abundance and variety of carbohydrate-active enzymes in the human gut microbiota. *Nat Rev Microbiol*. 2013;11:497–504.
- Van Dyk J, Pletschke B. A review of lignocellulose bioconversion using enzymatic hydrolysis and synergistic cooperation between enzymes—factors affecting enzymes, conversion and synergy. *Biotechnol Adv*. 2012;30:1458–80.
- Aulitto M, Fusco S, Fiorentino G, Limauro D, Pedone E, Bartolucci S, Contursi P. *Thermus thermophilus* as source of thermozymes for biotechnological applications: homologous expression and biochemical characterization of an  $\alpha$ -galactosidase. *Microb Cell Fact*. 2017;16:28.
- Ou MS, Mohammed N, Ingram L, Shanmugam K. Thermophilic *Bacillus coagulans* requires less cellulases for simultaneous saccharification and fermentation of cellulose to products than mesophilic microbial biocatalysts. *Appl Biochem Biotechnol*. 2009;155:76–82.
- Narwal RK, Bhushan B, Pal A, Panwar A, Malhotra S. Purification, physico-chemical kinetic characterization and thermal inactivation thermodynamics of milk clotting enzyme from *Bacillus subtilis* MTCC 10422. *Food Sci Technol*. 2016;65:652–60.
- Manfredi AP, Pisa JH, Valdeón DH, Perotti NI, Martínez MA. Synergistic effect of simple sugars and carboxymethyl cellulose on the production of a cellulolytic cocktail from *Bacillus* sp. AR03 and enzyme activity characterization. *Appl Biochem Biotechnol*. 2016;179:16–32.
- Priya I, Dhar M, Bajaj B, Koul S, Vakhlu J. Cellulolytic activity of thermophilic *Bacilli* isolated from Tattapani hot spring sediment in north east Himalayas. *Indian J Microbiol*. 2016;56:228–31.
- Kawaguchi H, Hasunuma T, Ogino C, Kondo A. Bioprocessing of bio-based chemicals produced from lignocellulosic feedstocks. *Curr Opin Biotechnol*. 2016;42:30–9.

29. Öhgren K, Bura R, Lesnicki G, Saddler J, Zacchi G. A comparison between simultaneous saccharification and fermentation and separate hydrolysis and fermentation using steam-pretreated corn stover. *Process Biochem.* 2007;42:834–9.
30. Olofsson K, Bertilsson M, Lidén G. A short review on SSF—an interesting process option for ethanol production from lignocellulosic feedstocks. *Biotechnol Biofuels.* 2008;1:7.
31. Olson DG, McBride JE, Shaw AJ, Lynd LR. Recent progress in consolidated bioprocessing. *Curr Opin Biotechnol.* 2012;23:396–405.
32. Elkins JG, Raman B, Keller M. Engineered microbial systems for enhanced conversion of lignocellulosic biomass. *Curr Opin Biotechnol.* 2010;21:657–62.
33. Kovács ÁT, van Hartskamp M, Kuipers OP, van Kranenburg R. Genetic tool development for a new host for biotechnology, the thermotolerant bacterium *Bacillus coagulans*. *Appl Environ Microbiol.* 2010;76:4085–8.
34. Altschul SF, Gish W, Miller W, Myers EW, Lipman DJ. Basic local alignment search tool. *J Mol Biol.* 1990;215:403–10.
35. Tamura K, Stecher G, Peterson D, Filipski A, Kumar S. MEGA6: molecular evolutionary genetics analysis version 6.0. *Mol Biol Evol.* 2013;30:2725–9.
36. Bradford MM. A rapid and sensitive method for the quantitation of microgram quantities of protein utilizing the principle of protein-dye binding. *Anal Biochem.* 1976;72:248–54.
37. Laemmli UK. Cleavage of structural proteins during the assembly of the head of bacteriophage T4. *Nature.* 1970;227:680–5.
38. Brock TD, Brock KM, Belly RT, Weiss RL. *Sulfolobus*: a new genus of sulfur-oxidizing bacteria living at low pH and high temperature. *Arch Mikrobiol.* 1972;84:54–68.
39. Fusco S, Aulitto M, Bartolucci S, Contursi P. A standardized protocol for the UV induction of *Sulfolobus* spindle-shaped virus 1. *Extremophiles.* 2015;19:539–46.
40. Fusco S, She Q, Fiorentino G, Bartolucci S, Contursi P. Unravelling the role of the F55 regulator in the transition from lysogeny to UV induction of *Sulfolobus* spindle-shaped virus 1. *J Virol.* 2015;89:6453–61.
41. Fusco S, Liguori R, Limauro D, Bartolucci S, She Q, Contursi P. Transcriptome analysis of *Sulfolobus solfataricus* infected with two related fuselloviruses reveals novel insights into the regulation of CRISPR-Cas system. *Biochimie.* 2015;118:322–32.
42. Verduyn C, Postma E, Scheffers WA, Van Dijken JP. Effect of benzoic acid on metabolic fluxes in yeasts: a continuous-culture study on the regulation of respiration and alcoholic fermentation. *Yeast.* 1992;8:501–17.
43. Wang R, Unrean P, Franzén CJ. Model-based optimization and scale-up of multi-feed simultaneous saccharification and co-fermentation of steam pre-treated lignocellulose enables high gravity ethanol production. *Biotechnol Biofuels.* 2016;9:88.
44. Warringer J, Blomberg A. Automated screening in environmental arrays allows analysis of quantitative phenotypic profiles in *Saccharomyces cerevisiae*. *Yeast.* 2003;20:53–67.
45. Wittmann S, Sharek F, Kluepfel D, Morosoli R. Purification and characterization of the CelB endoglucanase from *Streptomyces lividans* 66 and DNA sequence of the encoding gene. *Appl Environ Microbiol.* 1994;60:1701–3.
46. Théberge M, Lacaze P, Sharek F, Morosoli R, Kluepfel D. Purification and characterization of an endoglucanase from *Streptomyces lividans* 66 and DNA sequence of the gene. *Appl Environ Microbiol.* 1992;58:815–20.
47. Pleissner D, Dietz D, van Duuren JBJH, Wittmann C, Yang X, Lin CSK, Venus J. Biotechnological production of organic acids from renewable resources. *Adv Biochem Eng Biotechnol.* 2017; 1–38.
48. Maas RH, Bakker RR, Jansen ML, Visser D, De Jong E, Eggink G, Weusthuis RA. Lactic acid production from lime-treated wheat straw by *Bacillus coagulans*: neutralization of acid by fed-batch addition of alkaline substrate. *Appl Microbiol Biotechnol.* 2008;78:751–8.
49. Zhang Y, Chen X, Luo J, Qi B, Wan Y. An efficient process for lactic acid production from wheat straw by a newly isolated *Bacillus coagulans* strain IPE22. *Bioresour Technol.* 2014;158:396–9.
50. Irfan M, Safdar A, Syed Q, Nadeem M. Isolation and screening of cellulolytic bacteria from soil and optimization of cellulase production and activity. *Turk J Biochem.* 2012;37:287–93.
51. Adebayo-Tayo B, Elelu T, Akinola G, Oyinloye I. Screening and production of mannanase by *Bacillus* strains isolated from fermented food condiments. *Innov Roman Food Biotechnol.* 2013;13:53.
52. Heck JX, Flöres SH, Hertz PF, Ayub MAZ. Optimization of cellulase-free xylanase activity produced by *Bacillus coagulans* BL69 in solid-state cultivation. *Process Biochem.* 2005;40:107–12.
53. Odeniyi O, Onilude A, Ayodele M. Production characteristics and properties of cellulase/polygalacturonase by a *Bacillus coagulans* strain from a fermenting palm-fruit industrial residue. *Afr J Microbiol Res.* 2009;3:407–17.
54. Keller D, Farmer S, McCartney A, Gibson G. *Bacillus coagulans* as a probiotic. *Food Sci Technol Bull Funct Foods.* 2010;7:103–9.
55. Farmer S, Lefkowitz AR. Absorbent product containing absorbent structure and *Bacillus coagulans*. Patent US7025974; 2004.
56. Farmer S, Lefkowitz AR. Methods for reducing cholesterol using *Bacillus coagulans* spores, systems and compositions. Patent US6811786; 2004.
57. Dahod SK, Greasham R, Kennedy M. Raw materials selection and medium development for industrial fermentation processes. In: *Manual of industrial microbiology and biotechnology*, Third Edition. Washington: American Society of Microbiology; 2010. p. 659–668.
58. Hahn-Hägerdal B, Karhumaa K, Larsson CU, Gorwa-Grauslund M, Görgens J, Van Zyl WH. Role of cultivation media in the development of yeast strains for large scale industrial use. *Microb Cell Fact.* 2005;4:31.
59. Simair AA, Qureshi AS, Khushk I, Ali CH, Lashari S, Bhutto MA, Mangrio GS, Lu C. Production and partial characterization of  $\alpha$ -amylase enzyme from *Bacillus* sp. BCC 01-50 and potential applications. *Biomed Res Int.* 2017;2017:9.
60. Saimmai A, Sobhon V, Maneerat S. Molasses as a whole medium for biosurfactants production by *Bacillus* strains and their application. *Appl Biochem Biotechnol.* 2011;165:315–35.
61. Thomasser C, Danner H, Neureiter M, Saidi B, Braun R. Thermophilic fermentation of hydrolysates. *Appl Biochem Biotechnol.* 2002;98:765.
62. Bischoff KM, Liu S, Hughes SR, Rich JO. Fermentation of corn fiber hydrolysate to lactic acid by the moderate thermophile *Bacillus coagulans*. *Biotechnol Lett.* 2010;32:823–8.
63. Ouyang J, Cai C, Chen H, Jiang T, Zheng Z. Efficient non-sterilized fermentation of biomass-derived xylose to lactic acid by a thermotolerant *Bacillus coagulans* NL01. *Appl Biochem Biotechnol.* 2012;168:2387–97.
64. Ye L, Hudari MSB, Li Z, Wu JC. Simultaneous detoxification, saccharification and co-fermentation of oil palm empty fruit bunch hydrolysate for L-lactic acid production by *Bacillus coagulans* J112. *Biochem Eng J.* 2014;83:16–21.

## Manuscript 3-II:

### Seed culture pre-adaptation improves lactic acid production of *Bacillus coagulans* MA-13 in Simultaneous Saccharification and Fermentation

Aulitto M.<sup>1,2</sup>, Bartolucci S.<sup>1</sup>, Contursi P.<sup>1</sup>, Franzén C.J.<sup>2</sup>, Fusco S.<sup>1,2</sup>, Nickel D.<sup>2</sup>

<sup>1</sup>Dipartimento di Biologia, Università degli Studi di Napoli Federico II, Napoli (Italy)

<sup>2</sup>Division of Industrial Biotechnology, Department of Biology and Biological Engineering, Chalmers University of Technology, Göteborg (Sweden)

#### Abstract

One of the main barriers to the production of lactic acid (LA) from lignocellulosic biomass is the susceptibility towards biomass-derived growth inhibitors of the bacterial strains used for fermentation. Therefore, step of detoxification (i.e., water washing) to alleviate growth inhibition is required.

In this study, we assessed efficient strategy to overcome bacterial growth inhibition by performing pre-adaptation of the seed culture. Specifically, the seed medium was supplemented with different amounts of the liquid fraction obtained by filtration of pre-treated wheat straw by acid-catalysed (pre-)hydrolysis and steam-explosion. Afterwards, pre-adapted seed cultures were used to produce lactic acid in high-gravity simultaneous saccharification and fermentation (SSF).

The best results were obtained when the 30%-hydrolysate pre-adapted seed was used at a cell/biomass ratio of 0.01 g<sub>cell</sub>/g<sub>WIS</sub>. Indeed, the process time was reduced from 36 (not preadapted) to 15 hours with average and maximum volumetric productivities of 1.7 and 2.8 g/L·h, respectively. Noteworthy, the strength points of this strategy are: i) the use of a cheap carbon source (i.e., molasses); ii) the improved LA productivity upon physiological adaptation and iii) the saving of clean water that would have been otherwise used for biomass washing.

## 1. Introduction

Lactic acid (LA) is one of the most important carboxylic acid occurring in nature and exists in two optically active forms, i.e., L(+)- and the D(-)-lactic acid. LA is widely used in food, cosmetic, pharmaceutical and chemical industries, as well as for the production of bioplastics, such as poly-lactic acid (PLA) [1]. LA can be manufactured either by chemical synthesis or by microbial fermentation. However, petroleum-based synthesis produces always a racemic D/L-lactic acid solution. Bio-production via fermentation provides significant advantages over the chemical synthesis, such as reduced environmental impact and lower raw material costs [2]. Although lignocellulosic biomasses represent eco-friendly, abundant and inexpensive sources of feedstock, their utilization is still limited by several technical barriers [3]. At industrial scale, the biomass must be first chemically and physically pre-treated to deconstruct its complex structure, mainly to make cellulose and hemicellulose more accessible to the subsequent enzymatic hydrolysis (saccharification). After pre-treatment and saccharification, the fermentability of the biomass is generally hampered by toxic compounds, such as furfural, 5-hydroxymethyl furfural (HMF), and soluble phenolic compounds, which are released during the pre-treatment. Indeed, these chemicals inhibit the growth of the fermenting microorganisms and, in turn, affect the rate of biomass conversion to the end-product. One strategy to reduce the level of toxic compounds is the detoxification of the pre-treated hydrolysates, but this implies additional cost [3, 4]. Therefore, robust and tolerant microorganisms are required to keep the process economically feasible.

Saccharification is performed after the pre-treatment and consists in the depolymerisation of cellulose and hemicellulose to monomeric, fermentable sugars. This hydrolysis is commonly carried out by means of fungal hydrolytic enzyme cocktails either as a stand-alone phase (SHF: separate hydrolysis and fermentation) or in combination with the fermentation process (SSF: simultaneous hydrolysis and fermentation) [5]. The main benefit of performing the production in a SSF configuration is the reduced product inhibition experienced by the enzymes, because the sugar concentration is kept low by the microbial consumption [6]. On the other hand, the presence of a solid residue in the fermentation tank makes trickier the stirring of the medium. However, in many cases the operational conditions (i.e., temperature and pH) are not optimal neither for the enzymes and nor for the fermenting microorganism; thus, affecting the efficiency of these parallel processes [6]. Nowadays, several commercial bacterial strains, such as *Lactobacillus helveticus* and *Lactobacillus casei*, are already used to produce LA. However, high contamination risks make these mesophilic strains not suited for industrial production of LA [3]. For this reason, some studies have addressed to the use of a moderate thermophilic lactic acid bacteria (*Bacillus coagulans*), which is a facultative anaerobic bacterium able to grow in a range of temperatures from 37 to 55°C [7-10]. Recently, a new strain of *B. coagulans*, namely MA-13, was isolated from canned beans manufacturing residues and found to secrete soluble endo-1,4- $\beta$ -glucanase enzymes into the culture supernatant. Noteworthy, MA-13 showed temperature (55°C) and pH (5.5) optima for cell growth that are compatible with those required by the fungal hydrolytic enzymes used for the biomass saccharification. Moreover, MA-13 showed to tolerate well the toxicity of biomass-derived growth inhibitors when cultivated in the presence of high concentration of pre-treatment hydrolysate (up to 95%). The abovementioned features make this strain an attractive biocatalyst for the conversion of lignocellulosic residues into valuable chemicals [11].

In this study, *B. coagulans* MA-13 was used as microbial cell factory for the



production of LA in high-gravity SSF from wheat straw pre-treated by acid-catalysed (pre-)hydrolysis and steam-explosion. By adding the pre-treatment hydrolysate into the medium used for the propagation of the seed culture, we show that the strain MA-13 develops a certain tolerance towards to the biomass-derived growth inhibitors; therefore, performing better LA fermentation in high-gravity SSF than the control (not adapted) seed culture.

## 2. Material and Methods

### 2.1. Raw material

Pre-treated wheat straw used throughout this study was obtained from SP Biorefinery Demo Plant (Örnsköldsvik, Sweden). The lignocellulosic biomass was pre-treated by acid-catalysed hydrolysis with 1% (w/v)  $\text{H}_2\text{SO}_4$  and steam-explosion, as previously described [12]. After pre-treatment, the biomass slurry was separated by filtration into a water-insoluble solid (WIS) fraction (in SSF experiments) and a liquid hydrolysate, hereinafter referred to as pre-treatment hydrolysate (in seed cultivation). This latter, contains microbial growth inhibitors such as acetic acid (3.8 g/L), furfural (4.0 g/L) and hydroxymethylfurfural (1.4 g/L) [12].

For WIS saccharification Cellic CTec II enzymes (Novozymes) were used. Enzyme activity, expressed in filter paper units (FPU), was determined according to the NREL protocol TP-510-42628, with reduced reaction volume [13].

### 2.2. Strain and media

The recently isolated thermophilic and cellulolytic *B. coagulans* MA-13 [11] was used for the production of LA in high-gravity SSF configuration. The MA-13 strain was inoculated from a frozen glycerol stock, at an initial optical density ( $\text{OD}_{600}$ ) of 0.1, in 500 ml of LB medium: 1% (w/v) tryptone (AppliChem), 1% (w/v) NaCl (AppliChem) and 0.5% (w/v) yeast extract (VWR). The pre-culture was incubated at a temperature of 55°C and at a shaking rate of 200 rpm using a KS 4000i incubator shakers (IKA™) up to the early stationary phase (1.0-1.3  $\text{OD}_{600}$ ), prior to subsequent seed cultivations (see below).

The seed medium (SM) contained 5% (v/v) molasses, 1% (w/v) yeast extract, 1% (w/v) peptone, 1x CBS [0.75% (w/v)  $(\text{NH}_4)_2\text{SO}_4$ , 0.35% (w/v)  $\text{KH}_2\text{PO}_4$ , 0.07% (w/v)  $\text{MgSO}_4 \cdot 7\text{H}_2\text{O}$ ], 1x trace metals and 1x vitamins [14]. For the pre-adaptation of the seed cultures, the pre-treatment hydrolysate was added at different concentrations to the medium (i.e., 30, 40, 50, 70 and 95% v/v). The SSF medium was composed of 10% WIS (w/w, dry basis) supplemented with 1% (w/v) yeast extract, 1% (w/v) peptone and 0.05% (w/v)  $(\text{NH}_4)_2\text{HPO}_4$ . For both seed and SSF media, the pH was adjusted to 5.5 using 3M NaOH.

### 2.3. Optimization of lactic acid production from steam-exploded wheat straw

#### 2.3.1. Anaerobic seed pre-adaptation

MA-13 seed cultures were propagated in anaerobic batch fermentation in 3.6 L bioreactor vessels (INFORS HT), previously autoclaved at 121 °C for 20 min before usage. Pre-cultures were cultivated in 500 ml of LB medium in 2.0 L flasks at 55°C and 180 rpm, up to an  $\text{OD}_{600}$  value of about 1.0-1.3 (approximately 3-4 h). In order to remove the LB components, pre-culture aliquots (about 100 ml) were centrifuged at 4000 x g for 10 min to pellet the cells. Afterwards, 20-ml aliquots of sterile seed medium were collected from each bioreactor vessel and used to resuspend the bacterial pellets. At each round of experiments, at least three parallel anaerobic seed cultivations were started by injecting the cell suspensions into the bioreactors through

sterile rubber septa at an initial OD<sub>600</sub> of about 0.1. For pre-adaption experiments, the seed medium was supplemented with increasing concentrations of pre-treatment hydrolysate (see above) in order to allow the cells to adapt to the biomass-derived growth inhibitors present in the fermentation medium used for the downstream high-gravity SSF process. All seed cultivations were carried out in 1 L medium at 55 °C at a stirring speed of 500 rpm. Nitrogen was sparged at 1 VVM (volume of gas/volume of medium/minute), and pH was kept at 5.5 by automatic addition of 3 M NaOH. Antifoam 204 (Sigma-Aldrich) was added as required.

Samples were regularly withdrawn to measure OD<sub>600</sub> as well as to obtain cell-free culture supernatant (through centrifugation and filtration) for HPLC analysis of sucrose and fermentation products (lactic acid, acetic acid and acetoin) content. Once the seed cultures reached the early stationary phase (18-20 h), cells were collected through centrifugation at 4000 x g for 15 min, the supernatant was discarded and the pellets were resuspended in 0.9% w/v NaCl before being used for SSF fermentations.

### *2.3.2. LA production in open SSF configuration*

Batch SSF experiments were carried out in 3.6 L BioEtOH jacketed flat-bottom vessels (INFORS HT), autoclaved at 121 °C for 20 min before usage. An enzyme loading of 10 FPU·(g<sub>WIS</sub>)<sup>-1</sup> was applied to the SSF medium. The biomass pre-hydrolysis was carried out at 55°C with a stirring rate of 100 rpm for 30 minutes, before adding MA-13 at a cells/biomass ratio of either 0.005 or 0.01 g<sub>cells</sub>/g<sub>WIS</sub>. Samples were regularly collected to measure glucose, fermentation products and cell concentration (colony forming unit, CFU). The fermentation process was monitored until complete glucose consumption.

## *2.4. Analytical procedures*

### *2.4.1. HPLC*

After centrifugation and filtration, seed and SSF samples were analysed by high performance liquid chromatography (HPLC) to quantify glucose and fermentation products (lactic acid, acetic acid and acetoin). Concentrations were quantified with a refractive index and an UV detector (both Dionex) at 210 nm after separation with a Rezex ROA H+ (8%) (Phenomenex) column in an HPLC set to a flow rate of 0.8 mL/min and an oven temperature of 80 °C. For all calculations concentrations were converted into weights by multiplication with their corresponding volume.

### *2.4.2. Cell concentration*

To monitor cell growth during pre-culture and seed cultivations, optical density was spectrophotometrically measured at 600nm (OD<sub>600</sub>) after appropriate dilution and zeroing using sterile medium. For seed cultures, cell concentration was also measured by dry weight determination. In brief, 5 ml of culture was filtered through a pre-weighed 0.2 µm filter paper (PESU-membrane), washed three times with deionized water (ddH<sub>2</sub>O), dried at 105°C for 24 h and subsequently weighted.

Culturable cells concentration was assayed for seed and SSF fermentations by manual counting of colony forming units (CFU). For seed cultivations, the withdrawn samples were serially diluted (10-folds) with 0.9% w/v NaCl and 0.1 ml of each sample was spread on LB plates in triplicate. Given the high-solid content of SSF medium, prior serial dilution, collected samples were weighted (5 g) and 0.9% w/v NaCl was added up to a final volume of 50 ml. Plates were incubated at 55°C for 12-16 hours.

#### 2.4.3. Yield and productivity calculations

The glucose content of WIS samples was measured according to the NREL method for the determination of structural carbohydrates in biomass (Sluiter et al., 2008). After two-step hydrolysis, the glucose concentration was quantified by HPLC as described above (see 2.4.1). Yields were calculated as lactate produced per glucose consumed [g/g] according to equation (1), where  $m_{Glc,WIS}$  is the amount of glucose released during two-step hydrolysis,  $m_{Glc,L}$  the amount of glucose in the liquid phase,  $m_{Lac,L}$  the amount of lactate in the liquid phase and  $\sum m_{X,s}$  the sum of the amount of lactate or glucose removed by sampling. For calculations, following assumptions were made: (i) the concentration of glucose in the liquid phase before enzymatic hydrolysis is equal to the glucose concentration in the liquor fraction; (ii) all changes in the WIS occur upon cellulose depletion and (iii) the final volume is only dependent on sampling and not on evaporation and base titration which are assumed to equal out.

$$Y_{L/G} = \frac{Lactate_{produced}}{Glucose_{consumed}} = \frac{m_{Lac,L(t=t_{end})} - m_{Lac,L(t=0)} + \sum m_{Lac,s}}{(m_{Glc,WIS(t=t_{end})} - m_{Glc,WIS(t=0)}) + m_{Glc,L(t=0)} - m_{Glc,L(t=t_{end})} + \sum m_{Glc,s}} \quad (1)$$

Cell specific lactate productivities were calculated according to equation (2). The productivity is estimated by calculating the slope of lactate concentration over time. To account for unequal sampling intervals a weighing function was introduced. For calculations biomass measured as CFU/g was converted into CFU by multiplication with the mass of the reactor content.

$$q_{Lac} = \left( \frac{(t-t_{t-1})}{(t_{t+1}-t_{t-1})} \cdot \frac{(c_{Lac,t+1}-c_{Lac,t})}{(t_{t+1}-t)} + \frac{(c_{Lac,t}-c_{Lac,t-1})}{(t-t_{t-1})} \cdot \frac{(t_{t+1}-t)}{(t_{t+1}-t_{t-1})} \right) \cdot \frac{1}{c_{X,t}}$$

### 3. Results and Discussion

#### 3.1. Overall scheme of the pre-adaptation strategy and SSF

The underlying hypothesis of this work was that the fermentation performance of the bacterium used for the SSF depends on its physiological status after seed cultivation. Therefore, we have tested if *B. coagulans* MA-13 seed cultures could be pre-adapted to the presence of the pre-treatment hydrolysate. To do so, anaerobic seed propagations were performed in a medium supplemented with different amounts of hydrolysate as well as in a hydrolysate-free medium (Fig. 1). Pre-adapted and not pre-adapted seed cultures were used to inoculate high-gravity SSF bioreactors containing the WIS fraction of the wheat straw biomass mixed with a hydrolytic enzymes cocktail (Fig. 1). To evaluate the fermentation performance of the different seed cultures, cell culturability as well as LA productivity and yield were determined.

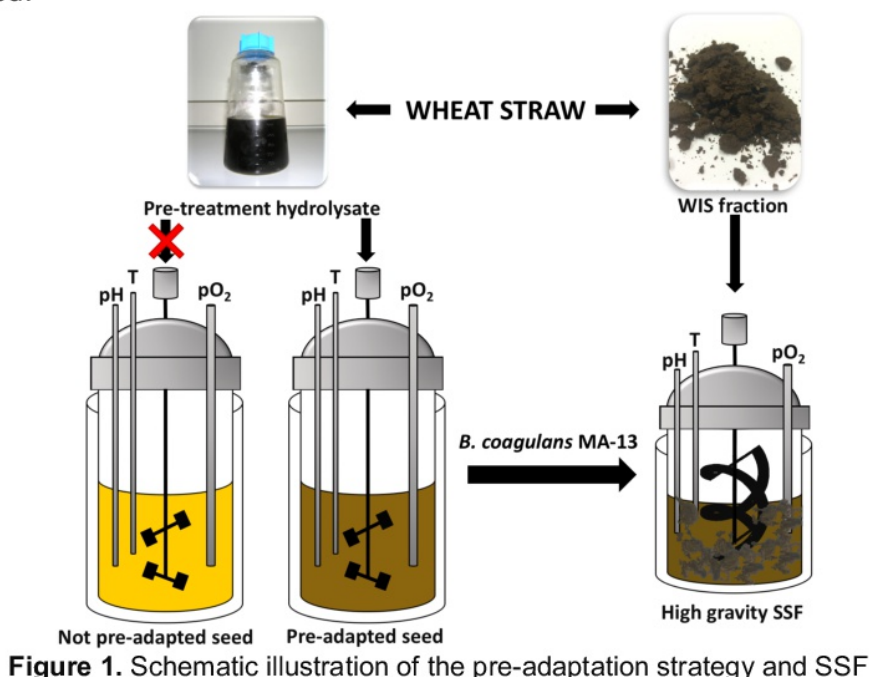


**Figure 1.** Schematic illustration of the pre-adaptation strategy and SSF

#### 3.2. Effect of pre-treatment hydrolysate supplementation on the seed cultures

Given the proved tolerance of MA-13 towards lignocellulose-derived growth inhibitors [11], this bacterium was pre-cultured in a molasses-based medium supplemented with different amounts of pre-treatment hydrolysate, in order to attempt a physiological pre-adaptation of the strain prior SSF. The LA maximum specific productivity resulted to be improved from 0.34 g/(L·h·OD) in the hydrolysate-free medium (Fig. 2, 0%) up to 0.51 g/(L·h·OD) at a hydrolysate concentration of 50% (Fig. 2, 50%); whereas higher concentrations resulted of hydrolysate resulted in a detrimental effect (i.e., a reduction of the LA maximum specific productivity and of the relative  $\mu_{max}$ ) (Fig. 2). The stimulated LA productivity in the hydrolysate-containing medium can be explained by a higher cellular requirement of energy needed for stress-response mechanisms. Indeed, under anaerobic conditions, cells can overproduce energy (i.e., ATP and reducing power) only by enhancing sugar fermentation, which results in the increase of LA production.

Compared to other *B. coagulans* strains [4, 10, 15-18], MA-13 turned out to be particularly robust towards growth inhibitors. In fact, most of the *B. coagulans* strains employed for the production of LA in high-gravity SSF have been cultivated in

hydrolysate-free rich media, because of their susceptibility to the biomass-derived growth inhibitors (Table 1). For this reason, a detoxification step consisting in the water washing of the biomass, is added prior the SSF to remove additional inhibitors inherently present in the WIS fraction of the biomass (Table 1). Conversely, the use of hydrolysate-containing medium provides a certain advantage over the conventional seed cultivation, because it allows reducing the amount of water to be used already at the stage of microbial propagation. Another important aspect affecting the economy of the whole LA production process is the cost of the carbon source used during cell propagation. In this regard, unlike other studies [4, 10, 15-18], the used of molasses (i.e., a renewable, easily available and relatively inexpensive source of sugars) for seed propagation makes the whole process more economically feasible.

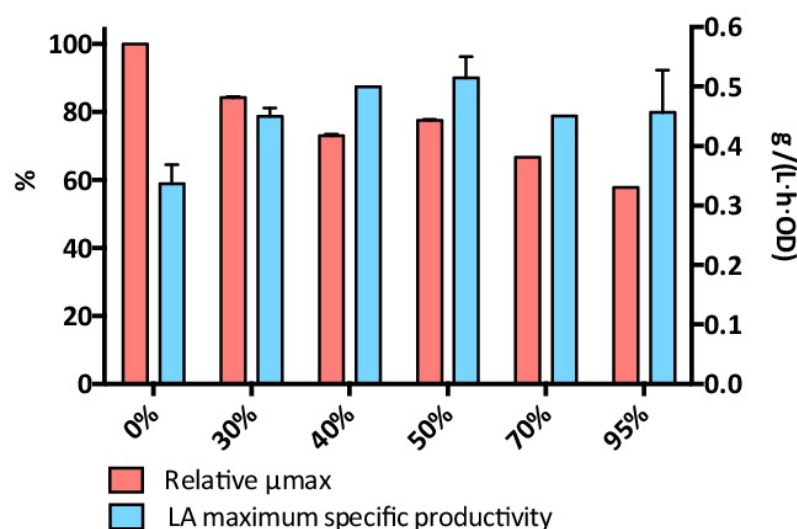


**Figure 2.** Seed cultures behavior upon supplementation of pre-treatment hydrolysate.



**Table 1.** Overview of representative recent studies on LA production in SSF using different *B. coagulans* strains

Biomass			Process					Lactic Acid				
Strain	Raw material	Pre-treatment	Detoxification	Seed culture medium	Fermentation set-up	Temperature (°C)	pH	Enzymes load	Process time (h)	LA Avg. Vol. productivity (g/L·h)	Yield (g/g)	Ref.
MA-13	wheat straw	H <sub>2</sub> SO <sub>4</sub> –steam explosion	–	SM-0%	SSF	55	5.5	10 FPU/g <sub>WIS</sub>	27	1.03	0.96 <sup>a</sup>	This work
			SM-30%	15					1.74	0.89 <sup>a</sup>		
DSM 2314	Birch wood	steam explosion	water washing	TSNT	SSF	50	5.5	2 mg/g <sub>DM</sub>	120	0.35	0.79 <sup>a</sup>	[17]
CC17	bagasse	sulfite pulping	water washing	GCY	Fed-batch SSF	50	5.0-5.5	10 FPU <sub>cellulase</sub> /g <sub>cellulose</sub> 120 U <sub>xylanase</sub> /g <sub>hemicellulose</sub>	120	0.92	0.72 <sup>a</sup> /0.60 <sup>b</sup>	[15]
LA204	corn cob	NaOH	water washing	YEX	Fed-batch SSF	50	6.0	30 (FPU/g <sub>cellulose</sub> )	90	1.37	0.77 <sup>c</sup>	[18]
		NH <sub>3</sub> -H <sub>2</sub> O <sub>2</sub>							90	1.32	0.74 <sup>c</sup>	
									72	1.10	0.43 <sup>c</sup>	
LA204	corn stover	NaOH	water washing	GY or XY	Fed-batch SSF	50	6.0	30 (FPU/g <sub>stover</sub> )	60	1.63	0.68 <sup>c</sup>	[16]
IPE22	wheat straw	H <sub>2</sub> SO <sub>4</sub> –steam explosion	–	mMRS	SSCF	50	5.0	20 FPU/g <sub>cellulose</sub>	60	0.43	0.46 <sup>c</sup>	[10]
DSM 2314	wheat straw	lime	–	GY	Fed-batch SSF	50	6.0	n.r.	55	0.68	0.81 <sup>b</sup> /0.43 <sup>c</sup>	[4]

DM = Dry Matter; FPU = Filter Paper Unit; n.r. = not reported; U = Unit; WIS = water-insoluble solid.

SM = Seed medium (see composition in Material & Methods section).

mMRS = commercial-available medium.

GY = 10 g/L glucose; 10 g/L yeast extract; 2g/L (NH<sub>4</sub>)<sub>2</sub>HPO<sub>4</sub>; 3.5 g/L (NH<sub>4</sub>)<sub>2</sub>SO<sub>4</sub>; 10 g/L Bis-Tris; 0.02 g/L MgCl<sub>2</sub> · 6H<sub>2</sub>O and 0.1 g/L CaCl<sub>2</sub> · 2H<sub>2</sub>O.

TSNT = 10 g/L tryptone; 5 g/L soytone; 3 g/L NaCl and 1 g/L Tween 80.

GCY = 20 g/L glucose; 2.5 g/L corn steep powder; 1 g/L yeast extract; 1 g/L NH<sub>4</sub>Cl; 0.2 g/L MgSO<sub>4</sub> and 10 g/L CaCO<sub>3</sub>.

GY (or XY) = 50 g/L glucose (or xylose) and 10 g/L yeast extract.

YEX = 10 g/L xylose and 10 g/L yeast extract.

<sup>a</sup>g of lactic acid / g of glucose released from cellulose

<sup>b</sup>g of lactic acid / g of released total sugars

<sup>c</sup>g of lactic acid / g of total stover



### 3.3. Lactic acid production by pre-adapted seed cultures in SSF

After filtration, the solid residue used for the production of LA in high-gravity SSF retains a certain content of pre-treatment hydrolysate. Therefore, it still contains growth inhibitors (see above, 2.1.) that can interfere with the microbial metabolism, thus affecting the fermentation performance during SSF. To test if pre-adaptation of the seed culture could alleviate the detrimental effect of these inhibitors, a control seed culture (i.e., pre-cultivated in hydrolysate-free medium) as well as pre-adapted ones (pre-cultivated in hydrolysate-containing media) were used to inoculate high-gravity SSF of unwashed WIS (see below, 3.3.1 and 3.3.2.). This experimental set-up gives the advantage of saving clean water that would otherwise be used for water-washing of the biomass prior SSF, as reported in several studies (Table 1). For all tested hydrolysate concentrations, the high-gravity SSF was carried out at 55°C and pH 5.5. These conditions were chosen because they are optimal for both the enzymes used for the saccharification (Cellic CTec II) and the microbial strain (*B. coagulans* MA-13) used for the fermentation [11]. Since a short pre-saccharification step (30 minutes) was performed for all the experiments, an initial glucose accumulation in the SSF medium was observed before the microbial cells started producing LA, as described below.

#### 3.3.1. High-gravity SSF using a cell/WIS ratio of 0.005g/g

For the control culture (not pre-adapted), when a cell/biomass ratio of 0.005 g/g<sub>WIS</sub> was used to inoculate the SSF an initial lag phase of about 12 h was observed for the LA production. In the same time frame, the total CFU increased of about two orders of magnitude (from 10<sup>9</sup> to 10<sup>11</sup> CFU) reflecting an active cell growth (Fig. 3A). Thereafter, a quite rapid lactate fermentation was detected with average and maximum volumetric productivities of 0.8 and 1.9 g/L·h, respectively (Table 2). Although this result confirms that the strain MA-13 can be used for LA production in high-gravity SSF configuration, this bacterium could not ferment all the released glucose from cellulose to LA (Fig. 3A). For this reason, the achieved LA yield was only of 0.8 g/g (Table 2).

To understand if pre-adaptation could improve LA production in high gravity SSF, pre-adapted seed cultures (propagated in 30%- and 40%-hydrolysate containing media) were used to inoculate the SSF bioreactors with the same cell/biomass ratio (i.e., 0.005 g/g<sub>WIS</sub>). For both pre-adapted seed cultures, a similar fashion of cell growth (from 10<sup>9</sup> to 10<sup>11</sup> CFU) was observed, as for the control seed culture (Fig. 3). On the other hand, as it concerns LA production, the 30%-hydrolysate pre-adapted seed culture was able to ferment glucose to LA already upon inoculation (Fig. 3B), without any apparent lag phase. Thus, indicating that the pre-adaptation strategy gives a clear advantage over using not pre-adapted cells. Indeed, the total process time was reduced from 36h (of the control seed) to 24h, with both average and maximum volumetric productivities increased up to 1.2 and 2.4 g/L·h, respectively (Table 2). Moreover, the yield increased from 0.8 of the control to 1.0 g/g of the 30%-hydrolysate pre-adapted seed culture (Table 2). This effect is due to the fact that, in this latter case, all the released glucose from cellulose was fermented to LA, unlike what observed for the not pre-adapted seed culture (Fig. 3A and Table 2). Although a similar yield was achieved by the 40%-hydrolysate pre-adapted seed, the occurrence of a lag phase in the LA production, as for the control seed (Fig. 3A and C), led to an increase of the total process time from 24 to 30h (Table 2). This result could be attributed to a more detrimental effect of the higher hydrolysate concentration (i.e., 40%) in the seed medium, compared previous

described condition. Nevertheless, altogether these results show that the strain MA-13 is well-suited for LA production in high-gravity SSF, given the shorter total time of the fermentation process (24 h), compared to what has been reported so far for other *B. coagulans* strains (i.e., from 55 up to 120 h; see Table 1).

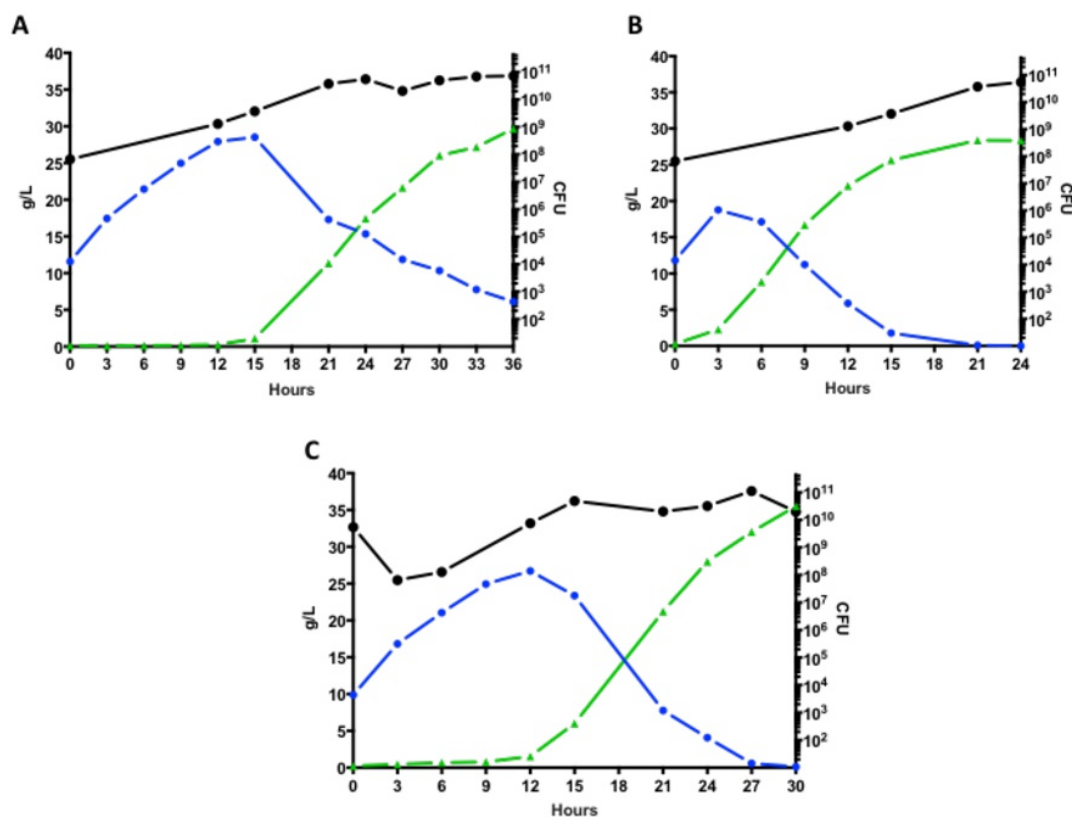


**Figure 3.** High-gravity SSF performed with *B. coagulans* MA-13 at a cell/biomass ratio of 0.005 g/g. Seed were cultivated in hydrolysate-free medium (A) as well as in 30%- (B) and 40%-hydrolysate (C) containing medium. Glucose consumption (blue circle), lactic acid production (green triangle) and total CFU (black circle) are reported.

**Table 2. Effect of the pre-adaptation on the lactic acid production by MA-13 in high-gravity SSF**

Hydrolysate in seed medium (%)	Cell concentration in SSF (g/g) <sup>a</sup>	Process time (h)	LA Avg. Vol. productivity (g/L·h)	LA Max. Vol. productivity (g/L·h)	Yield (g/g) <sup>b</sup>
0	0.005	36	0.8	1.9	0.8
0	0.01	30	1.0	1.9	1.0
30	0.005	24	1.2	2.4	1.0
<b>30</b>	<b>0.01</b>	<b>15</b>	<b>1.7</b>	<b>2.8</b>	<b>0.9</b>
40	0.005	30	1.2	2.3	1.0
40	0.01	24	1.2	1.9	0.8
50	0.01	24	1.2	2.0	0.7

<sup>a</sup>g of cells / g of WIS (water insoluble solid)

<sup>b</sup>g of lactic acid / g of glucose released from cellulose

### 3.3.2. High-gravity SSF using a cell/WIS ratio of 0.01g/g

In the attempt to improve the fermentation process, SSF experiments were carried out increasing the cell/biomass ratio to 0.01 g/g<sub>WIS</sub>. When the control seed culture (not pre-adapted) was inoculated into the SSF bioreactor, no lag phase was observed at the beginning of the process and the total cell biomass was stable (about  $10^{11}$  CFU) throughout the entire fermentation process (Fig. 4A). Unlike what was observed when a cell/biomass ratio of 0.005 g/g<sub>WIS</sub> was used (Fig. 3A), this time the strain managed to ferment all the glucose released from cellulose (Fig. 4A) in a shorted time frame (30 h), achieving a yield of 1.0 g/g (Table 2).

As it concerns the pre-adapted seed cultures (propagated in 30%-, 40%- and 50%-hydrolysate containing media), a reduction of the total process time was observed for all the cases (Fig. 4). However, for the 40%- and 50%-hydrolysate pre-adapted seed cultures, once again the detrimental effect of hydrolysate concentrations higher than 30% (see above, 3.3.1) is confirmed by both the longer total time of the fermentation process (24 h, Fig. 4C-D) and the reduction of the average and maximum volumetric productivities (Table 2). For this reason, seed cultures propagated in 70%- and 95%-hydrolysate containing media were not tested for LA fermentation in SSF.

Conversely, the 30%-hydrolysate pre-adapted seed performed better since it converted all the glucose released from cellulose to LA in half the time (15 h, Fig. 4B) compared to the control seed culture (30 h, Fig. 4A). Moreover, it showed the highest average and maximum volumetric productivities of 1.7 and 2.8 g/L·h, respectively (Table 2). So far, several strains of *B. coagulans* have been used for the production of LA from lignocellulosic biomasses in SSF configuration (Table 1). In most of these cases, the detoxification of the solid residue (i.e., water washing) is performed prior SSF, in order to remove the growth inhibitors inherently present in the pre-treated biomass and to get a better fermentation performance. This is even more evident when the same strain (i.e., LA204) was used for SSF with both washed and unwashed corncob [18]. Indeed, LA204 showed higher LA average volumetric productivity (1.32 g/L·h) and yield (0.74 g/g) when the biomass was subjected to water washing (Table 1). However, this approach is not industrially sustainable, because of the huge amount of clean water that would be required for the detoxification.

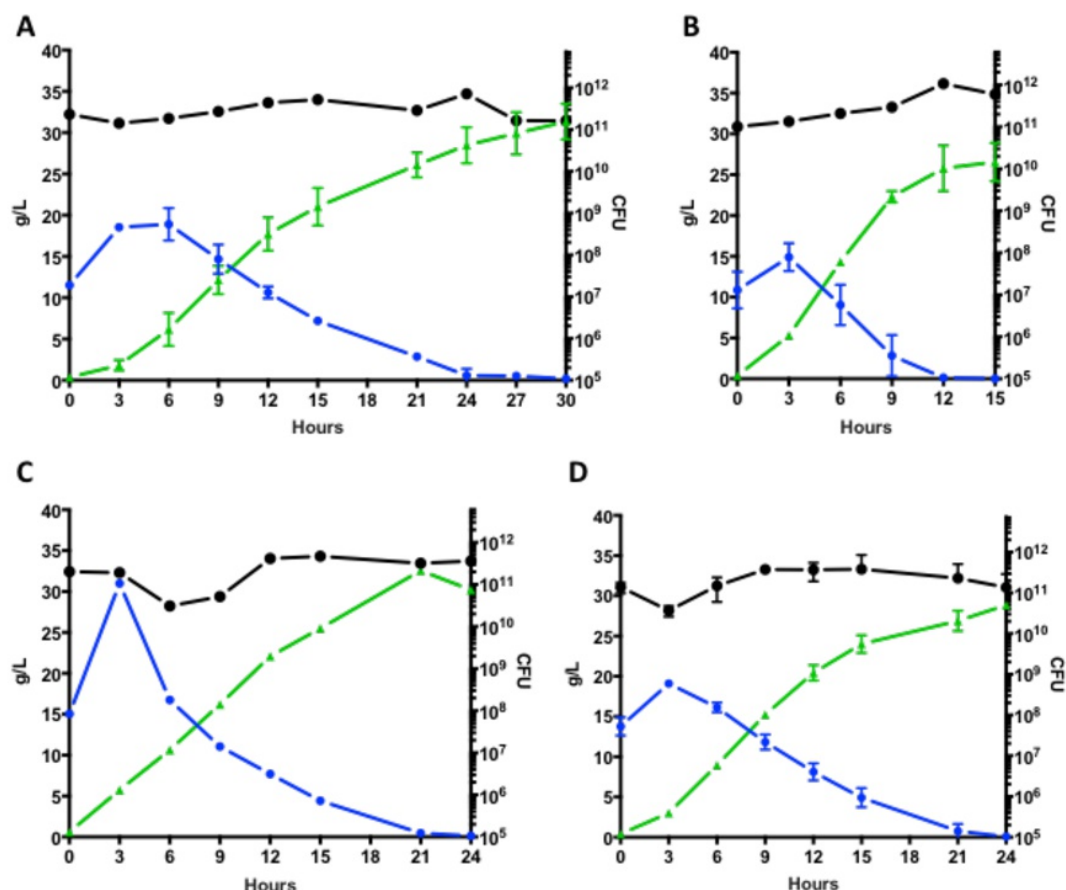


**Figure 4.** High-gravity SSF performed with *B. coagulans* MA-13 at a cell/biomass ratio of 0.01 g/g. Seed were cultivated in hydrolysate-free medium (A) as well as in 30%- (B), 40%- (C) and 50%-hydrolysate (D) containing medium. Glucose consumption (blue circle), lactic acid production (green triangle) and total CFU (black circle) are reported.

#### 4. Conclusions

By-products released from lignocellulosic biomass during thermo-chemical pre-treatments, act by hampering microbial growth and, in turn, affecting the fermentation performance. The main objective of this study was to test whether the pre-exposition of *B. coagulans* (strain MA-13) to the biomass-derived inhibitors could lead to the pre-adaptation of this microbial strain, prior production of lactic acid in high-gravity SSF configuration of pre-treated wheat straw. In our study, we have resolved to overcome the toxicity of *B. coagulans* towards inhibitors with a different strategy; i.e., by adapting the microbial strain to the biomass-derived growth inhibitors at the stage of cell propagation. This strategy has the advantage of saving additional clean water during cell propagation, because the pre-treatment hydrolysate represents a significant portion of the seed medium. Moreover, the use of a cheap carbon source (i.e., molasses) further decreases the cost of seed propagation. Noteworthy, this approach allows not only a cost-effective propagation of the seed culture compared to what reported for other *B. coagulans* strains (i.e., propagation in synthetic media), but it provides a pre-adapted seed culture that performs better in high-gravity SSF in terms of total fermentation time and LA productivity. This finding



could help to pave the way to the set-up of a low-cost solution by reducing the SSF process time and costs. However, a further development of the strain via genetic and/or metabolic strategies is envisaged to further increase the competitiveness of the SSF process at industrial scale.

## Aknowledgments

This project was partially supported by the Foundation Blanceflor Boncompagni Ludovisi, née Bildt, in the form of a fellowship awarded to Martina Aulitto to work at the Chalmers University in the division of Industrial Biotechnology.

## References

1. Chen Y, Geever LM, Killion JA, Lyons JG, Higginbotham CL, Devine DM: **A Review of Multifarious Applications of Poly (Lactic Acid)**. *Polymer-Plastics Technology and Engineering* 2016.
2. Komesu A, de Oliveira JAR, da Silva Martins LH, Maciel MRW, Maciel Filho R: **Lactic Acid Production to Purification: A Review**. *BioResources* 2017, **12**.
3. Abdel-Rahman MA, Tashiro Y, Sonomoto K: **Lactic acid production from lignocellulose-derived sugars using lactic acid bacteria: overview and limits**. *Journal of biotechnology* 2011, **156**:286-301.
4. Maas RH, Bakker RR, Jansen ML, Visser D, De Jong E, Eggink G, Weusthuis RA: **Lactic acid production from lime-treated wheat straw by *Bacillus coagulans*: neutralization of acid by fed-batch addition of alkaline substrate**. *Applied microbiology and biotechnology* 2008, **78**:751-758.
5. Öhgren K, Bura R, Lesnicki G, Saddler J, Zacchi G: **A comparison between simultaneous saccharification and fermentation and separate hydrolysis and fermentation using steam-pretreated corn stover**. *Process Biochemistry* 2007, **42**:834-839.
6. Ye L, Hudari MSB, Li Z, Wu JC: **Simultaneous detoxification, saccharification and co-fermentation of oil palm empty fruit bunch hydrolysate for l-lactic acid production by *Bacillus coagulans* J112**. *Biochemical Engineering Journal* 2014, **83**:16-21.
7. Ou MS, Mohammed N, Ingram L, Shanmugam K: **Thermophilic *Bacillus coagulans* requires less cellulases for simultaneous saccharification and fermentation of cellulose to products than mesophilic microbial biocatalysts**. *Applied biochemistry and biotechnology* 2009, **155**:76-82.
8. Bischoff KM, Liu S, Hughes SR, Rich JO: **Fermentation of corn fiber hydrolysate to lactic acid by the moderate thermophile *Bacillus coagulans***. *Biotechnology letters* 2010, **32**:823-828.
9. Ou MS, Ingram LO, Shanmugam K: **L (+)-Lactic acid production from non-food carbohydrates by thermotolerant *Bacillus coagulans***. *Journal of industrial microbiology & biotechnology* 2011, **38**:599-605.
10. Zhang Y, Chen X, Luo J, Qi B, Wan Y: **An efficient process for lactic acid production from wheat straw by a newly isolated *Bacillus coagulans* strain IPE22**. *Bioresource technology* 2014, **158**:396-399.
11. Aulitto M, Fusco S, Bartolucci S, Franzén CJ, Contursi P: ***Bacillus coagulans* MA-13: a promising thermophilic and cellulolytic strain for the production of lactic acid from lignocellulosic hydrolysate**. 2017.



12. Wang R, Unrean P, Franzén CJ: **Model-based optimization and scale-up of multi-feed simultaneous saccharification and co-fermentation of steam pre-treated lignocellulose enables high gravity ethanol production.** *Biotechnology for biofuels* 2016, **9**:88.
13. Sluiter A, Hames B, Ruiz R, Scarlata C, Sluiter J, Templeton D, Crocker D: **Determination of structural carbohydrates and lignin in biomass.** *Laboratory analytical procedure* 2008, **1617**:1-16.
14. Verduyn C, Postma E, Scheffers WA, Van Dijken JP: **Effect of benzoic acid on metabolic fluxes in yeasts: a continuous-culture study on the regulation of respiration and alcoholic fermentation.** *Yeast* 1992, **8**:501-517.
15. Zhou J, Ouyang J, Xu Q, Zheng Z: **Cost-effective simultaneous saccharification and fermentation of l-lactic acid from bagasse sulfite pulp by *Bacillus coagulans* CC17.** *Bioresource technology* 2016, **222**:431-438.
16. Hu J, Zhang Z, Lin Y, Zhao S, Mei Y, Liang Y, Peng N: **High-titer lactic acid production from NaOH-pretreated corn stover by *Bacillus coagulans* LA204 using fed-batch simultaneous saccharification and fermentation under non-sterile condition.** *Bioresource technology* 2015, **182**:251-257.
17. Müller G, Kalyani DC, Horn SJ: **LPMOs in cellulase mixtures affect fermentation strategies for lactic acid production from lignocellulosic biomass.** *Biotechnology and bioengineering* 2017, **114**:552-559.
18. Zhang Z, Xie Y, He X, Li X, Hu J, Ruan Z, Zhao S, Peng N, Liang Y: **Comparison of high-titer lactic acid fermentation from NaOH-and NH<sub>3</sub>-H<sub>2</sub>O<sub>2</sub>-pretreated corncob by *Bacillus coagulans* using simultaneous saccharification and fermentation.** *Scientific reports* 2016, **6**:37245.

## CONCLUDING REMARKS

---

Long-term scenarios resulting in a sustainable economic growth compulsorily rely on an increased utilization of renewable materials to satisfy the needs of our society, at the expenses of fossil resources that have a high environmental impact. Over the last years, several studies have established that lignocellulosic feedstocks (mainly composed of cellulose, hemicellulose and lignin) are an eco-friendly and relatively low-cost source for the production of non-fossil based fuel energy. In this context, my PhD thesis deals with the setting up of thermophilic biorefineries by exploiting the robustness of thermophilic microorganisms and their enzymes for the production of added value products from renewable resources.

With this aim an extremely **thermoactive and thermostable  $\alpha$ -galactosidase** from *T. thermophilus* HB27 (*TtGalA*) and potentially involved in lignocelluloses conversion into fermentable sugars, has been characterized. *TtGalA* can be used in the pre-saccharification step, when the temperature is still too high for the fungal enzymes currently used for the hydrolysis of the biomass. Indeed, this enzyme exhibited an optimal hydrolysis at 90°C and pH 6.0, retaining a significant activity in a wide range of pH and temperatures. The exceptional flexibility in its catalytic properties allows to foresee the employment of *TtGalA* in combination with other GHs for achieving an efficient hydrolysis of hemicellulose under a wide range of chemical-physical conditions. For instance, this enzyme proved to perform efficiently its catalytic activity also in **heterosynergistic association** with a thermophilic mannanase from *D. turgidum* (*DturCelB*), this latter one exhibiting an optimal hydrolytic activity at lower temperature (70°C) and different pH optimum (5.4). This novel synergistic association between *DturCelB* and *TtGalA* has high potential application to pre-hydrolyse the biomass right after the pretreatment, prior to the conventional saccharification step. Moreover, enzymatic thermophilic cocktails represent an interesting alternative to the conventional mesophilic counterparts to improve the yield of hydrolysis and the cost of the whole process. A more complex enzymatic cocktail including xylanases, cellulases, pectinases, suitable to achieve a complete degradation of lignocellulose biomass can be designed through mining of genomic and metagenomic data of thermophiles.

To further reduce the cost of biomass hydrolysis, a possible strategy is the use of immobilization carriers for recirculation of carbohydrate-active enzymes. **Thermophilic virus particles (VPs)** are suitable scaffold to withstand harsh conditions of industrial processes. Our long-term goal is to perform the immobilization of *TtGalA* and *DturCelB* as well as of other CAZymes on viral particles to improve their catalytic performance upon confinement on a nano-support. Since the VPs-based immobilization requires a large number of viral particles, part of this PhD thesis has been addressed to setting up an efficient irradiation protocol for *Sulfolobus* spindle-shaped virus 1 (SSV1) to overproduce VPs. Some studies have been focused on the use of virus particles as building blocks to engineer enzyme nano-carriers (ENCs). In this context, the exploitation of viruses' resistance to extreme acidic and thermophilic environments paves the way to their applications in thermophilic biorefineries.

The production of value added products from renewable biomasses can be achieved not only through enzymatic activities but also using whole cells. Specifically, agricultural wastes represent suitable source of cellulolytic microbes. With the aim of isolating new thermophilic microorganisms to be employed in biorefinery, we isolated and characterized a new thermophilic and cellulolytic ***Bacillus coagulans* strain (MA-13)** which is able to secrete cellulolytic enzymes and to ferment lignocellulose-derived

sugars to lactic acid (LA). During my period of internship abroad at Chalmers University of Technology, in collaboration with the Professor Carl Johan Franzén, the strain MA-13 was also characterized for its ability to ferment in media containing a hydrolysate derived from the pre-treatment of wheat straw by acid-catalyzed hydrolysis and steam explosion. Moreover, *B. coagulans* MA-13 has been successfully used in **high-gravity SSF** for the production of LA proving to be particularly resistant to biomass-derived inhibitors. Wide sugar utilization is a desirable feature for LA production strains. Since MA-13 is able to ferment only 6-carbon sugars (e.g., glucose), a further development of the strain via genetic and/or metabolic strategies is envisaged to expand the palette of sugars that this strain can ferment to LA (5-carbon sugars), thus increasing the competitiveness of the SSF process at industrial scale.

The production of added-value products from renewable sources is a hot topic in bioeconomy since lignocellulosic wastes cause serious environmental problems. This project strongly supports the use of thermostable enzymes and thermophilic microorganisms, as new biocatalysts in bioconversion of renewable raw materials into value added-products and supplies alternative and ecofriendly strategies for waste disposal. The results achieved during this PhD thesis will have an impact on multiple research fields expanding knowledge in the areas of biotechnology, molecular biology, biochemistry, microbiology, virology and process engineering of thermophiles.

## ACKNOWLEDGEMENTS

---

I thank Carl Johan Franzén, from the Chalmers University, for supervising my research activity during my doctoral project.

Acknowledgements go also to grants from:

- i) Foundation Blanceflor Boncompagni Ludovisi, née Bildt;
- ii) Add North AB;
- iii) Ministero dell'Istruzione, dell'Università e della Ricerca (IT) BIOPOLIS (PON03PE\_00107\_1 CUP: E48C14000030005);
- iv) Programma STAR, financially supported by UniNA and Compagnia di San Paolo (16-CSP UNINA007).

## APPENDIX I: Communications

---

Fusco S, Aulitto M, Qunxin S, Bartolucci S, Contursi P. **F55: a lisogeny regulator of fusellovirus SSV1"** PhD day 2013 Copenhagen 11 November 2013

Fusco S, Aulitto M, Qunxin S, Bartolucci S, Contursi P. **Exploring the life cycle regulation of *Sulfolobus* spindle-shaped virus 1: the role F55, A Ribbon-Helix-Helix viral protein"** 10th International Congress on Extremophiles (Extremophiles 2014), September 7 - 11, 2014, Saint Petersburg, Russia

Aulitto M, Bartolucci S, Contursi P. **Thermophilic microorganisms as source of enzymes for biofuel production.** 58th National Meeting of the Italian Society of Biochemistry and Molecular Biology September 14-16, 2015. This abstract was selected for an oral presentation during the National Meeting of the Italian Society of Biochemistry and Molecular Biology, in the protein session.

Aulitto M, Fusco S, Fusco FA, Limauro D, Bartolucci S, Contursi P. 2016. **A thermophilic *Bacillus coagulans* strain isolated from beans-waste is promising for cellulosic biomass saccharification.** XXI IUPAC CHEMRAWN CONFERENCE Rome April 6-8 2016. This abstract was selected for an oral presentation during the conference in the "Energy from urban waste" session.

Fusco FA, Ronca R, Aulitto M, Contursi P, Bartolucci S, Limauro D. **Biochemical characterization of a new endoglucanase from *Dictyoglomus turgidum*.** XXI IUPAC CHEMRAWN CONFERENCE. Rome April 6-8 2016. The poster was exhibited during the "Material recycling, transformation and recovery" session.

Fusco S, Aulitto M, Qunxin S, Bartolucci S, Contursi P. **The archaeal lysogeny regulator F55: from discovery to in vitro and in vivo characterizations.** The 59<sup>th</sup> Congress of the Italian Society of Biochemistry and Molecular Biology (SIB) will take place from the 20<sup>th</sup> to 22<sup>nd</sup> of September in Caserta.

## APPENDIX II: List of publications

---

Fusco S, Aulitto M, Bartolucci S, Contursi P. 2015. **A standardized protocol for the UV induction of Sulfolobus spindle-shaped virus 1.** *Extremophiles*. Mar;19:539-46.

Aulitto M, Fusco S, Fiorentino G, Limauro D, Pedone E, Bartolucci S, Contursi P. 2017. **Thermus thermophilus as source of thermozymes for biotechnological applications: homologous expression and biochemical characterization of an  $\alpha$ -galactosidase.** *Microbial cell factories*, 16(1), 28.

Gaglione R, Pirone L, Farina B, Fusco S, Smaldone G, Aulitto M, Dell'Olmo E, Roscetto E, Del Gatto A, Fattorusso R, Notomista E, Zaccaro L, Arciello A, Pedone E, Contursi P. 2017. **Insights into the anticancer properties of the first antimicrobial peptide from Archaea.** *Biochimica et Biophysica Acta (BBA)-General Subjects*.

Aulitto M, Fusco S, Bartolucci S, Franzén CJ, Contursi P. 2017. **Bacillus coagulans MA-13: a promising thermophilic and cellulolytic strain for the production of lactic acid from lignocellulosic hydrolysate.** *Biotechnology for biofuels*.

Aulitto M, Fusco FA, Fiorentino G, Bartolucci S, Limauro D, Contursi P. **A thermophilic enzymatic cocktail for galactomannans degradation.** *Submitted* (Manuscript 2-II).

Aulitto M, Bartolucci S, Contursi P, Franzén CJ, Fusco S, Nickel D. **Seed culture pre-adaptation improves lactic acid production of Bacillus coagulans MA-13 in Simultaneous Saccharification and Fermentation.** *In preparation* (Manuscript 3-II).

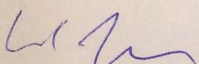


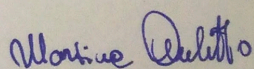
## APPENDIX III: Experiences in foreign laboratories

Prof. Giovanni Sannia  
Department of Chemical Sciences  
head of the PhD school in Biotechnology  
University of Naples FEDERICO II  
Via Cintia, 4 -80126 Naples, ITALY

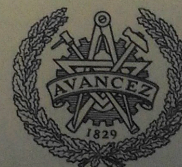
This is to certify that Martina Aulitto, student of the PhD course in Biotechnology 30<sup>o</sup>cycle, attended seminars and research activities for her thesis in the research group of Prof. Carl Johan Franzén at the Chalmers University of Technology, Göteborg (Sweden) from September 1<sup>st</sup> 2016 to December 22<sup>nd</sup> 2016.

Yours truly,

  
Carl Johan Franzén  
Ph.D., Associate Professor

  
Martina Aulitto  
PhD student

CHALMERS UNIVERSITY OF TECHNOLOGY  
*Department of Chemical and Biological Engineering*  
*Div. of Life Science – Industrial Biotechnology*  
SE-412 96 Göteborg, SWEDEN  
Visiting address: Kemigården 3  
Telephone: +46-(0)31 772 3808 Fax: +46-(0)31 772 3801  
Chalmers tekniska högskola AB, Reg. No: 556479-5598, VAT No. SE556479559801  
E-mail: franzen@chalmers.se



Web: [www.chalmers.se/chem/EN/divisions/industrial-biotechnology](http://www.chalmers.se/chem/EN/divisions/industrial-biotechnology)

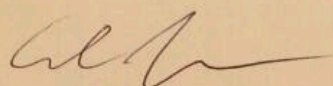
## CHALMERS

Göteborg April 13, 2017

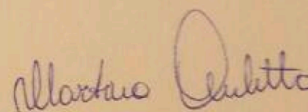
Prof. Giovanni Sannia  
Department of Chemical Sciences  
head of the PhD school in Biotechnology  
University of Naples FEDERICO II  
Via Cintia, 4 -80126 Naples, ITALY

This is to certify that Martina Aulitto, student of the PhD course in Biotechnology 30<sup>o</sup> cycle, attended seminars and research activities for her thesis in the research group of Prof. Carl Johan Franzén at the Chalmers University of Technology, Göteborg (Sweden) from January 12<sup>nd</sup> to January 29<sup>nd</sup> and February 26<sup>th</sup> to April 13<sup>th</sup>.

Yours truly,



Carl Johan Franzén  
Ph.D., Associate Professor



Martina Aulitto  
PhD student

CHALMERS UNIVERSITY OF TECHNOLOGY  
*Department of Chemical and Biological Engineering*  
*Div. of Life Science – Industrial Biotechnology*  
SE-412 96 Göteborg, SWEDEN  
Visiting address: Kemigården 3  
Telephone: +46-(0)31 772 3808 Fax: +46-(0)31 772 3801  
Chalmers tekniska högskola AB, Reg. No: 556479-5598, VAT No. SE556479559801  
E-mail: [franzen@chalmers.se](mailto:franzen@chalmers.se)



Web: [www.chalmers.se/chem/EN/divisions/industrial-biotechnology](http://www.chalmers.se/chem/EN/divisions/industrial-biotechnology)



# APPENDIX IV: Other papers

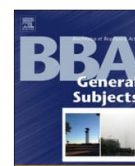
BBA - General Subjects 1861 (2017) 2155–2164



Contents lists available at ScienceDirect

BBA - General Subjects

journal homepage: [www.elsevier.com/locate/bbagen](http://www.elsevier.com/locate/bbagen)



## Insights into the anticancer properties of the first antimicrobial peptide from Archaea



Rosa Gaglione<sup>a,1</sup>, Luciano Pirone<sup>b,1</sup>, Biancamaria Farina<sup>b,c,1</sup>, Salvatore Fusco<sup>d,j,1</sup>, Giovanni Smaldone<sup>e</sup>, Martina Aulitto<sup>d</sup>, Eliana Dell'Olmo<sup>a</sup>, Emanuela Roscetto<sup>f</sup>, Annarita Del Gatto<sup>b,g</sup>, Roberto Fattorusso<sup>g,h</sup>, Eugenio Notomista<sup>d</sup>, Laura Zaccaro<sup>b,g</sup>, Angela Arciello<sup>a,i,\*</sup>, Emilia Pedone<sup>b,g,\*,2</sup>, Patrizia Contursi<sup>d,\*,2</sup>

<sup>a</sup> Department of Chemical Sciences, University of Naples Federico II, 80126 Naples, Italy

<sup>b</sup> Institute of Biostructures and Bioimaging, Italian Research National Council, Naples, Italy

<sup>c</sup> Advanced Accelerator Applications, 81100 Caserta, Italy

<sup>d</sup> Department of Biology, University of Naples Federico II, Complesso Universitario Monte S. Angelo, Via Cinthia, 80126 Naples, Italy.

<sup>e</sup> IRCCS SDN, Via E. Gianturco 113, 80143 Naples, Italy

<sup>f</sup> Department of Molecular Medicine and Medical Biotechnology, Federico II University Medical School, Italy

<sup>g</sup> Research Centre on Bioactive Peptides (CIRPeB), University of Naples "Federico II", Via Mezzocannone 16, 80134 Naples, Italy

<sup>h</sup> Department of Environmental, Biological and Pharmaceutical Sciences and Technologies, University of Campania-Luigi Vanvitelli, 81100 Caserta, Italy

<sup>i</sup> National Institute of Biostructures and Biosystems (INBB), Italy

<sup>j</sup> Division of Industrial Biotechnology, Department of Biology and Biological Engineering, Chalmers University of Technology, Göteborg, Sweden

### ARTICLE INFO

#### Keywords:

Antimicrobial peptide

Anticancer peptide

*Sulfolobus*

Archaea

Peptide-membrane interactions

### ABSTRACT

**Background:** The peptide VLL-28, identified in the sequence of an archaeal protein, the transcription factor Stf76 from *Sulfolobus islandicus*, was previously identified and characterized as an antimicrobial peptide, possessing a broad-spectrum antibacterial activity.

**Methods:** Through a combined approach of NMR and Circular Dichroism spectroscopy, Dynamic Light Scattering, confocal microscopy and cell viability assays, the interaction of VLL-28 with the membranes of both parental and malignant cell lines has been characterized and peptide mechanism of action has been studied.

**Results:** It is here demonstrated that VLL-28 selectively exerts cytotoxic activity against murine and human tumor cells. By means of structural methodologies, VLL-28 interaction with the membranes has been proven and the binding residues have been identified. Confocal microscopy data show that VLL-28 is internalized only into tumor cells. Finally, it is shown that cell death is mainly caused by a time-dependent activation of apoptotic pathways.

**Conclusions:** VLL-28, deriving from the archaeal kingdom, is here found to be endowed with selective cytotoxic activity towards both murine and human cancer cells and consequently can be classified as an ACP.

**General significance:** VLL-28 represents the first ACP identified in an archaeal microorganism, exerting a trans-kingdom activity.

### 1. Introduction

Antimicrobial peptides (AMPs) are short peptides endowed with direct and broad-spectrum antimicrobial activity and represent essential components of the innate immune system of higher eukaryotes, being the first line of defense against microbial invasions [1,2]. In

addition to a direct antimicrobial action, AMPs show a wide panel of biological activities including anti-inflammatory, anti-viral, chemotactic and pro-angiogenic activity [1,3–6]. AMPs are very heterogeneous in length, amino-acid composition, secondary structure and mechanism of action; however, the majority of them shows a peculiar abundance of cationic and hydrophobic residues. These AMPs, also

\* Correspondence to: A. Arciello, Department of Chemical Sciences, University of Naples Federico II, 80126 Naples, Italy.

\*\* Correspondence to: E. Pedone, Institute of Biostructures and Bioimaging, Italian Research National Council, Naples, Italy.

\*\*\* Corresponding author.

E-mail addresses: [anarciel@unina.it](mailto:anarciel@unina.it) (A. Arciello), [empedone@unina.it](mailto:empedone@unina.it) (E. Pedone), [contursi@unina.it](mailto:contursi@unina.it) (P. Contursi).

<sup>1</sup> These authors equally contributed.

<sup>2</sup> These authors equally contributed to the study and are therefore both last names on this manuscript.

called Host Defence Peptides (HDPs) [7], kill bacterial cells through a specific mechanism i.e. targeting bacterial membranes [2,6,8]: the net positive charge drives the adsorption of the peptide onto the surface of bacterial membranes which are richer in anionic lipids than eukaryotic membranes, hence the hydrophobic residues mediate the insertion of the peptide into the membrane. The accumulation of peptide molecules in the membrane causes the alteration of its structure/permeability, accompanied by a severe impairment of the membrane functions that eventually lead to the death of bacterial cells, often by cell lysis [2,6,8]. Since eukaryotic plasma membranes show an asymmetric distribution of negatively charged phospholipids, generally present only in the inner leaflet of the membrane, HDPs are not able to effectively adsorb to eukaryotic cells. The presence of cholesterol further prevents the insertion into and the perturbation of the eukaryotic membranes. Nonetheless, it is worth mentioning that at high concentration several HDPs become toxic also for eukaryotic cells.

Intriguingly, several AMPs endowed with anti-cancer activity [9] are defined as “anti-cancer peptides” (ACPs), because they show a much stronger toxicity for cancer cells than that towards normal cells. This differential toxicity has been attributed to the fact that transformation of eukaryotic cells is often associated to alterations of the membrane composition [10], such as: i) loss of the asymmetric distribution of phospholipids with exposure of phosphatidylserine on the outer leaflet, ii) increased production of anionic lipids (e.g. sulfated lipids), sialic acid containing glycolipids and glycoproteins, and sometimes iii) decreased production of cholesterol. Altogether these events lead to an augmented negative charge at the external surface of tumor cells that, in turn, would favor the binding of ACPs. However, differently from bacterial killing mechanisms, the death of tumor cells is not necessarily due to accumulation of the peptide into the membrane followed by their lysis. Indeed, in several cases it has been demonstrated that ACPs are internalized and the cell death occurs upon the interaction with one or more intracellular targets, such as mitochondria, DNA, cytoplasmic and nuclear proteins (e.g. HSP70 [11] and DNA polymerase  $\beta$  [12], respectively). Moreover, it is worth noting that these ACPs usually induce apoptosis rather than necrosis [9].

Due to the severe side effects of conventional chemotherapeutic agents and the ability of some tumor cells to develop the multidrug resistant phenotype, ACPs have attracted considerable attention. Indeed, these peptides could help to develop a new generation of anti-cancer drugs with a mechanism of action well distinguished from those of conventional chemotherapeutic agents.

As not all the HDPs are ACPs and the killing mechanism seems to differ for each ACP and tumor cell line, the rationale development of new antitumor agents based on CAMPs/ACPs requires further investigations. In particular, the identification and characterization of new ACPs could help to better define the requirements for a strong and selective antitumor activity.

Recently, we have developed an *in silico* tool allowing to identify HDP-like peptides hidden into the sequences of proteins not necessarily involved in host defense [13]. Using this tool we have already identified three new human HDPs [14–16]. Furthermore, we have demonstrated that DNA binding proteins can be a convenient source of new HDP-like peptides by identifying the first HDP from an archaeal protein, the transcription factor Stf76 encoded by the hybrid plasmid-virus pSSVx from *Sulfolobus islandicus* [17]. This archaeal HDP, named VLL-28 from its sequence [16], has a broad-spectrum antibacterial activity and exhibits selective leakage and fusogenic capability on vesicles with a lipid composition similar to that of bacterial membranes. Moreover, we have shown that VLL-28 retains the ability of the parental protein to bind nucleic acids (both single and double strand DNA). Using a fluorescent derivative, we have demonstrated that VLL-28 localizes not only on the cell membrane but also in the cytoplasm of *Escherichia coli*, thus suggesting that it could target both membranes and intracellular components of bacterial cells.

Here we report for the first time the characterization of the

antitumor activity of VLL-28. By means of a multidisciplinary approach including biochemical, cellular biology and spectroscopic techniques, the action mechanism of VLL-28 has been elucidated. Intriguingly, it has been proved to be an effective ACP able to selectively kill tumor cells by inducing apoptosis.

## 2. Materials and methods

### 2.1. Peptide synthesis reagents

Polypropylene reaction vessels and sintered polyethylene frits were supplied by Alltech Italia (Milan, Italy). NovaSyn TGR resin, 2-(1H-benzotriazole-1-yl)-1,1,3,3-tetramethyluronium hexafluorophosphate (HBTU), cyano-hydroxyimino-acetic acid ethyl ester (Oxyma) and all amino acids were purchased from Novabiochem-Merck (Nottingham, U.K.). *N,N'*-diisopropylethylamine (DIPEA), piperidine, Kaiser test, trifluoroacetic acid (TFA), scavengers, fluorescein isothiocyanate (FITC) and *N*-methylmorpholine (NMM) were purchased from Sigma-Aldrich (Milan, Italy). *N,N*-Dimethylformamide (DMF) was purchased from CARLO ERBA Reagents (Milan, Italy). Acetonitrile (ACN), dichloromethane (DCM) and diethyl ether were purchased from VWR International (Milan, Italy). All aqueous solutions were prepared by using water obtained from a Milli-Q gradient A-10 system (Millipore, 18.2 M $\Omega$ -cm, organic carbon content  $\geq$  4  $\mu$ g/L).

### 2.2. Peptide synthesis

VLL-28 and FITC-VLL-28 (VLL-28 derivative with an additional glycine residue at the C-terminus as spacer and a lysin residue for FITC labeling) peptides were manually synthesized using the fluorenylmethyloxycarbonyl (Fmoc) solid-phase strategy (0.2 mmol). The syntheses were performed on NovaSyn TGR resin (loading 0.24 mmol/g), using all standard amino acids. The Fmoc protecting group was removed by treatment with 30% piperidine in DMF ( $3 \times 10$  min). The amino acids in 10-fold excess were pre-activated with HBTU (9.8 equiv)/Oxyma (9.8 equiv)/DIPEA (10 equiv) in DMF for 5 min and then added to the resin suspended in DMF. The reaction was performed for 1 h and the coupling efficiency was assessed by the Kaiser test. In the case of FITC-VLL-28 peptide, once synthesis was completed, the ivDde protecting group of Lys(ivDde) residue was selectively removed by treatment of the peptidyl resin with a solution of 2% hydrazine in DMF ( $20 \times 3$  min). FITC labeling was then performed with 2 equiv of fluorescein isothiocyanate and 4 equiv of NMM in DMF for 5 h.

The peptides were finally cleaved off the resins by treatment with a mixture of trifluoroacetic acid (TFA)/water/triisopropylsilane (95:2.5:2.5 v/v/v) for 3 h at room temperature. The resins were filtered, the crude peptides were precipitated with diethyl ether, dissolved in H<sub>2</sub>O/ACN solution, and lyophilized. The products were purified by preparative RP-HPLC on a Shimadzu system equipped with a UV-visible detector SPD10A using a Phenomenex Jupiter Proteo column (21.2  $\times$  250 mm; 4  $\mu$ m; 90 Å) and a linear gradient of H<sub>2</sub>O (0.1% TFA)/ACN (0.1% TFA) from 10%–55% of ACN (0.1%TFA) in 15 min at a flow rate of 20 mL/min. The collected fractions containing the peptides were lyophilized giving a final yield of about 35% of each pure product. The identity and purity of the compounds were assessed by the AGILENT Q-TOF LC/MS instrument equipped with a diode array detector combined with a dual ESI source on a Agilent C18 column (2.1  $\times$  50 mm; 1.8  $\mu$ m; 300 Å) at a flow rate of 200  $\mu$ L/min and a linear gradient of H<sub>2</sub>O (0.01% TFA)/ACN (0.01% TFA) from 5%–70% of ACN (0.01% TFA) in 15 min.

### 2.3. Cell culture

Malignant SVT2 murine fibroblasts (BALBc 3T3 cells transformed by SV40 virus), parental BALBc 3T3 murine cells, and HEK-293 human embryonic kidney cells were cultured in Dulbecco's Modified Eagle's



Medium (Sigma-Aldrich), supplemented with 10% fetal bovine serum (HyClone), 2 mM L-glutamine and antibiotics, in a 5% CO<sub>2</sub> humidified atmosphere at 37 °C. HRCE (Human Renal Cortical Epithelial) cells (Innoprot) were cultured in basal medium, supplemented with 2% fetal bovine serum, epithelial cell growth supplement and antibiotics, all from Innoprot, in a 5% CO<sub>2</sub> humidified atmosphere at 37 °C [18].

#### 2.4. Cytotoxicity assays

Cells were seeded in 96-well plates (100 µL per well) at a density of  $5 \times 10^3$  per well (SVT2, HEK-293, and HRCE cells) or  $2.5 \times 10^3$  per well (BALBc 3T3 cells). VLL-28 peptide was added to the cells 24 h after seeding for time- and dose-dependent cytotoxic assays. At the end of incubation, cell viability was assessed by the MTT assay, as previously described [19]. In brief, MTT reagent, dissolved in DMEM in the absence of phenol red (Sigma-Aldrich), was added to the cells (100 µL per well) to a final concentration of 0.5 mg/mL. After a 4-h incubation at 37 °C, the culture medium was removed and the resulting formazan salts were dissolved by adding isopropanol containing 0.1 N HCl (100 µL per well). Absorbance values of blue formazan were determined at 570 nm using an automatic plate reader (MicrobetaWallac 1420, Perkin Elmer). Cell survival was expressed as percentage of viable cells in the presence of the peptide, with respect to control cells grown in the absence of the peptide. In all of the experiments described in this paper, controls were performed by supplementing the cell cultures with identical volumes of peptide buffer for the same time span. Obtained data represent the mean ( $\pm$  standard deviation) of at least 4 independent experiments, each one carried out with triplicate determinations. Statistical analysis was performed using a Student's *t*-Test, and significant differences were indicated as  $^*(P < 0.05)$ ,  $^{**}(P < 0.01)$  or  $^{***}(P < 0.001)$ .

#### 2.5. Analysis of cell death

Cells were plated in 6-well plates (1 mL per well) at a density of  $1 \times 10^6$  cells per well in complete medium for 24 h and then exposed to 20 µM VLL-28 for 6, 12 or 24 h to prepare cell lysates. Both untreated and treated cells were scraped off in PBS, centrifuged at  $1000 \times g$  for 10 min and resuspended in lysis buffer (1% NP-40 in PBS, pH 7.4) containing protease inhibitors. After 30 min of incubation on ice, lysates were centrifuged at  $14,000 \times g$  for 30 min at 4 °C. Upon determination of total protein concentration in the supernatant by the Bradford assay, samples were analyzed by SDS-PAGE followed by Western blotting using specific antibodies directed towards procaspase-3 (Cell Signaling Technology) or p62 (Novus Biologicals) proteins. For normalization to internal standard signals, antibodies against  $\beta$ -actin (Sigma-Aldrich) were used. In parallel experiments, cells were treated with puromycin (10 µg/mL) for 12 h or with rapamycin (20 µM) for 24 h, which were used as positive controls for apoptosis and autophagy induction, respectively.

For morphological analyses, cells were seeded on glass coverslips in 24-well plates and grown to semi-confluency. Cells were then incubated for 72 h with 20 µM VLL-28 peptide in complete medium, after which cells were washed with PBS, fixed for 10 min at room temperature (RT) with 4% paraformaldehyde in PBS and mounted in 50% glycerol in PBS. Samples were then examined using a confocal laser-scanner microscope Zeiss LSM 700. All images were taken under identical conditions.

#### 2.6. Fluorescence studies

Fluorescence analyses were performed as previously described [20]. Briefly, cells were seeded on glass coverslips in 24-well plates, grown to semi-confluency, and then incubated for 12 h with 20 µM FITC-labeled VLL-28. Following incubation, cells were washed with PBS and then fixed for 10 min at RT with 4% paraformaldehyde in PBS. Cell membranes were labeled by incubating the cells with Wheat Germ

Agglutinin (WGA, 5 µg/mL) Alexa Fluor®594 Conjugate (ThermoFisher Scientific) for 10 min at RT. Cells were then washed twice in PBS following the manufacturer's instructions. Confocal microscopy analyses were performed with a confocal laser-scanner microscope Zeiss LSM 700.

#### 2.7. Circular dichroism analyses

Far-UV CD spectra were recorded on a Jasco J-810 spectropolarimeter (JASCO Corp) equipped with a PTC-423S/15 Peltier temperature controller in the wavelength interval of 198–260 nm. Experiments were performed using a 20 µM VLL-28 solution (in PBS pH 7.4) in a 0.1 cm path-length quartz cuvette as already reported in Notomista et al. [16].

CD spectra in the presence of intact cells were registered using  $8 \times 10^5$  BALBc 3T3 cells or SVT2 cells at different incubation times (0, 10, 30, 60 min and 24 h) in PBS buffer at 20 °C. The baseline was corrected by subtracting the spectrum of the cells alone at the same time of incubation [21–23].

#### 2.8. Membrane preparation

Membranes used in NMR experiments were isolated from BALBc 3T3 or SVT2 cells and obtained as reported in Farina et al. [24]. In details, cells were detached from the flask with trypsin and washed twice with PBS. Then the cells were transferred into homogenization buffer containing PBS and homogenized by means of a pellet pestle (Sigma). Particulate matter was removed by centrifuging at 3500 rpm for 15 min. The supernatant was then centrifuged at 28000 rpm for 1 h at 4 °C. The pellet was washed and centrifuged at 28000 rpm for 30 min at 4 °C. 180 µL of PBS plus 20 µL D<sub>2</sub>O were added to the pellet, and the membrane was re-suspended by 20 passages through a 25 gauge needle.

#### 2.9. NMR spectroscopy

All NMR experiments were carried out at 298 K using an Inova 600 MHz spectrometer (Varian Inc., Palo Alto, CA, USA), equipped with a cryogenic probe optimized for <sup>1</sup>H detection.

NMR samples were prepared as follows. For chemical shift assignment and conformational analysis, 1 mg of VLL-28 was dissolved either in 500 µL sodium phosphate 20 mM pH 7.0 with 10% v/v D<sub>2</sub>O or in 500 µL of the same buffer containing 25% (v/v) TFE (2,2,2-trifluoroethanol-D<sub>3</sub> 99.5% isotopic purity, Sigma-Aldrich). One-dimensional (1D) <sup>1</sup>H spectra were acquired with a spectral width of 7191.66 Hz, relaxation delay 1.03 s, 7k data points for acquisition and 16k for transformation. Bi-dimensional (2D) [<sup>1</sup>H, <sup>1</sup>H] total correlation spectroscopy (TOCSY) [25], double quantum filtered correlated spectroscopy (COSY) [26] and nuclear Overhauser effect spectroscopy (NOESY) [27] were acquired with 32 or 64 scans per t1 increment with a spectral width of 7191.66 Hz along both t1 and t2, 2048  $\times$  256 data points in t2 and t1, respectively, and recycle delay 1.0 s. Water suppression was achieved by means of Double Pulsed Field Gradient Spin Echo (DPFGSE) sequence [28,29]. TOCSY experiments were recorded using a DIPSI-2 mixing scheme of 70 ms with 7.7 kHz spin-lock field strength. NOESY spectra were carried out with a mixing time of 250 ms. Data were typically apodized with a square cosine window function and zero filled to a matrix of size 4096  $\times$  1024 before Fourier transformation and baseline correction.

According to the procedure recently reported [24] for interaction studies of VLL-28 with intact cells and isolated membranes of BALBc 3T3 and SVT2 cell lines, pellet of  $18 \times 10^6$  cells and membranes from  $18 \times 10^6$  cells, obtained as reported above, were re-suspended in 150 µL of PBS buffer (pH 7.4) and 10% <sup>2</sup>H<sub>2</sub>O, to obtain reference spectra, or of VLL-8 (430 µM) in PBS buffer. STD spectra were acquired with 10,000 scans with on-resonance irradiation at 0.2 ppm or 5.2 ppm for saturation of membrane proteins or lipids resonances, respectively,



and off-resonance irradiation at 30 ppm. A train of 40 Gaussian shaped pulses of 50 ms with 1 ms delay between pulses were used, for a total saturation time of 2 s. STD spectra were obtained by internal subtraction of saturated spectrum from off-resonance spectrum by phase cycling. STD spectrum of the only peptide was also acquired and did not show any signal. 2D [ $^1\text{H}$ ,  $^1\text{H}$ ] TOCSY and NOESY spectra of VLL-28 in presence of isolated membranes were also acquired, similarly to those of the peptide alone.

All NMR data were processed with the software VNMRJ 1.1.D (Varian Inc.). 1D spectra were analyzed using ACD/NMR Processor 12.0 [www.acdlabs.com]. 2D TOCSY, COSY and NOESY spectra for proton chemical shift assignment were analyzed using Homoscope, a tool available in CARA (Computer Aided Resonance Assignment) software. Chemical shift assignments of VLL-28 in the absence of TFE are referred to residual water proton signals, (4.75 ppm), whereas in 25% TFE to residual TFE proton signals (3.88 ppm). Chemical shift deviations from random coil values for  $\text{H}_\alpha$  were calculated using the ChemShiftDeviationsFile script available in CARA.

### 2.10. Zeta-potential measurements of bacterial and eukaryotic cells in the presence of VLL-28

BL21 (DE3) *E. coli* cells were plated on Luria-Bertani agar overnight at 37 °C. An isolated bacterial colony was used to inoculate Mueller Hinton Broth (MHB; OXOID, Hampshire, UK), and the bacterial culture was allowed to grow overnight at 37 °C. 100  $\mu\text{L}$  of culture was used to freshly inoculate 5 mL of MHB. The suspension was incubated at 37 °C for ~2 h, until a final bacterial concentration of  $\sim 3 \times 10^8$  colony forming units per mL (CFU/mL) was reached ( $\text{OD}_{600\text{nm}} \sim 0.1$ ). Bacterial suspensions were diluted using fresh MHB to  $3 \times 10^7$  CFU/mL for zeta-potential studies. Afterwards, cells were centrifuged at  $12,000 \times g$  for 5 min, and washed three times using 20 mM sodium phosphates buffer, pH 7.4. The zeta-potential of bacterial cells was determined at 25 °C from the mean of 3 measurements (50 runs each), in the absence and presence of different VLL-28 concentrations (0–10  $\mu\text{M}$ ). Zeta-potential values were obtained by phase analysis light scattering (PALS) in a Zetasizer Nano ZS (Malvern Instruments, Malvern, UK), using disposable zeta cells with gold electrodes. Values of viscosity and refractive index were set to 0.8872 cP and 1.330, respectively.

Confluent BALBc 3T3 and SVT2 cells were washed with PBS buffer followed by trypsinization. Zeta potential measurements of eukaryotic cells were performed using the Diffusion Barrier Technique (Malvern, Application Note).  $4 \times 10^5$  cells were dispensed into the disposable zeta cells with gold electrodes in PBS with and without the peptide (from 0 to 50  $\mu\text{M}$ ) and allowed to equilibrate for 30 min at 37 °C. One measurement (~70 runs each) was performed with a constant voltage of 40 V. The complete experiment was carried out at least two times using independent cellular suspensions.

## 3. Results and discussion

### 3.1. Selective antitumor action of VLL-28 peptide

To assess whether VLL-28 was endowed with anti-cancer activity, cytotoxicity assays were performed on malignant SVT2 mouse fibroblasts and parental non-malignant BALBc 3T3 mouse fibroblasts. Interestingly, these studies have shown that the peptide VLL-28 exerts a dose- and time-dependent inhibition of viability on malignant SVT2 murine fibroblasts (see Fig. 1a). Conversely, the peptide was found to be inactive towards the non-malignant line of BALBc 3T3 fibroblasts (Fig. 1b). This evidence was also confirmed by morphological analyses through light microscopy, where a severe alteration of cell morphology with the presence of cell debris was observed only in the case of SVT2 cancer cells, with an  $\text{IC}_{50}$  value of 10  $\mu\text{M}$  at 72 h (Fig. S1). Remarkably, this peptide was also found to be effective and selective against human tumor cell lines, as demonstrated by MTT assays performed on

transformed HEK-293 cells (with an  $\text{IC}_{50}$  value of 10  $\mu\text{M}$  at 72 h) and human primary renal cortical epithelial (HRCE) cells (Fig. S2). In agreement with these results, it has been previously reported that other AMPs, which are toxic for bacteria but not for normal mammalian cells, are instead cytotoxic for cancer cells [30].

### 3.2. Internalization of VLL-28 peptide

Most AMPs and ACPs share a common membranolytic mechanism of action that results first either in the selective disruption or permeation of the cancer cell membrane and then in the swelling of mitochondria. Nonetheless, a non-membranolytic mechanism of action is increasingly recognized as an alternative ACPs mechanism [31]. To test whether the selective antitumor activity of VLL-28 was associated to a membranolytic mechanism and/or to its internalization, we performed experiments by using the peptide labeled with fluorescein isothiocyanate (FITC). To this purpose, SVT2 and BALBc 3T3 cells were incubated for 12 h with 20  $\mu\text{M}$  FITC-labeled VLL-28, since this concentration of peptide turned out to be the most effective in terms of cytotoxicity. As shown in Fig. 2a, in the case of SVT2 cells, VLL-28 fluorescent signal appears to be mostly intracellular already after 12 h of incubation, thus indicating that the peptide is internalized into the target cancer cells. On the other hand, the peptide (green) mainly colocalizes with WGA (red) at the plasma membrane in BALBc 3T3 cells (as indicated by arrows in Fig. 2b). The lack of VLL-28 internalization into these latter cells is consistent with the absence of cytotoxicity emerged from viability tests (Fig. 1b). Fluorescent staining was found to be specific, as no fluorescent signals were observed in the absence of FITC-labeled peptide (data not shown). Since the internalization has been observed at a time point preceding the cell death (48–72 h), the molecular target of VLL-28 might be a not yet identified intracellular component.

### 3.3. VLL-28 CD analyses in the presence of intact eukaryotic cells

Since differences in the plasma membrane composition between normal and cancer cells are supposed to contribute to the selective permeability and toxicity of ACPs towards the latter, we resolved to examine if the presence of the two different cell lines affects differently the secondary structure of VLL-28. Interestingly, VLL-28 CD spectra registered in the presence of either BALBc 3T3 or SVT2 whole cells revealed a different behavior (Fig. 3). In particular, in the presence of BALBc 3T3 cells, VLL-28 seems to gradually get structured over time until a prevalence of helical structure is observed upon 1 h incubation (Fig. 3a). Indeed, the spectrum shows two minima, at 208 and 222 nm, typical of helical structure, in agreement with CD data obtained in the presence of *n*-dodecyl-phosphatidylcholine (DPC), a well-known eukaryotic membrane mimetic agents [16]. Differently, in the presence of SVT2 intact cells, a drop in the CD signal is observed suggesting a fast internalization process of VLL-28, occurring already after 10 min (Fig. 3b), as confirmed by confocal microscopy data (Fig. 2).

### 3.4. NMR conformational analysis of VLL-28

In order to gain insight into the mechanism of action of VLL-28 and provide information on the basis of the different behaviors of VLL-28 with regard to the two studied cell lines, a NMR conformational analysis of the peptide in the absence and in the presence of TFE, a well-known structuring solvent, has been initially carried out (Figs. S3 and S4). According with what previously observed by CD analysis [16], VLL-28 does not adopt a well-defined conformation in phosphate neutral solution, as indicated by sharp and low-dispersed resonances in both the amide/aromatic and the aliphatic regions (Fig. S3a). Upon addition of TFE (25% v/v), amide, aromatic and aliphatic proton resonances resulted significantly more dispersed (Fig. S3b). In particular, the tryptophan side chain  $\text{H}_\text{N}$ , clearly distinguishable at 10.14 ppm in

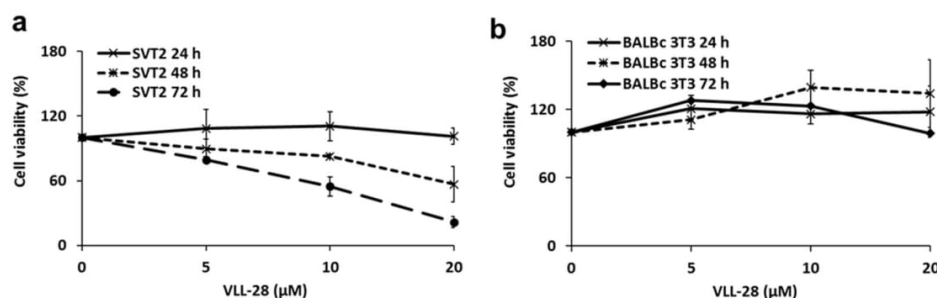


**Fig. 1.** Effects of the peptide VLL-28 on the SVT2 (a) and BALBc 3T3 (b) cell viability. MTT assays were performed on cells treated with increasing amounts of the peptide (5, 10 and 20  $\mu$ M) for different time spans (24, 48 and 72 h). The viability of cell samples was expressed as the percentage of MTT reduction with respect to control cells, tested under the same conditions but in the absence of the peptide. Data represent the mean ( $\pm$  standard deviation, SD) of at least 4 independent experiments, each one carried out with triplicate determinations. \* $P < 0.05$ , \*\* $P < 0.01$ , or \*\*\* $P < 0.001$  were obtained for control versus treated samples in the case of SVT2 cells treated with VLL-28 peptide for 48 and 72 h.

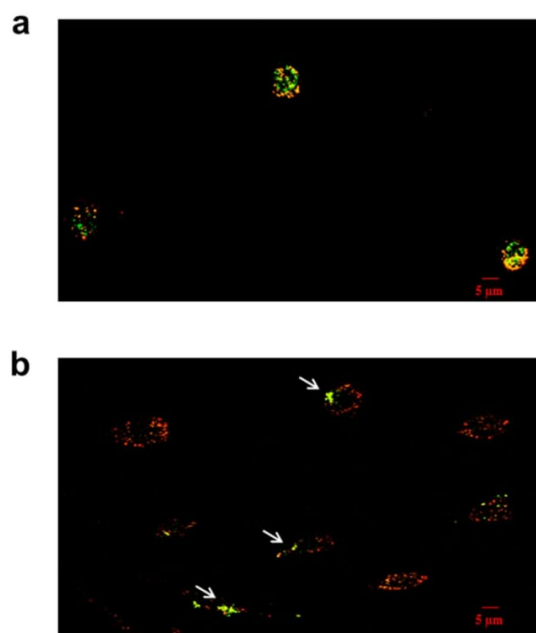


**Fig. 2.** Internalization of VLL-28 peptide in SVT2 (a) and BALBc 3T3 (b) cells. Cells were cultured on coverslips, incubated for 12 h with 20  $\mu$ M VLL-28 peptide (green) and stained with WGA (5  $\mu$ g/mL, Alexa Fluor®594 Conjugate). Cells were analyzed by confocal microscopy.

the absence of TFE (Fig. S3a, left), exhibits up-field shift at 9.94 ppm upon addition of TFE (Fig. S3b, left), possibly induced by an aromatic-aromatic long-range interaction. Moreover, 2D [ $^1\text{H}$ ,  $^1\text{H}$ ] NOESY spectrum of VLL-28 peptide contains a consistent higher number of cross-peaks with respect of that recorded in the absence of TFE, indicating a more structured conformation (Fig. S4). Almost complete assignment of proton resonances of VLL-28 has been achieved in 25% TFE by using a combination of TOCSY and NOESY spectra, according to the standard procedures (Table S1).

To assess the secondary structure of VLL-28 in 25% TFE, analyses of the  $H_\alpha$  chemical shift deviations from random coil values ( $\Delta\delta H_\alpha$ ) and of the NOE patterns were performed. Interestingly, two regions encompassing residues  $V^{37}$ - $R^{48}$  and  $V^{50}$ - $S^{59}$  showed large negative deviations ( $\Delta\delta H_\alpha < -0.1$  ppm), suggesting that the peptide mostly assumes a helical conformation, which is lost in the last C-terminal amino acids (Fig. 4a). Accordingly,  $H_N$ - $H_N$  NOEs, together with  $H_{\alpha i}$ - $H_{Ni+3}$  and  $H_{\alpha i}$ - $H_{\beta i+3}$  NOEs, were observed starting from residues  $V^{37}$  to  $S^{59}$  only in the presence of TFE (Fig. 4b and c), further confirming the helical

structure of that region in TFE.

### 3.5. STD NMR interaction studies of VLL-28 with tumor and normal cell membranes and definition of its binding epitopes

To identify binding residues of VLL-28 saturation transfer difference (STD) NMR binding experiments of the peptide in the presence of intact SVT2 and BALBc 3T3 cells [32], as well as of their isolated membranes, were performed. Unfortunately,  $^1\text{H}$  NMR VLL-28 proton resonances vanish in the presence of each of the two cell lines, thus hampering a detailed molecular analysis of the VLL-28 interaction with the cellular membranes (data not shown).

Very recently, we described the use of native cell membranes to overcome peptide cell internalization issues in “on-cell” NMR binding experiments [24]. This approach provides a significant improvement of NMR peptide spectra with respect to those acquired by using intact cells. Particularly, in the presence of isolated membranes, the  $^1\text{H}$  NMR signals of the peptide are sharper and better resolved, the STD signals appear significantly stronger, and background signals of the cellular components result much weaker in both the  $^1\text{H}$  and the STD spectra [24]. On the basis of the biochemical evidences of peptide internalization (see above), we carried out STD NMR experiments of the VLL-28 peptide in the presence of isolated membranes.

Interestingly,  $^1\text{H}$  NMR peptide signals resulted well visible in the presence of both SVT2 and BALBc 3T3 cell membranes as in the sole buffer (Fig. S5), thus allowing to perform STD NMR binding studies. In particular, we evaluated the binding capability of VLL-28 to the two different components of the cell membrane, proteins and lipids, acquiring STD spectra at two different saturation frequencies, i.e. one to selectively saturate proteins (0.2 ppm) and another one to saturate lipids (5.2 ppm) [33]. Remarkably, the  $^1\text{H}$  STD spectra showed that VLL-28 receives a detectable saturation transfer in the presence of cell membranes only when lipids are saturated (Fig. 5). This effect, which is negligible in the absence of cell membranes (Fig. 5b), provides a direct observation of the binding of VLL-28 to the lipid component of the cell membranes. This finding is in agreement with previous results showing that the peptide is able to interact with lipids mimicking bacterial membranes [16]. It is worth of note that differences in the STD spectra were observed for BALBc 3T3 and SVT2 cell membranes (Fig. 5). In particular, a higher number of STD signals, with stronger intensities, was observed in the presence of BALBc 3T3 cell membranes compared with those of SVT2 (Fig. 6a). In particular, all the binding residues of VLL-28 to the SVT2 cell membranes are in common with that of the BALBc 3T3 cell membranes. Specifically, VLL28 residues involved in both BALBc 3T3 and SVT2 interaction are  $G^{49}$ ,  $Y^{52}$  and  $W^{55}$  (Fig. 6b, highlighted in magenta). Moreover, one or both of the two threonine residues,  $T^{41}$  and  $T^{43}$ , appear involved in the VLL-28 interaction with both cell lines. On the other hand,  $Q^{47}$ ,  $V^{50}$ ,  $I^{51}$  and  $F^{58}$ , together with the acetyl N-terminal, show protons that are saturated only in the



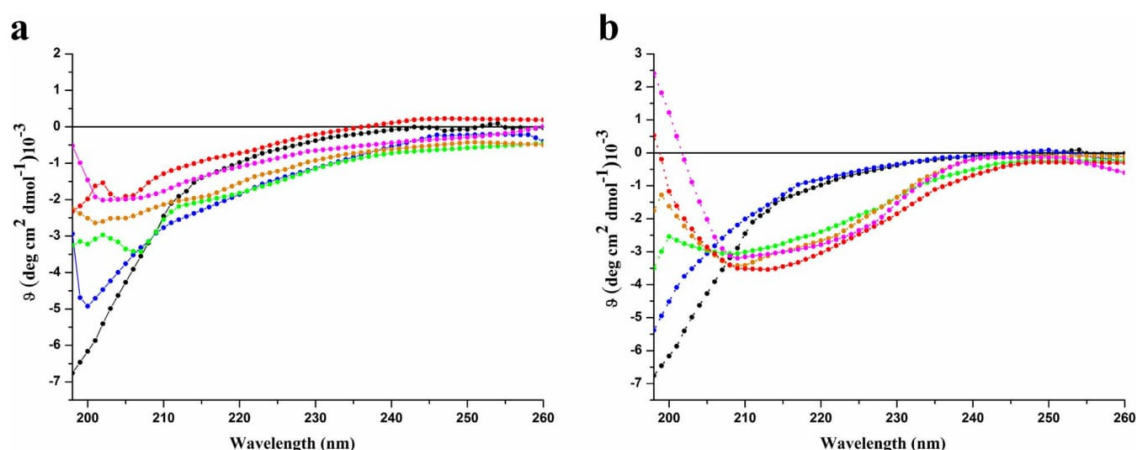


Fig. 3. Far UV VLL-28 CD spectra (black) recorded in the presence of a) BALBc 3T3 cells and b) SVT2 cells at 0 (blue), 10 (green), 30 (orange), 60 (red) min and 24 h (magenta) of incubation.

presence of BALBc 3T3 membranes (Fig. 6b, highlighted in red). Furthermore, strong STD effects were observed for side-chains of arginine and lysine residues. However, due to the spectral overlap and to the presence of a high number of basic residues in the peptide sequence they could not be identified unambiguously. Moreover, methyl of leucine (L) and valine (V) localized in the N-terminal region, seem to be involved as well.

Overall, these data indicate that the interaction of VLL-28 with cell membranes is mediated by the N-terminal and the central regions (V<sup>37</sup>-F<sup>58</sup>) (Fig. 6), which interestingly correspond to the portions of the

peptide that assume helical conformation in presence of TFE. Specifically, the binding to both the cell membranes seems to be mainly mediated by aromatic and basic residues, as could be expected for peptide-lipid interactions.

Different STD intensities of the peptide induced by the interaction with BALBc 3T3 and SVT2 cell membranes are likely ascribed to a different interaction mechanism between the peptide and the two membranes. In particular, stronger STD effects observed in the presence of non-tumor BALBc 3T3 membranes indicates that a fast-exchange equilibrium between the free form and a well-recognized bound

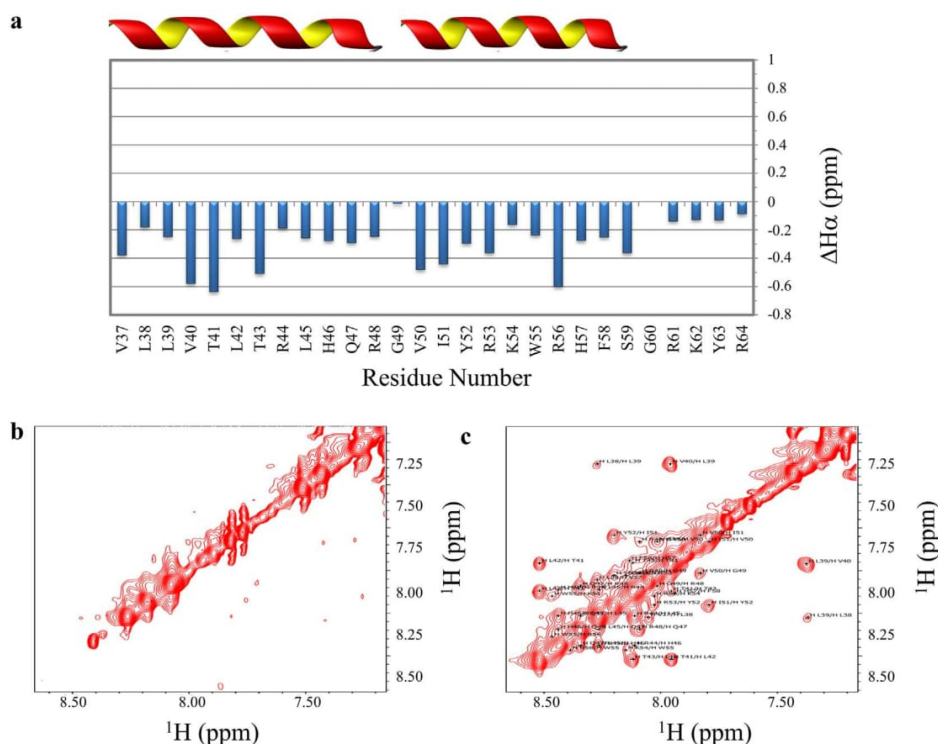
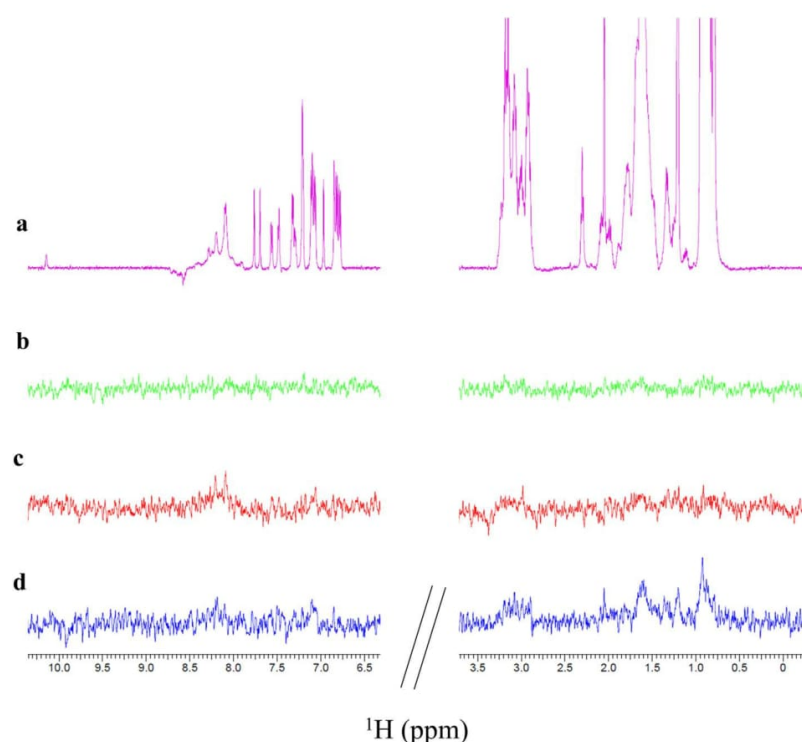


Fig. 4. (a) Chemical shift deviation from random coil values of H $\alpha$  backbone atoms ( $\Delta H\alpha$ ) plotted as a function of residue number. Two segments with helical conformation encompassing residues V37-R58, V50-S59, as suggested from the  $\Delta H\alpha$ s, are indicated above the plot. (b) and (c) Expansions of the H $_N$ -H $_N$  correlation region of the 2D [ $^1H$ ,  $^1H$ ] NOESY spectra of VLL-28 in phosphate buffer pH 7.0 at 298 K in the absence and presence of TFE 25%, respectively. HN $_i$ -HN $_{i+1}$  cross-peaks, observed only in (C), are labeled.

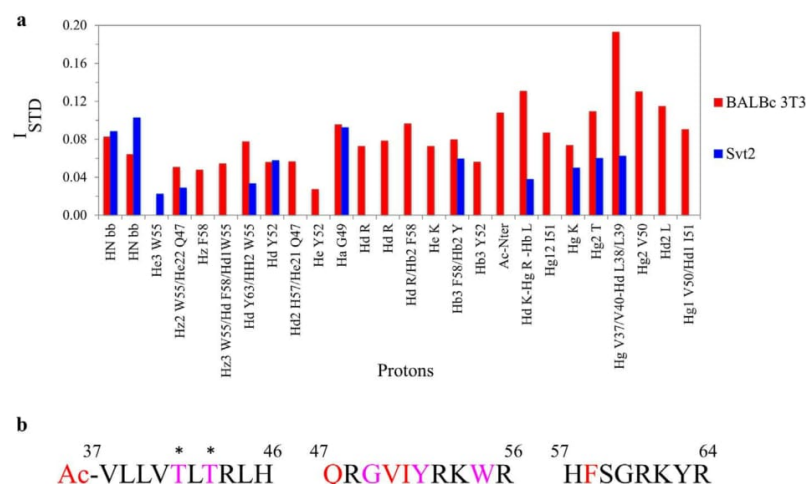


conformation occurs. Since fast-exchange regime is observed with lower affinity interaction, this could explain the inability of VLL-28 to penetrate these cell membranes. Differently, the reduced STD effects, observed in the presence of SVT2 membranes, can be ascribed to a stronger interaction with the cell membranes possibly being the first step of an internalization process.

### 3.6. Effect of VIL-28 on zeta-potential of cell membranes

Zeta potential of cell membranes has been used as a possible marker for the assessment of membrane damage and could be suitable to study the permeabilizing property of the VLL-28 peptide [34]. Zeta potential analyses were performed on *E. coli*, BALBc 3T3 and SVT2 cells. The

measured zeta potential in our experimental conditions for the cells in the absence of any peptide is  $-43.93$  mV for *E. coli* (Fig. S6),  $-6.91$  mV for BALBc 3T3 and  $-11.2$  mV for SVT2 cells, respectively, indicating that their surfaces are all negatively charged and, as already known, that the surface of the bacterial membranes is more negatively charged than mammalian cells [35,36]. This is due to both lipid composition and negatively charged cell surface macromolecules, as described also for other systems [9]. Furthermore, Z-potential measurements clearly demonstrated that the surface of SVT2 has a more negative charge than BALBc 3T3 cells. The addition of VLL-28 caused an increase of Z-potential values towards neutralization indicating that the peptide is interacting with the surface of all the cells tested (Fig. 7a and b and S6). Given the role of electrostatic interactions in driving the



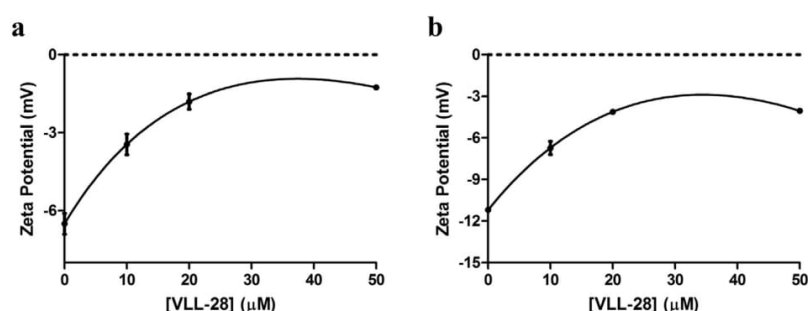


Fig. 7. a) VLL-28 effect on the Z-potential of BALBc 3T3 cells. b) VLL-28 effect on the Z-potential of SVT2 cells. At  $4 \times 10^5$  cells/mL cells were incubated and stabilized for 30 min with different peptide concentrations and the potential was measured at 37 °C. Data represent the mean ( $\pm$  standard deviation, SD) of 2 independent experiments.

AMPs initial adsorption onto the extracellular surface, it is reasonable to question if VLL-28, as ACP, exerts the same kind of action. In accordance with the general mechanism of action of AMPs, VLL-28 fully neutralizes *E. coli* cell's surface potential to exert its antimicrobial action (Fig. S6). Differently, on eukaryotic cells, VLL-28 is able to increase the Z-potential but never reaching full neutralization even at concentrations  $\geq 20$  μM thus indicating that total surface neutralization is not necessary to elicit its anticancer action [37].

### 3.7. Cell death pathway activated by cell treatment with VLL-28

To elucidate cell death pathways selectively activated by cell treatment with VLL-28, we performed western blot analyses by using antibodies specifically recognizing pro-caspase 3 and p62 proteins. The activation of procaspase-3 to caspase-3 is a key event in the apoptotic execution phase, since caspase-3 is considered the most important among executioner caspases and is activated by any of the initiator caspases (caspase-8, caspase-9, or caspase-10) [38]. p62, instead, is generally used as a marker to study the autophagic flux, since it accumulates when autophagy is inhibited, whereas p62 decreased levels can be observed when autophagy is induced [39].

To get insight into cell death pathway induced by VLL-28, western blot analyses were performed on SVT2 cells in comparison with BALBc 3T3 (Fig. 8a–d). In SVT2 cells it was found a significant increase of p62 levels upon 6 h treatment with 20 μM VLL-28 (Fig. 8a, d), indicative of

a stress leading to cell death with a consequent block of autophagy flux [40]. Accordingly, procaspase-3 levels appear lower than in control cells upon 6 and 12 h treatment (Fig. 8a, b), indicating a significant (about 30%) activation of procaspase-3 to caspase-3 associated to apoptosis induction. This activation appears even stronger (about 50%) after 24 h of treatment (Fig. 8a, b), and is associated to a significant decrease of p62 levels (Fig. 8a, d), in agreement with a time-dependent activation of apoptotic cell pathway.

In the case of non-malignant BALBc 3T3 cells, instead, no significant effects on procaspase-3 levels were observed upon cell treatment with 20 μM VLL-28 peptide at different time intervals (6, 12 and 24 h) (Fig. 8b, c), in agreement with the results reported above. This indicates that these cells are not susceptible to VLL-28 peptide toxic effects. Moreover, no significant effects were observed also when p62 levels were analyzed, except for 72 h treatment, where a slight increase of p62 levels was observed (Fig. 8b, d). Since no effects on cell viability were detected by MTT assays, this might be indicative of a slight cell perturbation counteracted by autophagy activation.

Hence, experimental data revealed that VLL-28 exerts its action through a time-dependent activation of apoptotic cell pathways as demonstrated by the maturation of procaspase-3 to the caspase-3 [41]. This is in agreement with data reported in the literature indicating that several potential ACPs are able to induce apoptosis in human cancer cell lines of different origin, such as breast, uterine cervix, liver and prostate [9]. Apoptosis induction, with some degree of selectivity

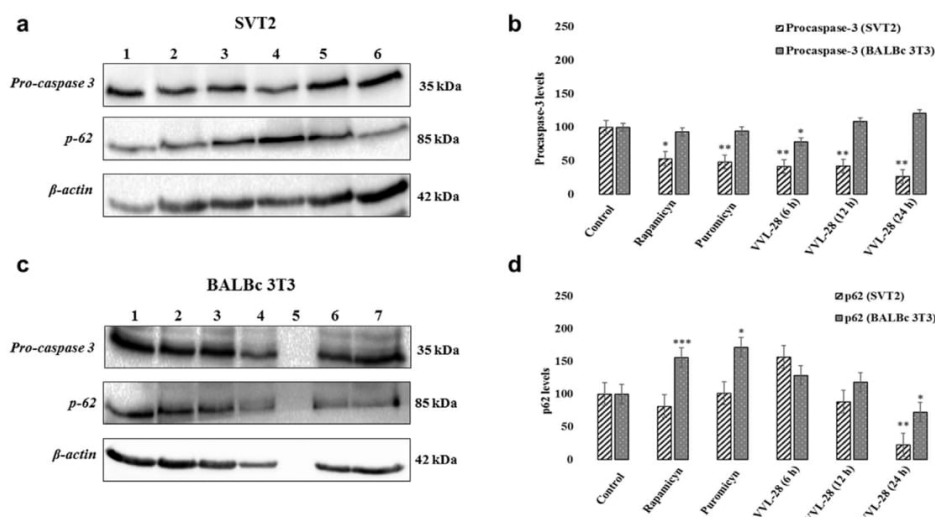


Fig. 8. Analysis of cell death pathway activated by the treatment with 20 μM VLL-28 peptide of SVT2 (a) and BALBc 3T3 (c) cells. Lane 1, cell lysate of untreated cells; lane 2, lysate of cells treated with rapamycin; lane 3, lysate of cells treated with puromycin; lane 4, lysate of cells treated with the peptide for 6 h; lane 5, lysate of cells treated with the peptide for 12 h; lane 6, lysate of cells treated with the peptide for 24 h. Western blots were performed by using antibodies directed towards procaspase-3, p62, and endogenous β-actin used as an internal standard (a, c). Densitometric analyses of protein bands specifically recognized by anti-procaspase-3 and anti-p62 antibodies are reported in b and d, respectively, where data represent the mean ( $\pm$  standard deviation, SD) of 3 independent experiments. \* $P < 0.05$ , \*\* $P < 0.01$ , or \*\*\* $P < 0.001$  were obtained for control versus treated samples.



towards cancer cells, has been described also in the case of ACPs effective on metastatic tumor cells or on cancer endothelial cells [9]. Since metastases are the main cause of conventional therapy failure, peptides able to specifically interfere with the process of metastases formation by stimulating apoptosis induction in neoplastic cells represent valuable resources in cancer treatment [9]. These observations associated to the strong and selective toxic effects exerted by VLL-28 peptide towards cancer cells open interesting perspective to future applications of this peptide.

#### 4. Concluding remarks

The cytotoxic activities of several AMPs turn this group of molecules into an amazing pool of new templates for anticancer drug development [42]. Accordingly, VLL-28, previously identified as an AMP [16], is here found to be endowed also with selective cytotoxic activity towards both murine and human cancer cells, thus pointing to VLL-28 as a potential chemotherapeutic agent. Microorganisms belonging to the archaeal kingdom have been so far considered as source of biotechnologically relevant enzymes and proteins [43–51], but there are no reports regarding potential ACPs isolated from this kingdom. This paper represents the first evidence that archaeal microorganisms could bear also an unexplored repertoire of such kind of molecules exerting a trans-kingdom action. Given the intrinsic stability to physical and chemical agents of Stf76, the parental source of VLL-28, it is foreseen that VLL-28 might be a promising “lead compound” for future development of novel drugs, upon chemical modifications, i.e. D-amino acids, an all-hydrocarbon bridge, and/or modified amide bounds to further increase its stability to proteases [22].

#### Transparency document

The <http://dx.doi.org/10.1016/j.bbagen.2017.06.009> associated with this article can be found, in online version.

#### Appendix A. Supplementary data

Supplementary data to this article can be found online at <http://dx.doi.org/10.1016/j.bbagen.2017.06.009>.

#### References

- [1] S.C. Mansour, O.M. Pena, R.E. Hancock, Host defense peptides: front-line immunomodulators, *Trends Immunol.* 35 (2014) 443–450.
- [2] J. Wiesner, A. Vilcinskis, Antimicrobial peptides: the ancient arm of the human immune system, *Virulence* 1 (2010) 440–464.
- [3] A.L. Hilchie, K. Wuerth, R.E.W. Hancock, Immune modulation by multifaceted cationic host defense (antimicrobial) peptides, *Nat. Chem. Biol.* 9 (2013) 761–768.
- [4] K.C.L. Mulder, L.A. Lima, V.J. Miranda, S.C. Dias, O.L. Franco, Current scenario of peptide-based drugs: the key roles of cationic antitumor and antiviral peptides, *Front. Microbiol.* 4 (2013).
- [5] M. Pushpanathan, P. Gunasekaran, J. Rajendhran, Antimicrobial peptides: versatile biological properties, *Int. J. Pept.* 2013 (2013) 675391.
- [6] S. Riedl, D. Zwegitck, K. Lohner, Membrane-active host defense peptides — challenges and perspectives for the development of novel anticancer drugs, *Chem. Phys. Lipids* 164 (2011) 766–781.
- [7] R.E.W. Hancock, E.F. Haney, E.E. Gill, The immunology of host defence peptides: beyond antimicrobial activity, *Nat. Rev. Immunol.* 16 (2016) 321–334.
- [8] V. Teixeira, M.J. Feio, M. Bastos, Role of lipids in the interaction of antimicrobial peptides with membranes, *Prog. Lipid Res.* 51 (2012) 149–177.
- [9] D. Gaspar, A.S. Veiga, M.R.B. Castanho, From antimicrobial to anticancer peptides. A review, *Front. Microbiol.* 4 (2013).
- [10] G. Gabernet, A.T. Muller, J.A. Hiss, G. Schneider, Membranolytic anticancer peptides, *Med. Chem. Commun.* 7 (2016) 2232–2245.
- [11] A.L. Rerole, J. Gobbo, A. De Thonel, E. Schmitt, J.P. Pais de Barros, A. Hammann, D. Lanneau, E. Fourmaux, O.N. Demidov, O. Micheau, L. Lagrost, P. Colas, G. Kroemer, C. Garrido, Peptides and aptamers targeting HSP70: a novel approach for anticancer chemotherapy, *Cancer Res.* 71 (2011) 484–495.
- [12] I. Kuriyama, A. Miyazaki, Y. Tsuda, H. Yoshida, Y. Mizushima, Inhibitory effect of novel somatostatin peptide analogues on human cancer cell growth based on the selective inhibition of DNA polymerase beta, *Bioorg. Med. Chem.* 21 (2013) 403–411.
- [13] K. Pane, L. Durante, O. Crescenzi, V. Cafaro, E. Pizzo, M. Varcamonti, A. Zanfardino, V. Izzo, A. Di Donato, E. Notomista, Antimicrobial potency of cationic antimicrobial peptides can be predicted from their amino acid composition: application to the detection of “cryptic” antimicrobial peptides, *J. Theor. Biol.* 419 (2017) 254–265.
- [14] R. Gaglione, E. Dell’Omo, A. Bosso, M. Chino, K. Pane, F. Ascione, F. Itri, S. Caserta, A. Amoresano, A. Lombardi, H.P. Haagsman, R. Piccoli, E. Pizzo, E.J. Veldhuizen, E. Notomista, A. Arciello, Novel human bioactive peptides identified in apolipoprotein B: evaluation of their therapeutic potential, *Biochem. Pharmacol.* (2017).
- [15] K. Pane, V. Sgambati, A. Zanfardino, G. Smaldone, V. Cafaro, T. Angrisano, E. Pedone, S. Di Gaetano, D. Capasso, E.F. Haney, V. Izzo, M. Varcamonti, E. Notomista, R.E.W. Hancock, A. Di Donato, E. Pizzo, A new cryptic cationic antimicrobial peptide from human apolipoprotein E with antibacterial activity and immunomodulatory effects on human cells, *FEBS J.* 283 (2016) 2115–2131.
- [16] E. Notomista, A. Falanga, S. Fusco, L. Pirone, A. Zanfardino, S. Galdiero, M. Varcamonti, E. Pedone, P. Contursi, The identification of a novel *Sulfolobus islandicus* CAMP-like peptide points to archaeal microorganisms as cell factories for the production of antimicrobial molecules, *Microb. Cell Factories* 14 (2015).
- [17] P. Contursi, B. Farina, L. Pirone, S. Fusco, L. Russo, S. Bartolucci, R. Fattorusso, E. Pedone, Structural and functional studies of Stf76 from the *Sulfolobus islandicus* plasmid-virus pSSVx: a novel peculiar member of the winged helix-turn-helix transcription factor family, *Nucleic Acids Res.* 42 (2014) 5993–6011.
- [18] E. Galano, A. Arciello, R. Piccoli, D.M. Monti, A. Amoresano, A proteomic approach to investigate the effects of cadmium and lead on human primary renal cells, *Metallomics* 6 (2014) 587–597.
- [19] D.M. Monti, D. Guarnieri, G. Napolitano, R. Piccoli, P. Netti, S. Fusco, A. Arciello, Biocompatibility, uptake and endocytosis pathways of polystyrene nanoparticles in primary human renal epithelial cells, *J. Biotechnol.* 193 (2015) 3–10.
- [20] A. Arciello, N. De Marco, R. Del Giudice, F. Guglielmi, P. Pucci, A. Relini, D.M. Monti, R. Piccoli, Insights into the fate of the N-terminal amyloidogenic polypeptide of ApoA-I in cultured target cells, *J. Cell. Mol. Med.* 15 (2011) 2652–2663.
- [21] G. Smaldone, D. Diana, L. Pollegioni, S. Di Gaetano, R. Fattorusso, E. Pedone, Insight into conformational modification of alpha-synuclein in the presence of neuronal whole cells and of their isolated membranes, *FEBS Lett.* 589 (2015) 798–804.
- [22] I. de Paola, L. Pirone, M. Palmieri, N. Balasco, L. Esposito, L. Russo, D. Mazza, L. Di Marcotullio, S. Di Gaetano, G. Maligneri, L. Vitagliano, E. Pedone, L. Zaccaro, Cullin3-BTB interface: a novel target for stapled peptides, *PLoS One* 10 (2015).
- [23] S. Corrales, C. Esposito, L. Pirone, L. Vitagliano, S.D. Gaetano, E. Pedone, A biophysical characterization of the folded domains of KCTD12: insights into interaction with the GABAB2 receptor, *J. Mol. Recognit.* 26 (2013) 488–495.
- [24] B. Farina, I. de Paola, L. Russo, D. Capasso, A. Liguoro, A. Del Gatto, M. Saviano, P.V. Pedone, S. Di Gaetano, G. Maligneri, L. Zaccaro, R. Fattorusso, A combined NMR and computational approach to determine the RGDchi-hCit-alpha(v)beta(3) integrin recognition mode in isolated cell membranes, *Chem. Eur. J.* 22 (2016) 681–693.
- [25] A. Bax, D.G. Davis, Mlev-17-based two-dimensional homonuclear magnetization transfer spectroscopy, *J. Magn. Reson.* 65 (1985) 355–360.
- [26] M. Rance, O.W. Sorensen, G. Bodenhausen, G. Wagner, R.R. Ernst, K. Wuthrich, Improved spectral resolution in cosy 1H NMR spectra of proteins via double quantum filtering, *Biochem. Biophys. Res. Commun.* 117 (1983) 479–485.
- [27] A. Kumar, R.R. Ernst, K. Wuthrich, A two-dimensional nuclear Overhauser enhancement (2D NOE) experiment for the elucidation of complete proton-proton cross-relaxation networks in biological macromolecules, *Biochem. Biophys. Res. Commun.* 95 (1980) 1–6.
- [28] T.L. Hwang, A.J. Shaka, Water suppression that works — excitation sculpting using arbitrary wave-forms and pulsed-field gradients, *J. Magn. Reson. Ser. A* 112 (1995) 275–279.
- [29] C. Dalvit, Efficient multiple-solvent suppression for the study of the interactions of organic solvents with biomolecules, *J. Biomol. NMR* 11 (1998) 437–444.
- [30] D.W. Hoskin, A. Ramamoorthy, Studies on anticancer activities of antimicrobial peptides, *BBA-Biomembranes* 1778 (2008) 357–375.
- [31] F. Schweizer, Cationic amphiphilic peptides with cancer-selective toxicity, *Eur. J. Pharmacol.* 625 (2009) 190–194.
- [32] G. Maligneri, C. Avitabile, M. Palmieri, L.D. D’Andrea, C. Isernia, A. Romanelli, R. Fattorusso, Structural basis of a temporin 1b analogue antimicrobial activity against gram negative bacteria determined by CD and NMR techniques in cellular environment, *ACS Chem. Biol.* 10 (2015) 965–969.
- [33] X. Pan, M. Wilson, C. McConville, M.-A. Brundler, T.N. Arvanitis, J.P. Shockcor, J.L. Griffin, R.A. Kauppinen, A.C. Peet, The lipid composition of isolated cytoplasmic lipid droplets from a human cancer cell line, BE(2)M17, *Mol. Biosyst.* 8 (2012) 1694–1700.
- [34] S. Halder, K.K. Yadav, R. Sarkar, S. Mukherjee, P. Saha, S. Halder, S. Karmakar, T. Sen, Alteration of zeta potential and membrane permeability in bacteria: a study with cationic agents, *Spring* 4 (2015).
- [35] R.E.W. Hancock, H.G. Sahl, Antimicrobial and host-defense peptides as new anti-infective therapeutic strategies, *Nat. Biotechnol.* 24 (2006) 1551–1557.
- [36] D. Gaspar, J.M. Freire, T.R. Pacheco, J.T. Barata, M.A.R.B. Castanho, Apoptotic human neutrophil peptide-1 anti-tumor activity revealed by cellular biomechanics, *BBA-Mol. Cell. Res.* 1853 (2015) 308–316.
- [37] D. Gaspar, A.S. Veiga, C. Sinthuvanich, J.P. Schneider, M.A.R.B. Castanho, Anticancer peptide SVS-1: efficacy precedes membrane neutralization, *Biochemistry* 51 (2012) 6263–6265.
- [38] S. Elmore, Apoptosis: a review of programmed cell death, *Toxicol. Pathol.* 35 (2007) 495–516.
- [39] G. Bjorkoy, T. Lamark, S. Pankiv, A. Overvatn, A. Brech, T. Johansen, Monitoring